Mechanistic studies of the desorption ionization process in fast atom bombardment mass spectrometry by Jentaie Shiea

A thesis submitted in partial fulfillment of the requirements for the degree of Doctor of Philosophy in Chemistry
Montana State University

Abstract:
The mechanisms involved in Desorption Ionization (DI) continue to be a very active area of research. The answer to the question of how involatile and very large molecules are transferred from the condensed phase to the gas phase has turned out to involve many different phenomena. The effect on Fast Atom Bombardment (FAB) mass spectra of the addition of acids to analyte bases has been quantitatively investigated. Generally, the pseudomolecular ion (M+H+) intensity increased with the addition of acid, however, decreases in ion intensity were also noted. For the practical use of FAB, it is important to clarify the reasons for this acid effect. By critical evaluation, a variety of different explanations were found. However, contrary to other studies, no unambiguous example was found in which the effect of "preformed ions" could adequately explain the observed results. The mechanistic implications of these findings are briefly discussed. The importance of surface activity in FAB has been pointed out by many researchers. A systematic study was conducted, involving the addition of negatively charged surfactants to samples containing small organic and inorganic cations. An enhancement of the positive ion spectra of these analytes was observed. The study of mass transport processes of two surfactants was performed by varying the analyte concentration and matrix temperature in FAB. The study of the desorption process in SIMS by varying the viscosity of the matrix solutions shows that such studies may help to bridge the mechanisms in solid and liquid SIMS and, in the process, increase our understanding of both techniques. It also shows that in the ionization process (precursor ion formation versus ion-molecule reactions), the role of radiation chemistry, transport processes, and the desorption process show characteristic changes with matrix viscosity. The ionization efficiency and competition effects in FAB for the precharged alkali and tertiary alkyl ammonium (TAM) ions were investigated. The competition between alkali ions themselves and alkali ions and TAM ion is too weak to be detected. However, TAM ion as well as the alkali ions, have a strong suppressing effect on the ion signal from amine bases. The most significant finding is a strong enhancement of Cs+ ion signal at a low matrix temperature. It was also found that the formation of mixed alkali chloride clusters in FAB are formed with a statistical distribution. Finally, a 2D molecular dynamics calculation simulating the bulk desorption in FAB was performed. The shockwave, spinodal decomposition, extensive cooling and the molecular desorption are all observed from the simulation. These are in agreement with the concepts presented earlier in the "phase explosion model".

MECHANISTIC STUDIES OF THE DESORPTION IONIZATION PROCESS IN FAST ATOM BOMBARDMENT MASS SPECTROMETRY

by

Jentaie Shiea

A thesis submitted in partial fulfillment
of the requirements for the degree

of

Doctor of Philosophy

in

Chemistry

MONTANA STATE UNIVERSITY
Bozeman, Montana

March 1991

APPROVAL

of a thesis submitted by

Jentaie Shiea

This thesis has been read by each member of the thesis committee and has been found to be satisfactory regarding content, English usage, format, citations, bibliographic style, and consistency, and is ready for submission to the College of Graduate Studies.

March 8, 91
Date

Jan Sun
Chairperson,
Graduate Committee

Approved for the Major Department

3/8/91
Date

Edwin H. Abbott
Head, Major Department

Approved for the College of Graduate Studies

March 20, 1991
Date

Henry L Parsons
Graduate Dean

STATEMENT OF PERMISSION TO USE

In presenting this thesis in partial fulfillment of the requirements for a doctoral degree at Montana State University, I agree that the Library shall make it available to borrowers under rules of the Library. I further agree that copying of this thesis is allowable only for scholarly purposes, consistent with "fair use" as prescribed in the U.S. Copyright Law. Requests for extensive copying or reproduction of this thesis should be referred to University Microfilms International, 300 North Zeeb Road, Ann Arbor, Michigan 48106, to whom I have granted "the exclusive right to reproduce and distribute copies of the dissertation in and from microfilm and the right to reproduce and distribute by abstract in any format."

Signature Jentai Shiea

Date Mar 15, 1991

ACKNOWLEDGMENTS

I would like to express my sincere appreciation to Dr. Jan Sunner for all of his supervision during this study. I also would like to give my special thanks to Dr. Joe Sears for the help of setting up the mass spectrometers for this study and for all of his suggestions and invaluable help during my graduate studies.

I thank the Department of Chemistry at Montana State University for the financial support through the last five and half years.

My special thanks to my wife Shwuneu for her assistance and love support.

TABLE OF CONTENTS Page

TABLE OF CONTENTS - Continued Page

LIST OF FIGURES

LISTS OF FIGURES - Continued

Figures Page

LISTS OF FIGURES - Continued

Figures Page

LIST OF FIGURES - Continued

Figures Page

LIST OF FIGURES - Continued

Figures Page

LIST OF FIGURES - Continued

Figures Page

ABSTRACT

The mechanisms involved in Desorption Ionization (DI) continue to be a very active area of research. The answer to the question of how involatile and very large molecules are transferred from the condensed phase to the gas phase has turned out to involve many different phenomena. The effect on Fast Atom Bombardment (FAB) mass spectra of the addition of acids to analyte bases has been quantitatively investigated. Generally, the pseudomolecular ion ($M+H^+$) intensity increased with the addition of acid, however, decreases in ion intensity were also noted. For the practical use of FAB, it is important to clarify the reasons for this acid effect. By critical evaluation, a variety of different explanations were found. However, contrary to other studies, no unambiguous example was found in which the effect of "preformed ions" could adequately explain the observed results. The mechanistic implications of these findings are briefly discussed. The importance of surface activity in FAB has been pointed out by many researchers. A systematic study was conducted, involving the addition of negatively charged surfactants to samples containing small organic and inorganic cations. An enhancement of the positive ion spectra of these analytes was observed. The study of mass transport processes of two surfactants was performed by varying the analyte concentration and matrix temperature in FAB. The study of the desorption process in SIMS by varying the viscosity of the matrix solutions shows that such studies may help to bridge the mechanisms in solid and liquid SIMS and, in the process, increase our understanding of both techniques. It also shows that in the ionization process (precursor ion formation versus ion-molecule reactions), the role of radiation chemistry, transport processes, and the desorption process show characteristic changes with matrix viscosity. The ionization efficiency and competition effects in FAB for the precharged alkali and tertiary alkyl ammonium (TAM) ions were investigated. The competition between alkali ions themselves and alkali ions and TAM ion is too weak to be detected. However, TAM ion as well as the alkali ions, have a strong suppressing effect on the ion signal from amine bases. The most significant finding is a strong enhancement of Cs^+ ion signal at a low matrix temperature. It was also found that the formation of mixed alkali chloride clusters in FAB are formed with a statistical distribution. Finally, a 2D molecular dynamics calculation simulating the bulk desorption in FAB was performed. The shockwave, spinodal decomposition, extensive cooling and the molecular desorption are all observed from the simulation. These are in agreement with the concepts presented earlier in the "phase explosion model".

INTRODUCTION

It was a substantial development in Analytical Chemistry when the mass spectrometer (MS) was first successfully used in determining the structure and molecular weight of chemicals in this century. Until recently, sample volatility was one of the principal requirements for mass spectrometry. Samples are amenable to electron impact ionization (EI) only if the sample molecules interact with energetic electrons (usually 70 eV) in the gas phase (see Figure 1). Traditional sample-inlet systems, at best, transport the sample only to the periphery of the ion source. By virtue of its vapor pressure, the molecules have to diffuse into the central region of the ionization chamber (focal point) to be ionized. The ions are extracted from the chamber by a small repulsion voltage (ca. 50 V) applied to the ion source and later focused and accelerated by a series of ion optical lenses. The requirement of adequate sample volatility imposed a practical limit of roughly 1,000 a.m.u. or less on the molecular weight of samples that were amenable to EI or chemical ionization (CI) mass spectrometry.

The development of desorption-ionization (DI) techniques has broken the shackles of sample volatility in mass spectrometry (Watson, 1985). This breakthrough has been especially important in the biochemical area, where most compounds (e.g. peptides, proteins and nucleic acids) are

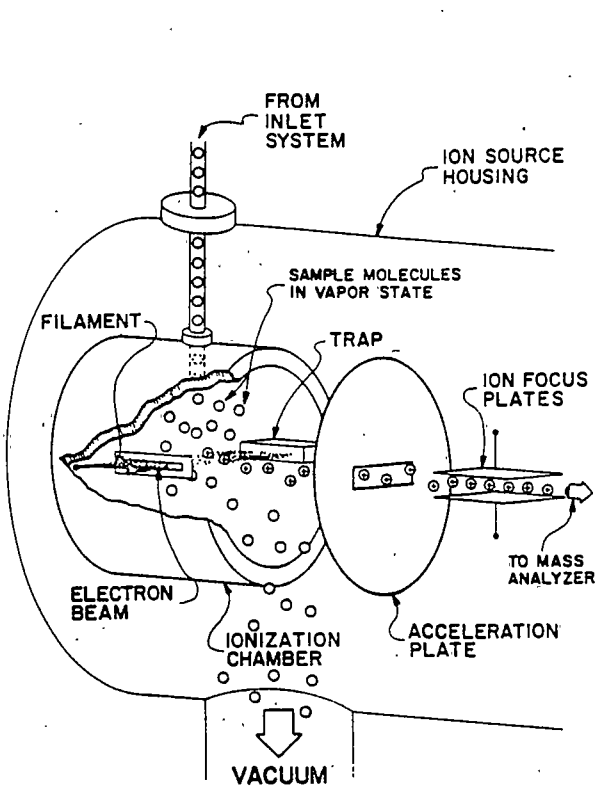

Figure 1. Diagram of EI ion source in mass spectrometer (from Watson, 1985).

quite polar or are in the form of polymers having very high molecular weights and thus low or no appreciable vapor pressure. In addition, these compounds are with few exceptions thermally labile and decompose easily at the operational temperature in EI.

There are four main DI techniques. These are particle induced DI techniques which include Secondary Ion Mass Spectrometry (SIMS), Fast Atom Bombardment (FAB), and Plasma Desorption (PD) and laser induced DI technique- Laser

Desorption (LD). In particle induced DI technique, the analyte is introduced into the ion source in the condensed phase (pure solid or as a solution in a viscous solvent). Desorption and ionization are induced by bombardment by energetic particles. The techniques are distinguished by the type of particle used for bombardment. For example, in SIMS a solid surface is bombarded by ions; in FAB by atoms; and in PD by fission fragments. In LD, the energy is deposited in the sample by pulse from the laser beam. A schematic representation of the four techniques is presented in Figure 2. It is interesting to note that although the energy of the primary ions (or atoms) of the various techniques range over several orders of magnitude, the resulting mass spectra are similar. That is, most of the ions formed contain the intact molecule in the form of an adduct with H^+, Na^+, K^+, or other cations or clusters. One rarely observes a peak for the molecular ion per se. Fragmentation is generally less than that observed in EI. Because of this particular characteristic, DI is termed a "soft ionization method".

A short summary of the history of developments in DI techniques will be given here. In 1969 Beckey published a mass spectrum of glucose, a polar compound of very low volatility (Beckey, 1969). The method he used, so called Field Desorption (FD), proved to be the precursor of the family of desorption ionization methods. In FD, ions are desorbed by the combined action of heat and the very high

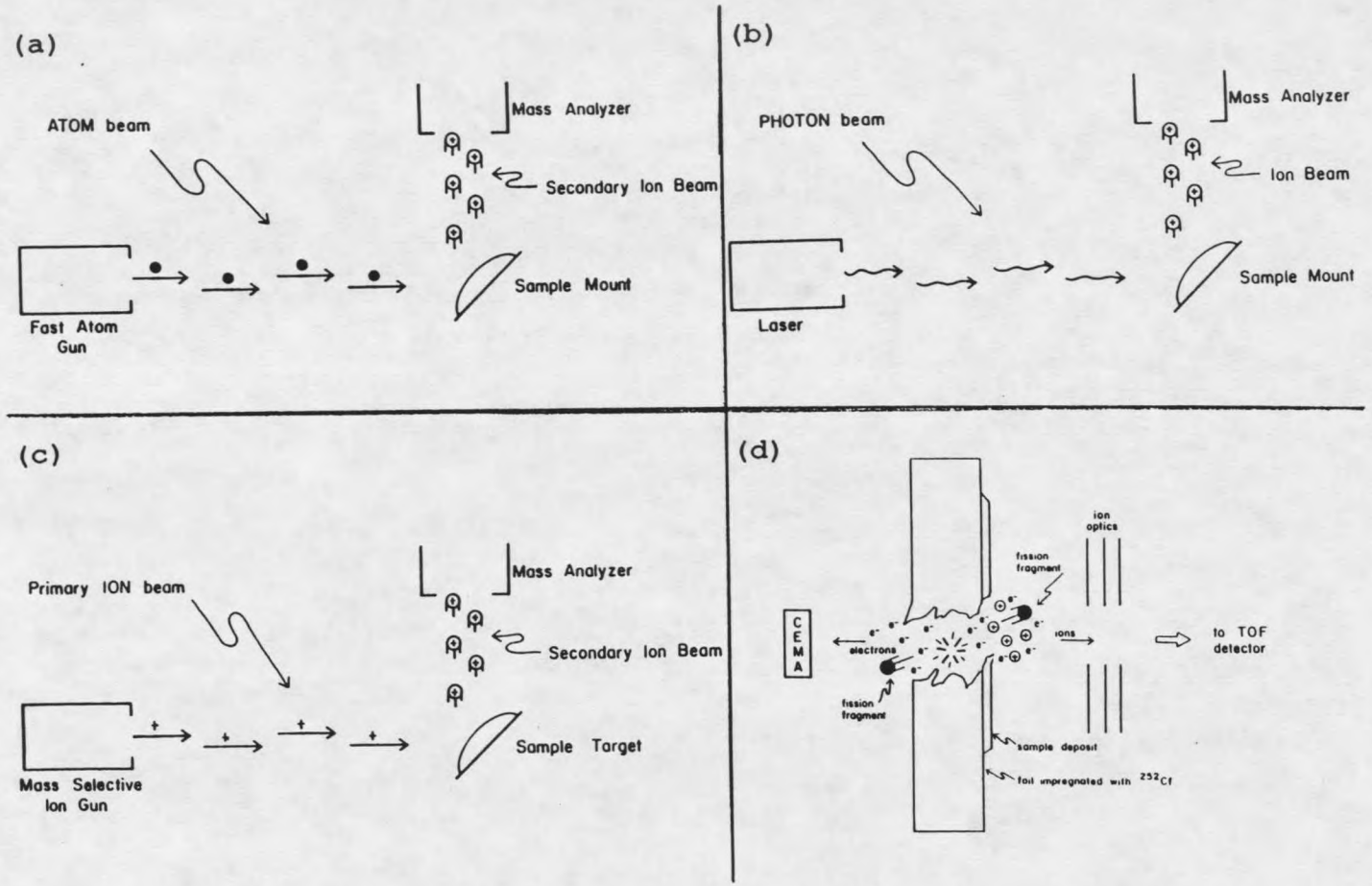

Figure 2. Schematic representation of the four variations of desorption ionization (DI) techniques- (a) FAB, (b) LD, (c) SIMS, (d) Cf PDMS (from Watson, 1985).

fields present in the source (Beckey, 1977). Beckey's work was built on an understanding of the physics of field emission and ionization. His contribution was the translation of this knowledge into a device having practical value in the molecular sciences.

The development of particle induced DI techniques began with the introduction of californium-252 Plasma Desorption Mass Spectrometry (PDMS) in 1974 by MacFarlane and coworkers (Torgerson et al., 1974). In this method, heavy ions (with hundreds of MeV of kinetic energy from the spontaneous fission of ^{252}Cf) bombard a solid matrix and induce desorption and ionization processes. Large polar thermally labile molecules are able to survive intact and to sublime from the surface as ionized species (Torgerson et al., 1974; MacFarlane and Torgerson, 1976; MacFarlane, 1982; McNeal and MacFarlane, 1981; Hakansson et al., 1982). After the initial report, it was soon realized that an essential feature of PDMS was that the deposition of energy is highly concentrated and that the excitation is very short-lived. This technique has been very important for the analysis of biological compounds.

In 1976, Benninghoven demonstrated that the mass spectra of amino acids derived from keV ions impinging on the surface of a thin film of the sample are essentially the same as those observed in ^{252}Cf PDMS (Benninghoven, 1976). This method, Secondary Ion Mass Spectrometry (SIMS), had been used routinely in surface analysis of inorganic species or organic

compounds but had never been applied to thermally labile biomolecules. So far, two types of SIMS have been developed. Atomic SIMS is used in surface analysis of inorganic materials under dynamic conditions. In this technique, high primary ion dose densities (usually $>10^{-6}$ A·cm^{-2}) at ultra-low pressure (ca. 10^{-10} torr) was used. Low ion fluxes ($<1 * 10^{-8}$ A·cm^{-2}) and low pressure ($< 10^{-5}$ Torr) are used in molecular SIMS to effect depth profile measurement. Most of the organic compounds were analyzed by molecular SIMS under static conditions.

In 1978, Posthumus et al. showed that excitation by short (< 10 ns) laser pulses created mass spectra that are essentially the same as in ^{252}Cf PDMS and SIMS (Posthumus et al., 1978). This third variant of DI technique is called Laser Desorption (LD).

The fourth variation, introduced by Barber et al. in 1981, uses a keV beam of neutral atoms for bombardment and is called Fast Atom Bombardment (FAB) (Barber et al., 1981a; 1981b). However, it was later shown that the use of atoms as opposed to ions was of little importance. Instead, what is significantly different about FAB is the medium from which desorption-ionization occurs; a liquid solution matrix. Since the development of this technique in 1981, several thousand papers dealing with FAB have been published. Today, FAB is used in routine analysis in most major mass spectrometry laboratories.

Since FAB has become such an important DI method in

analytical mass spectrometry and because the majority of this dissertation deals with the desorption process in FAB (see below), a detailed description of this technique will be given here.

Fast Atom Bombardment Mass Spectrometry

FAB is the most recent DI technique and has acquired the widest usage in the fields of analytical bioorganic and pharmaceutical chemistry. This is because of

1) quick and easy sample preparation
2) a relatively stable and persistent ion signal
3) high flexibility for the FAB source to add-on several types of mass spectrometers.

In FAB, the analyte is usually dissolved in a polar, viscous, low boiling point solvent such as glycerol, diethanolamine, ethylene glycol, and thioglycerol. The sample is then mounted on a probe that is introduced through a vacuum-lock assembly such that the sample surface rests at the focal point of the instrument.

The beam of fast atoms is produced by first ionizing the corresponding gas to produce ions and accelerating the ions (in the range of 6 to 10 keV) into a dilute gas where the fast ions capture an electron, thereby being converted from fast ions to fast atoms (Lew, 1976; Frank, 1983; Mahoney et al., 1983; Rudat and McEwen, 1983). FAB with xenon atoms gives the best spectra among those gases that have been studied (Morris

et al., 1983; Martin et al., 1982). The beam of bombarding atoms is usually maintained at a large angle relative to the axis of the beam of ions extracted by the ion optics. A typical incidence angle is between 45° and 70° (Martin et al., 1982). Many particles (ions and neutrals) are disrupted from the surface and are spewed over a wide solid angle. Positive or negative ions focused by the ion optics provide a glimpse of the process in the form of a mass spectrum. The ions available are by no means solely related to the analyte, even if pure. Many ions emanate from the glycerol or solvent itself. A diagram of the arrangement of the atom gun and sample probe in the mass spectrometer is illustrated in Figure 3(a).

The FAB technique has been successfully used in analyzing numerous biological and organic compounds (such as peptides, pigments, saccharides, polar lipids, nucleic acids and underivatized, polar, high-molecular-weight, nonvolatile organic synthetic compounds), however, the FAB mass spectrum does not always provide a simple straightforward indication of the molecular weight. Evidence for the intact molecule comes in the form of adduct ions consisting of the molecule together with a Na^+, K^+, or H^+. Dehydrated adduct ions frequently produce intense peaks also. A peak representing the molecular ion is rarely observed, as one might find in EI. Figure 3(b) is a typical FAB mass spectrum of a dipeptide (tyrosyl-arginine) in glycerol. The spectrum shows a peak for the

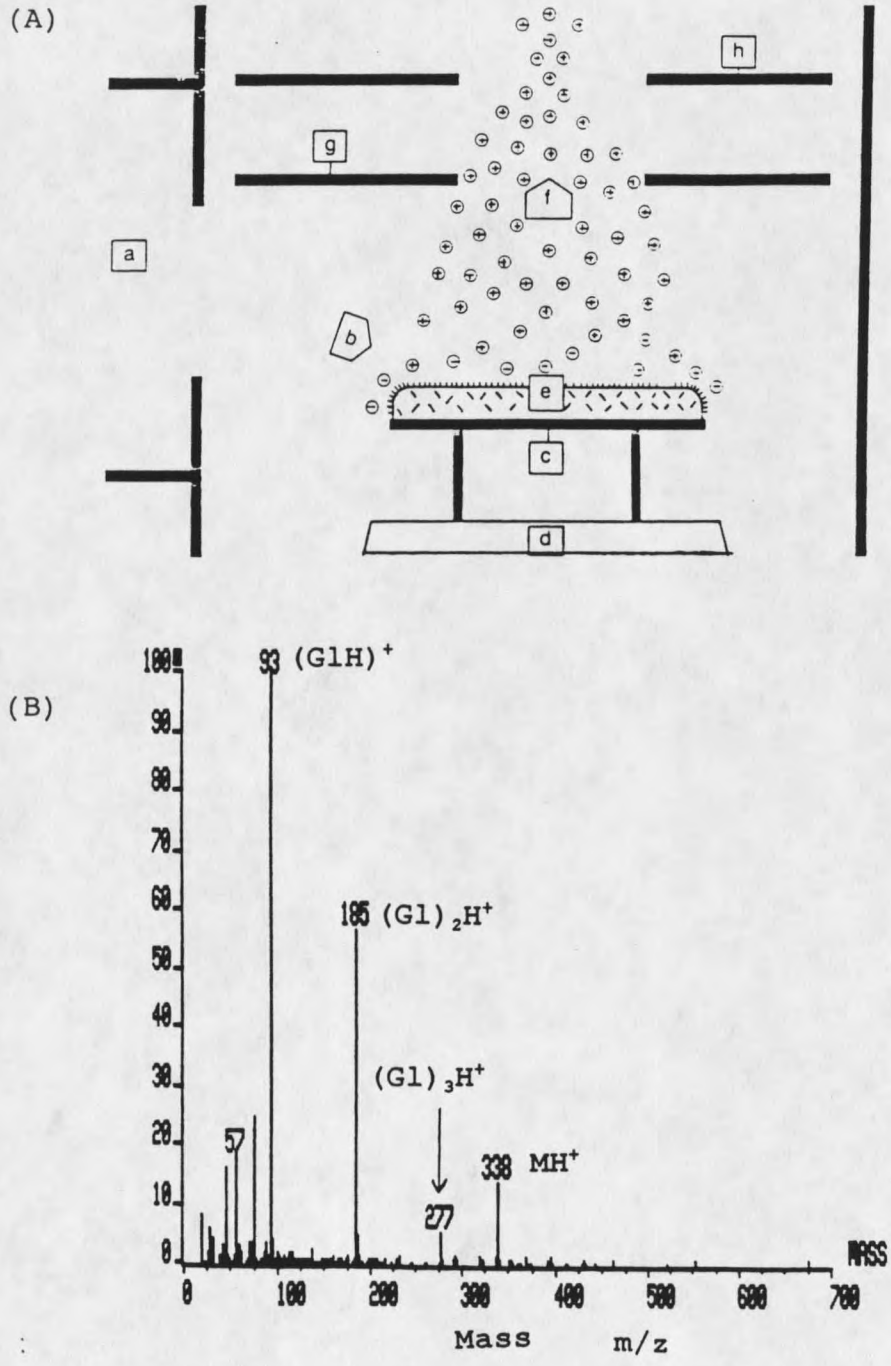

Figure 3. (A) Schematic diagram of the FAB source. (a) atom gun; (b) atom beam; (c) metal sample holder; (d) end of probe; (e) sample in low volatility solvent; (f) positive ion beam; (g) ion extraction plate; (h) lens system leading to the mass analyzer (revised from Barber et al., 1982). (B) FAB mass spectrum of 0.1 mol% dipeptide (tyrosyl-arginine) in glycerol.

adduct ion $(M+H)^+$ (also named pseudomolecular ion) at m/z 338. The ions at m/z 136 are fragments from the dipeptide. All of the other major ions arise from the glycerol matrix (major glycerol fragments: m/z 29, 31, 45, 57, 75; glycerol monomer: m/z 93; glycerol dimer: m/z 185; and glycerol trimer: m/z 277). The chemical noise, the low intensity background of ions occurring at every mass, which is characteristic in FAB mass spectra is also observed in this spectrum. As can be seen in Figure 3(b), the most useful information obtained from most FAB spectra is the molecular weight of the analyte. Usually limited information about the structure is obtained from a few ion fragments in the mass spectrum (only one fragment from the dipeptide is observed in the mass spectrum).

Recently, a number of studies using FAB/MS/MS have succeeded in deriving structural information from small molecules (e.g. peptides). In this technique, the intact protonated molecular ion produced in the ion source is selected by a first mass analyzer and then accelerated into a field free collision chamber. Many ions can be made to dissociate as a result of collisions with the neutral molecules (e.g. air or argon) preexisted in this region. The fragment ions generated by this process are analyzed by the second mass analyzer located after the collision chamber. Although this technique has been successfully used in analyzing small and simple molecules, large and complex compounds usually give very complicated fragment mass spectra

and it becomes very difficult to interpret the spectra.

FAB has been successfully used in qualitative analysis of many biological compounds. However, it is known for its lack of accuracy in quantitative analysis. It has been observed that in FAB mass spectra, the signal intensity from the analyte usually is not proportional to its concentration in the solution. The situation becomes worse when the sample contains more than one analyte. In many cases, it has been shown that with two analytes at equal-concentration, one analyte often dominates in the mass spectrum whereas the signal from the other analyte may show only weak intensity or totally disappear. Some analyte ions cannot compete with the ions formed by the matrix itself and are not seen in the FAB spectra. These suppression effects have restricted the development of FAB for quantitative analysis.

The research community has spent a great deal of energy in trying to solve practical problems encountered in FAB. From these studies, four major factors have been suggested as playing the main roles in determining good FAB spectra:

1) bringing the sample to the solution
2) bringing the sample to the surface layers
3) precharging the sample before the bombardment
4) choosing the right matrix

Later, each of these factors will be shortly discussed. There are also various theoretical studies on the fundamental mechanisms of the desorption ionization process in FAB.

Several of these studies and models derived from them will also be presented and discussed shortly in this section.

Bringing the Sample to the Solution

There is general agreement that secondary ion currents are stronger if the analyte molecule is actually dissolved, either in the matrix liquid or in a cosolvent, as opposed to being present as a suspension. It is thus an important task for the FAB practitioner to find a way to bring the analyte into solution in the matrix. Cosolvents such as water, methanol, chloroform and dimethyl sulfoxide have been used, miscible with the less volatile matrix solvents.

Bringing the Sample to the Surface

In many cases, ion currents are observed to increase when the analyte is enriched at the surface of the matrix. Experimental measurements are easily made on surface tension, and thus surface-active analytes have been most readily studied. Several approaches have been conducted to concentrate the sample in the upper layer of the matrix (Zhang et al., 1984; Ligon and Dorn; 1986a; Ligon and Dorn; 1986b) and have led to improvements in analyte-to-matrix signal ratio. For example, derivatization may increase the surface activity of the molecule, or one may add a surfactant with an opposite charge to bring the molecule to the surface through charge neutrality in the surface layers.

Precharging the Sample Before the Bombardment

The observation that the majority of the ions detected in FAB are pseudomolecular ions (i.e. $(M+H)^+$) suggests that they are formed before the bombardment. Most FAB practitioners have added some salts or acids to the sample try to increase the ratio of the precharged analyte molecules in the matrix. In some cases, the addition of acids or salts does increase the $(M+H)^+$ signal, however, in other cases the method fails. The overall effect of adding acids and salts to the sample is still unclear, however, the practice of using this strategy to enhance the precharged molecules still is very common and acceptable in routine FAB analysis.

Choosing the Right Matrix

Although all parameters used in controlling the primary beam and ion optics of the mass spectrometer are critical to obtain good FAB spectra, many of these parameters are not variable or even optimized on commercial instruments. However, it is easy to change the liquid matrix. Indeed, the choice of matrix in FAB can spell the difference between success and failure. The multiple contributions of the matrix have been discussed (dePauw, 1986; Fenselau, 1984; Todd, 1986, Todd and Groenewold, 1986). It has been suggested that the matrix should be chosen with the objectives of optimizing and persisting absolute secondary ion currents. Its selection can

also influence fragmentation and signal-to-noise ratios. According to the studies, several characteristics of the matrix such as viscosity, vapor pressure, and background contribution (i.e. chemical noise level) have been suggested as important factors in determining a good FAB mass spectrum (Falic, et al.,1986; Ligon, 1983a; Todd, 1986; Wong et al.,1986; Katz et al., 1986; Gower, 1985). From these studies, a general picture of a good FAB matrix in qualitative analysis can be given as follows:

1) the matrix itself should possess low volatility and enough fluidity to prolong the ion currents and the viscosity should not be too high to inhibit the self cleaning process (i.e. the radiation products formed by FAB are removed by the desorption process itself).
2) the matrix should be able to dissolve the sample well (i.e. bring the analyte molecule into the solvent) and also provide a precharged analyte molecule.
3) Compared to the matrix, the surface activity of a given analyte should be high.
4) A matrix is preferred which provides a clear window (i.e. low chemical noise level) in the mass range of analytical interest.

Only very few existing organic solvents match all the criteria described above (Cook et al., 1989). It needs to be mentioned here that the matrix selection is also highly dependent on the chemical properties of analyte itself. These criteria are the

reasons why, in many cases, the FAB practitioner must try several matrices to get a signal from an analyte. However, for some compounds, regardless of the choice of matrix, the desired analytical signal may still be totally missing. This was not understood until some of the researchers began to investigate the mechanisms of the FAB process.

Understanding the mechanisms of desorption-ionization is important not only from a theoretical point of view but also from the perspective of increasing the analytical utility of the method. To discuss the molecular SIMS and FAB mechanisms, atomic SIMS represents a useful starting point, since it provides a vocabulary and a theoretical foundation on which to build (Pachuta and Cooks, 1985). Three major mechanistic studies of atomic SIMS which address different aspects of atomic desorption will be outlined. The discussion will be followed by the models suggested for FAB and molecular and liquid SIMS.

Collision Cascade Model

The model involves momentum-transfer processes (Thompson, 1968; Sigmund, 1969; Sigmund, 1981). The primary atom enters a surface and gradually slows down as it strikes surface and substantial atoms until it has lost its excess kinetic energy. The collisions displace target atoms, as well as alter the initially linear trajectory of the primary ion. Recoiling target atoms can strike other atoms, and this so-called

"collision cascade" proceeds until the impact energy is dissipated in a volume radiating outward from the point of impact. In the course of the cascade, some atoms may acquire momentum in a direction toward the surface and, if the energy of such an atom is greater than the surface-binding energy, the atom will be emitted from the surface. In this case, the kinetic energy of the ejected atoms is usually high. The model was formulated by Sigmund and has received wide currency, primarily because it provides a quantitative basis for many observations. However, it is still the subject of intense debate and its restriction to binary collisions is thought by some to be an oversimplification (Cooks and pachuta, 1987).

Thermal Spike Model

This model explains the emission of low-energy and high-energy particles from the DI process and it is very useful in molecular SIMS (Kelly, 1977; Sigmund and Claussen, 1981). Kelly and Sigmund considered that bombardment of a material induces elastic collisions between atoms in the matrix, and this collision-induced excited region (the "slevedge") behaves much like a dense gas at high temperature. Emission of low kinetic energy particles occurs by evaporation from the "slevedge". Atoms with high-energy can be emitted by a direct recoil process which is similar to the processes suggested in the collision cascade model (Magee, 1983; Schultz et al.,

1983; Rabalais and Chen, 1986). This involves ejection of high-energy-recoil particles produced by direct momentum transfer from primary ions. The thermal spike model explains the emission of low and high energy particles, but cannot explain the emission of the vast majority of particles with intermediate energies.

Bond Breaking Model

This model is often invoked to explain ion emission from ionic compounds (Soldzian, 1975; Gnaser, 1984). A typical lattice (e.g. NaCl) will contain a valence band of anionic states and a conduction band of cationic states, separated by a band gap (e.g. 10 eV for NaCl) (Williams, 1979; Poole et al., 1975). According to this model, half of the lattice energy is consumed when a cation is removed, but in order to remove a neutral an electron has to cross the band gap and the atom must go to the gas phase, which is energetically less favorable. Then, for ionic compounds the emission of ions is preferred, when the lattice energy is much less than the band gap. The model can also be used to explain ion emission from covalent compounds. As long as there is some polar character, a band gap will exist, and ion emission will be favored if the lattice energy is much less than this band gap. While the bond-breaking model is appealing, it applies mainly to polar materials, and it fails to explain the enhanced emission of negative ions from oxygenated surfaces.

In addition to the main models, several other models have also been suggested. Some of them tried to improve the existing models and can only be applied to specific cases. These models include a "molecular model" (Thomas, 1977), "band structure model" (Van der Weg and Bierman, 1969; Kelly and Kerkdijk, 1974; Murray and Rabalais, 1981), "local thermal equilibrium model" (Andersen and Hinthorne,1973), "surface polarization model" (Williams and Evans, 1978), "local bond-breaking model" (Yu and Mann, 1986), "sudden perturbation model" (Krueger, 1983), and "electron-tunneling model" (Yu and Lang, 1983; Yu and Lang, 1986). Unfortunately, none of the above models can explain all the experimental results.

Molecular species were observed as contaminants in SIMS spectra. However, molecular SIMS did not evolve until after the development of the static SIMS method. As described before, the key innovation in static SIMS was the use of a low primary ion current density to minimize sample damage which is opposite to that in molecular SIMS. In the mechanism of molecular emission in SIMS, a first step might be to attempt to correlate molecular data with the wealth of atomic SIMS theory. There may be similarities between the processes resulting in atom and in molecule emission, but an energetic collision cascade alone would seem an improbable means by which to eject intact molecules, particularly large biomolecules. Most of the molecular SIMS models that have been advanced therefore incorporate a thermal component into

the mechanism. In the following discussion, several different views of molecular desorption will be described, beginning with the models most closely resembling those in atomic SIMS and then toward models focused mainly on FAB or molecular and liquid SIMS.

Classical Dynamics Simulations of Collision Cascade

A number of the computer simulations of desorption process in SIMS have been developed by Garrison and co-workers (Garrison and Winograd, 1982; Brenner and Garrison, 1986; Garrison, 1982; Garrison, 1983; Garrison, 1985). The simulations are based in large part on those first developed by Harrison (Harrison et al., 1968; Harrison et al., 1973; Harrison and Delaplain, 1976). It was found that some aspects of molecular SIMS can be explained by assuming a collision cascade model which is developed from atomic SIMS. In a typical calculation, parameters such as primary ion mass, energy, and angle, and the size, depth, and crystal structure of the target are first defined. Classical equations of motion are then applied to compute the position and momentum of each particle as a function of time (Harrison et al., 1978). The time scale is in femtoseconds, with molecular ejection usually occurring in less than 200 fs. Classical dynamics simulations have a number of obvious advantages and disadvantages. The major advantage is that it allows semiquantitative predictions of actual behavior, including the

species ejected and their energy and angular distributions. It is conceptually simple and has a basis in reasonably well-understood atomic sputtering theory. The disadvantage is that it is primarily a model for sputtering, and not for ionization; parallels must therefore be established between neutral and ion emission.

Preformed Ion Formation Model

The idea that precharged analyte ions are observed preferentially to ionized forms of the initially neutral analyte is the key to the preformed ion or precursor model (Day et al.,1980; Benninghoven, 1983a and b). Benninghoven, drawing chiefly from results for monolayers of amino acids on clean metal surfaces, describes this idea for pseudomolecular ion emission. In this model, Benninghoven suggested that an excited region (10-100 Å in diameter) is formed around the path of the bombarding particle, due to the dissipation of its kinetic energy. Very rapid energy transfer causes emission of the precursor ions from the surface, with the high probability of maintaining their charge state during the whole process. Fragmentation occurs in some cases and may result from transfer of a large amount of energy near the impact point or from gas-phase decomposition of an excited molecule.

Gas Flow Model

The essential part of this model is that gas may be

formed in the cavity (created by primary atom impact) as a result of the thermal spike effect. This gas may then flow from the cavity into vacuum and various chemical reactions may also occur during this process (Michl, 1983; David et al., 1986; Urbassek and Michl, 1987). The model was suggested by Michl et al. as follows: at very short times after primary ion impact ($< 10^{-12}$ s) collision cascades result in secondary ion formation, but at somewhat longer times ($> 10^{-12}$ s) thermal processes take on a dominant role. Ions arising from collision cascades are called "first batch" ions, while those emitted from thermal spikes are called "second batch" ions. A thermal regime is presumably created during quenching of the collision cascade as energy is transferred to the cold surroundings in the solid. As the thermal spike spreads, second batch particles are ejected in an "explosive expansion of high-pressure gas into vacuum". During this expansion, clusters can be formed by recombination, and molecular fragmentation can occur. Ionization is thought to originate in the spike also.

Vibrational Desorption Model

The model was developed by Cooks and co-workers (Unger and Cooks, 1981; Busch and Cooks, 1982; Cooks and Bush, 1983; Busch et al., 1983b; Zakett et al., 1981). On the basis of the observation that the mass spectra obtained by SIMS, FAB, LD, and PD are essentially the same, these authors suggested

that although the initial form of energy deposition is different among these techniques at some point, the energy should be present in a common form. This so-called "energy isomerization" has been proposed to involve energy transfer to low-energy vibrational and translational models. This causes heating and emission of electrons, photons, neutral molecules and ions. As in the gas flow model, the concepts of quasi-thermal emission and "selvedge" reactions (e.g. ion-molecular reaction) are thought important by Busch et al. (1983). The model also includes the idea that for organic samples examined under static conditions most fragmentation results from unimolecular decay of metastable ions in the free vacuum.

Droplet or Spray Model

The idea of this model originates from the high sputtering yields and the ejection of vibrationally cold cluster ions and pseudomolecular ions in FAB (Vestal, 1983; Wong and Rollgen, 1986). The model suggests the following sputtering mechanism: First, the incident particle penetrates into the liquid, probably with a mean penetration depth between 50 and 100 Å, and creates a collision cascade which contains dense gas. A high gas pressure is built up causing the ejection of large clusters of matrix and sample molecules originally from the dense cascade region. Later, the decomposition of these clusters produces the pseudomolecular ions. The unimolecular decay of the clusters also gives rise

to some vibrational cooling of the remaining molecules. Sputtering of radiation damage products also takes place. As for the ionization process, it is assumed that the clusters initially formed are randomly charged, and their rapid decomposition leads to the most stable ions. Therefore, the ion intensity distribution reflects the ion chemistry in solution.

Gas Collision Model

The model primarily deals with the sequential chemical reactions occurring in the gas phase in the collision cascade. It was suggested that the incident primary atom forms ionized fragments from matrix or analyte molecules in the collision cascade, and that these react to give protonated molecules and clusters through a sequence of proton transfer and clustering reaction in a dense gas type condition (Sunner et al., 1988a). The intensity of the intact molecules is then dependent on the gas-phase basicity not the liquid-phase basicity. A kinetic analysis by the authors showed that significant number of gas-phase collisions may occur. This also strongly indicates that some thermalization must take place. From the model a "residence time distribution" in the 10^{-10} to 10^{-9} second range for the ions in the "gas" was deduced. The best agreement with experiments was found for a distribution that was inversely proportional to time. This is also the expected distribution if ion-ion recombination is the dominant ion loss

mechanism.

Phase Explosion Model

In this model, the liquid to gas transition in the collision cascade is explained as a result of the liquid approaching the "limit of absolute instability" or "spinodal" state (Sunner et al., 1988b). The role of the collision cascade is to heat the matrix (thermal spike). As the liquid is heated rapidly in vacuum it penetrates deeply into the metastable region and approaches the state so called "spinodal". This is the limit of absolute instability since beyond the spinodal the pressure increases as the volume increases (at constant temperature). As a result, the liquid undergoes an irreversible expansion into a gas without the formation of vapor nuclei. Consideration of the energetics of the process showed that the exploding "gas" rapidly cools down and that for this reason extensive clustering must occur.

The phase explosion model offers a qualitative explanation for the extent of clustering in different matrices and suggests how thermally labile analyte molecules can survive the desorption process and also how extensive ion-molecule chemistry can occur in FAB.

In the next section, the objectives of the work in this thesis will be presented and discussed shortly.

Objective of The Thesis

Role of Preformed Ion Formation

It was shown by Sunner and Kebarle that solutions of diethanolammonium·hydrochloride (DEA·HCl) in glycerol, where DEA is precharged in the matrix, have nearly identical FAB spectra to solutions of neutral DEA in glycerol (Sunner et al., 1987). Further, when a salt such as KCl (dissociates in the matrix thereby increasing the concentration of precharged ions) was added into glycerol, the total ion current (TIC) was not increased (Sunner et al., 1986a). Such experimental evidence would seem to suggest that preformed ion formation is not very important in FAB. On the other hand, there are a large number of reports in the literature showing a much improved pseudomolecular ion signal in FAB when the analyte is preionized by adding an acid to the matrix. Also, sometimes when large molecules (e.g. bovine insulin) are desorbed in FAB under acidic conditions, multiply charged ions dominate over singly charged ions (Schronk and Cotter, 1986). This seems to imply that there even fewer neutral molecules are desorbed. Such results seem to favor a precursor ion formation model. To clarify the problem, systematic studies of the FAB spectra with the addition of acid into the matrix will be conducted.

Role of Surface Activity

It is clearly established that surface active compounds give a much enhanced signal in FAB. It was observed by Ligon

and Dorn that the signal intensity from a small inorganic anion can be enhanced by adding a positive charged surfactant. They suggested that because of the requirement of charge neutrality in the surface layers, the small anion will be brought up to the surface by the positive charged surfactant. This results in increasing the surface concentration of the anionic analyte and also in enhancing the signal intensity in FAB. However, the report was presented only in a very qualitative aspect. In this study, the role of surface activity has been examined with respect to the analysis of cationic analytes by the addition of negatively charged surfactants. Systematic studies of the FAB spectra with the concentration of the surfactant have also been conducted. Mass transportation process for the surfactants in FAB have been explored by varying the concentration of the surfactants and viscosity.

Viscosity of Matrix

As described before, viscosity is suggested to be one of the important factors in determining a good FAB spectrum. In a previous paper, Sunner et al. found that the intensity of analyte ions relative to matrix ions increased as the matrix temperature was increased (Morales et al., 1989). At the same time, fragmentation of the glycerol matrix decreased, clustering increased and there was a marked decrease in the chemical noise intensity, as measured in percent of TIC. A kinetic model for ion-molecular reactions in a high pressure

"gas" and the concept from the phase explosion model were used to explain the experimental results. In this study, further progress has been made in the clarification of temperature effects on the change of FAB spectra. Sensitivity and competition effects between alkali ions and tertiary ammonium ions have also been studied.

Molecular Dynamics (MD) Simulations for DI Processes

Garrison and co-workers pioneered MD calculation of molecular desorption by keV bombardment. They have studied metallic solids (Garrison, 1982), and molecules absorbed on metal surfaces (Garrison and Winograd, 1983). Momentum-induced desorption dominate both of these simulations. However, from the experimental results, a bulk desorption is believed to occur in FAB because of its high ion yield. Abraham et al. (1982) have performed MD simulation of spinodal decompositions by instantaneously dropping the temperature below the critical point. They found a characteristic pattern of "wave creation and growth" (Figure 4). This is very similar to the concepts presented in the "phase explosion model" by Sunner et al. (1988b). In this study, a two dimensional MD calculation of the bulk desorption processes has been performed. The goal of this program of MD simulations is to gradually "develop our intuition" about the bulk desorption process by performing increasingly realistic simulations.

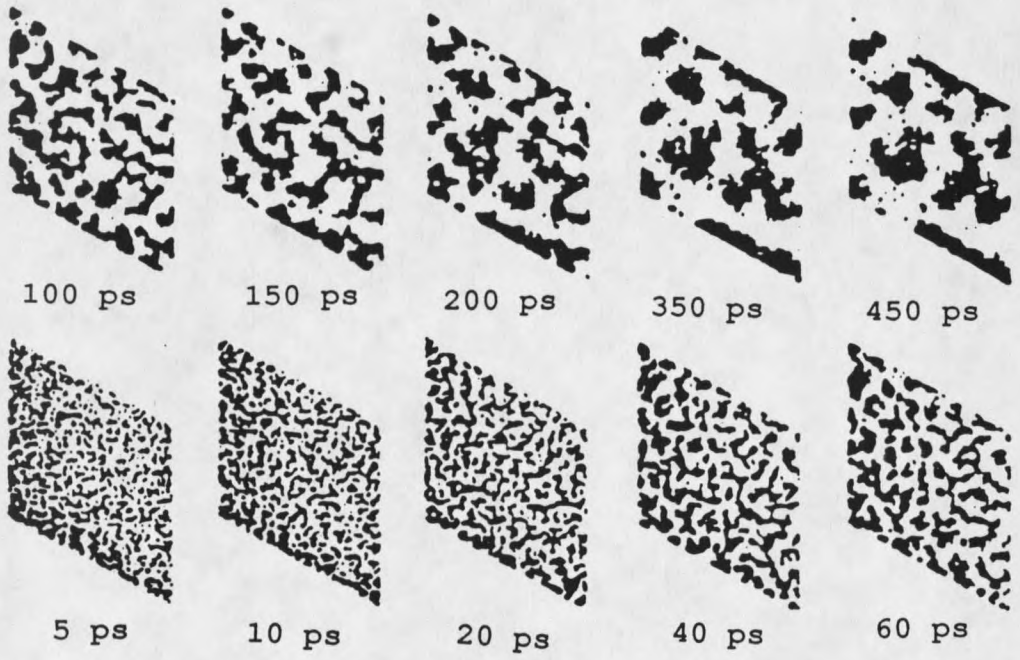

Figure 4. Snapshot pictures of the constant-temperature simulation for various times shown in picoseconds after the simulation (from Abraham et al., 1982).

MATERIALS AND METHODS

Mass Spectrometer

The experiments were performed on a VG 70E-HF mass spectrometer with a VG 11-250J data system. A schematic of mass spectrometer is shown in Figure 5. The accelerating voltage was 5,000 volts and the magnet was scanned from m/z 1,000 down to m/z 10 with a rate of 10 seconds per decade and 0.5 second for interscan delay time. The % of TIC of the ions from the first three mass spectra recorded were calculated and averaged by the computer data system. A computer program-Quattro Spreadsheet was used to evaluate the data. The mass resolution was usually set around 1,500. The mass spectra of neat glycerol and glycerol plus sodium or lithium were used for mass calibration. In one case cesium iodide was used for mass calibration.

Fast Atom Bombardment

The VG 70E-HF FAB source is equipped with a VG FAB insertion probe and a saddle-field FAB gun (Ion Tech. Co.). The FAB gun was operated with Xenon gas, a discharge current of 1.0 mA and voltage of 8 kV. The angle between the ion exit path and line normal to the probe tip surface is 20° and the angle between the exit path and the incident atom beam is 70°. The FAB probe was fitted with a VG FAB tip or a home-built copper-tip with a diameter of 6.5 mm.

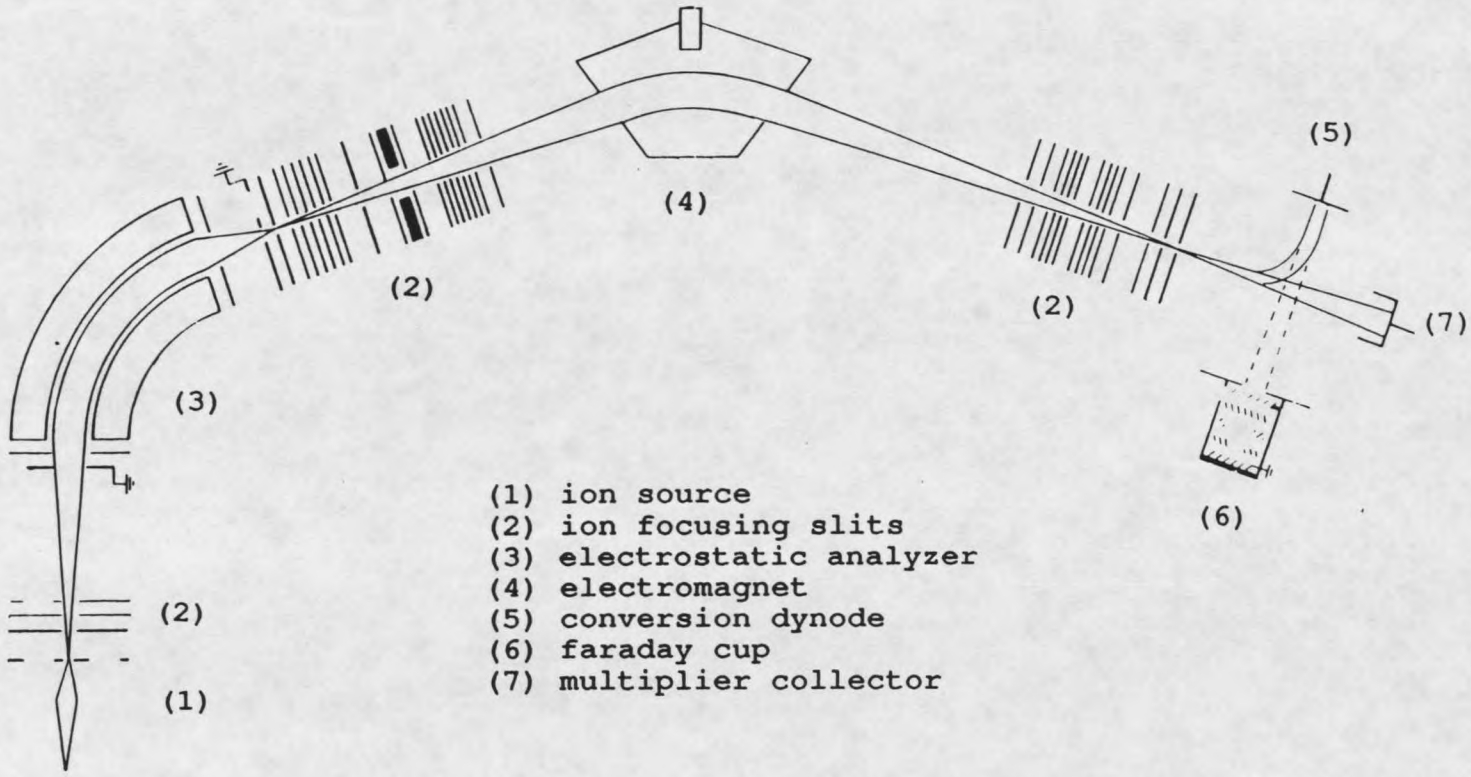

Figure 5. Diagram of a double focusing mass spectrometer (VG 70E-HF).

The temperature of the probe tip was measured in situ using a thermistor (Fenwal 30F1725, 10 kohm at 25°C) attached by epoxy to the inside of the probe tip and connected to the two electrical posts on the VG FAB probe. One of the posts also supplied the probe voltage (5000 volts). The thermistor resistance, R, was measured during the experiment with a volt-ohm-meter. Heat conduction from the copper probe tip to the probe rod was minimized by mounting the tip on a 1.5 mm diameter nylon rod. The probe tip temperature relaxed toward 30°C with a half life of ca. 40 min.. The calibration curve for R versus temperature was obtained from pure methanol and methanol/dry ice solution (temperature range: -60°C to 25°C) with a mercury filled thermometer.

Sample Preparation

The chemicals were obtained commercially (Sigma Co. or Aldrich Co.) and used without further purification. Samples were dissolved in the matrices by stirring and in some cases by gentle heating to produce supersaturated solutions. Glucose-glycerol solutions were prepared by heating and vigorous stirring. About 2 μl of solution was applied on the FAB probe tip for analysis. The viscosities of the solutions were measured by recording the rate of settling of a sphere (3 mm diameter glass beads) in a liquid (Daniels and Alberty, 1961):

$$\frac{dx}{dt} = \frac{2 * r^2 (\rho - \rho_0) * g}{9 * \gamma}$$

where dx/dt is the setting rate, r is the radius of the bead, ρ is the density of the sphere, ρ_0 is the density of the viscous medium, g is the acceleration of free fall and γ is the coefficient of viscosity. For temperature studies, the sample was cooled by immersing the tip together with the applied solution into a dry ice bath prior to FAB analysis. To prevent excessive condensation of moisture from the air on the FAB tip at low temperature, the tip was wrapped with alumina foil prior to cooling. After the sample became cold enough (ca. 10 min.), the probe tip was pulled out of the bath and the alumina foil was removed and the sample immediately inserted into the FAB source.

Tetraethanolammonium·bromide salt used in the surface activity study was synthesized by reflux distillation of triethanolammonium·chloride (50% by volume) together with 2-bromoethanol (50% by volume) in anhydrous methanol at 115 °C for 22 hours. Tetraethanolammonium·bromide was separated from the unused triethanolammonium·chloride by recrystalization in ethanol-methanol (4:1 by volume) solution. Tetraethanolammonium·bromide remained in crystal form in the methanol, it was then dried under vacuum by a rotary evaporator.

The absorption spectrum of the solution of porphyrin in thioglycerol was measured by a Cary model 14 spectrophotometer

scanning continuously from 850 nm to 400 nm.

Molecular Dynamic Simulation

The MD code used the leap-frog or Verlet scheme (van Gunsteren, 1988) with a timestep of 2 fs. The MD codes used in this calculation were written in BASIC language and were run on a PC-386 computer with a PC-387 coprocessor. The codes comprise three parts- initialization of the parameters used in the simulation (see Appendices, Figure 45), calculation for the new position and energy of each molecule after each time step (see Appendices, Figure 46), and color code of temperature for each molecule (see Appendices, Figure 47). Typically, a 16 ps MD simulation took about 60 hours and 25 megabytes of space in the computer.

THE ACID EFFECTS IN FAB

In FAB, it is well known that addition of acid to the sample frequently enhances the intensity of the pseudomolecular ion of many analytes. This effect will be referred to as the "acid effect". The common explanation for this signal enhancement is that the secondary ions produced in FAB originate from the preformed ion in the matrix, therefore, the analyte ion signal increases when more of the analyte molecules become "preformed" in the matrix on addition of acid (Pachuta and Cooks, 1987; Fenselau and Cotter, 1987; Detter, et al., 1988).

From published reports, the acid effect in solid SIMS is quite convincing. For example, Inchaouh et al. studied the MH^+ ion signal of nucleotides as a function of the Ph of the solution used to deposit the analyte on a silver foil. A sharp change in the MH^+ ion signal intensity around the pKa value for each analyte was found (Inchaouh, et at., 1984). Strong signal enhancement was also found when p-toluenesulfonic acid was added to zwitterionic compounds such as amino acids and aminohexanoate on silver (Benninghoven and Scichtermann, 1978; Busch, et al., 1982). A similar acid effect has also been observed in field desorption (FD) (Keough and DeStafano, 1981).

Although acids are often used to improve FAB mass spectra of many biological compounds (Martin, et al., 1982; Malorni,

et al., 1986; Gegarly, et al., 1989; Allmaier and Schmid, 1985), some experimental results are contradictory. For example, it was found that the addition of HCl, $HClO_4$ or H_2SO_4 to a solution of pentapeptide in glycerol did not significantly enhance the MH^+ signal in FAB (Malorni, et al., 1986). In another report, only a two-fold increase in MH^+ intensities were found for physalaemin when acids were added (Gegarly, et al., 1989).

Ligon and Dorn have argued that, at least in some cases, the acid effect has an explanation different from increasing preformed ion concentration (Ligon and Dorn, 1984b; 1988). They found that by adding a surface-active acid, the signal intensities of protonated analyte increased dramatically. They suggested that the analyte is brought up to the surface by the acid in order to maintain charge neutrality (Ligon and Dorn, 1984b). In contrast, they found that the analyte signal of surface active amines decreased with the addition of the acid! This was explained as a result of increasing solubility and decreasing surface concentration as the analyte is protonated (Ligon and Dorn, 1988).

In 1986, Musselman et al. published a very interesting study about the acid effect on porphyrins (Musselman et al., 1986). This paper is frequently quoted as supporting the preformed ion formation mechanism in FAB. In that study, porphyrin was first dissolved in dichloromethane. This solution was then mixed with thioglycerol. The concentration

of protonated porphyrin at different Ph was measured by visible absorption spectroscopy. A qualitative correlation was found between the intensity of the pseudomolecular ion in the FAB mass spectra and the concentration of protonated porphyrin in the matrix. However, no quantitative correlations were presented.

The experimental evidence for the acid effect may be summarized thus: in solid SIMS, the evidence seems strong. Very large effects are observed and preformed ion formation would seem to be involved. In FAB (or liquid SIMS), however, the situation is not all that clear. Although the addition of acids is frequently beneficial in practical analysis, different studies have given very mixed results. This study, has critically investigated the acid effect for a wide range of analytes and experimental conditions. A major reason for the study was to determine the practical use of acids and bases in FAB and to have some guidance to the physical basis of observed and expected effects. During this work, a number of different reasons for the FAB acid effect were identified. These different explanations will be discussed individually and be illustrated with specific examples.

Improved Solvation of Analyte

As described before, well solvated analyte molecules are essential for an intense and long-lasting FAB signal. The situation is often attained by first dissolving the analyte in

a co-solvent. The co-solvent is usually volatile and quickly evaporates after the sample has been inserted into the vacuum, leaving a supersaturated solution of analyte in the matrix (Junker, et al., 1989). Water, methanol and dichloromethane are common co-solvents used in FAB. In the absences of a co-solvent, a supersaturated analyte solution can also be made by gentle heating.

Figure 6 is a simple but dramatic illustration of the importance of analyte solvation. The figure shows the effect of adding HCl to (a) an equilibrated suspension of 1.7 mol% adenosine in glycerol and (b) the same mixture as in (a) but prepared in an acid-free supersaturated state by heating. The dramatic enhancement observed for the suspension continues until the sum of the analyte signal is brought to the same level as in the supersaturated solution. In this case, the main effect of the acid is to improve the solubility of the analyte molecules in the matrix. In comparison, any preformed ion formation effect must be small.

The study of the acid effect with porphyrins by Musselman et al. (1986) was mentioned above. Based on the simple adenosine results, it is speculated that solvation and solubility of porphyrins in the solution may also be important factors, especially since the problems with bringing porphyrin molecules into solution are well known (Smith, 1975). For this reason, extensive experiments with porphyrin were conducted. Figure 7 shows a simple and convincing result for

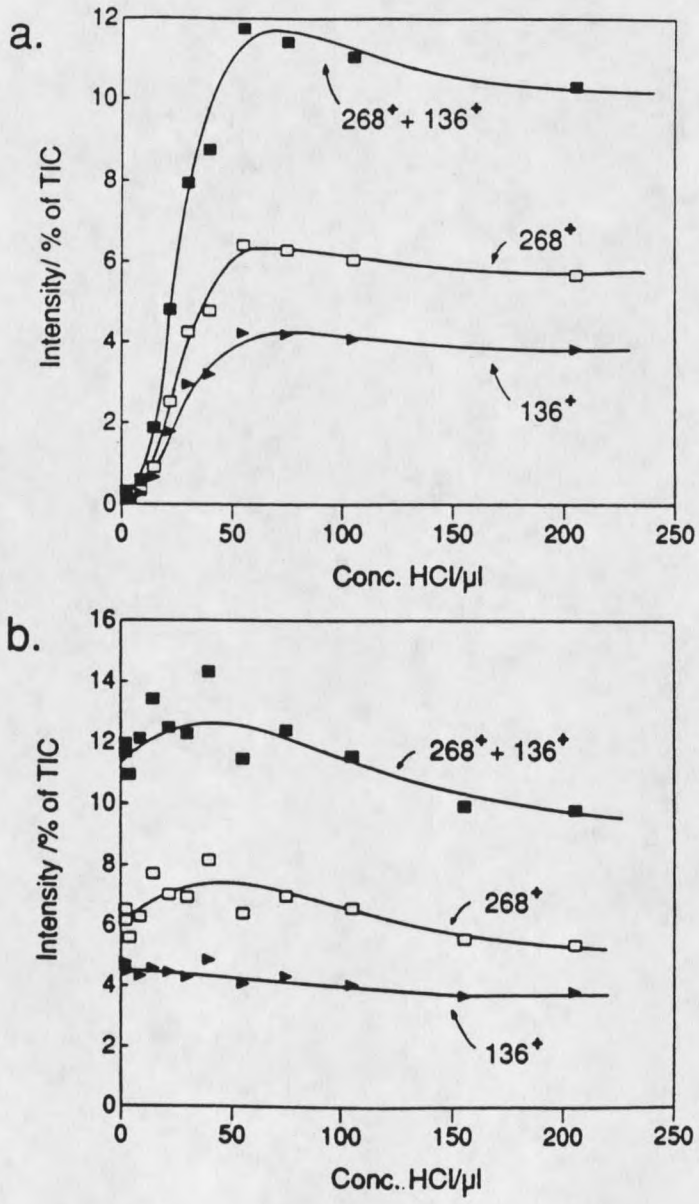

Figure 6. (a) Effect of adding concentrated HCl to an equilibrated suspension of adenosine in glycerol with nominal concentration 1.7 mol%. The MH^+ ion at m/z 268 and the only major fragmentation at m/z 136 are shown. A 15.3 µl volume of acid is equimolar with the amount of adenosine. (b) Same as (a), but homogeneous (supersaturated) solution was achieved by heating prior to acid addition.

octaethylporphyrin (MW 534.5). As did Musselman et al., it was found that the use of dichloromethane as a co-solvent in the analysis of porphyrin gave a good FAB signal (Figure 7(a)). Addition of trifloroacetic acid further increased the signal to give a spectrum similar to that shown in Figure 7(b). However, this spectrum was really obtained from a supersaturated solution, without added acid, and made simply by gentle heating a porphyrin suspension in thioglycerol. It should be mentioned here that when adding the trifloroacetic acid, the color of solution changed from red to pink. This is due to the transition of porphyrin molecules from partial to full protonated form (Musselman et al, 1986). Color change (reddish) was not observed in the solution before and after heating. This suggests that the amount of protonated porphyrin molecules does not increase even after heating. Addition of trifluoroacetic acid into this supersaturated solution changed the sample color from red to pink but had no further effect on the intensity of the porphyrin ion in FAB mass spectrum. The examination of the visible absorption spectra of these samples with and without adding acid confirmed this conclusion (Figure 6(c) and (d)). This simple result shows that the acid effect observed with octaethylporphyrin is indeed a solubility effect and not a preformed ion formation effect.

The fact that the co-solvent method did not yield the full mass spectrum signal as obtained from the supersaturated

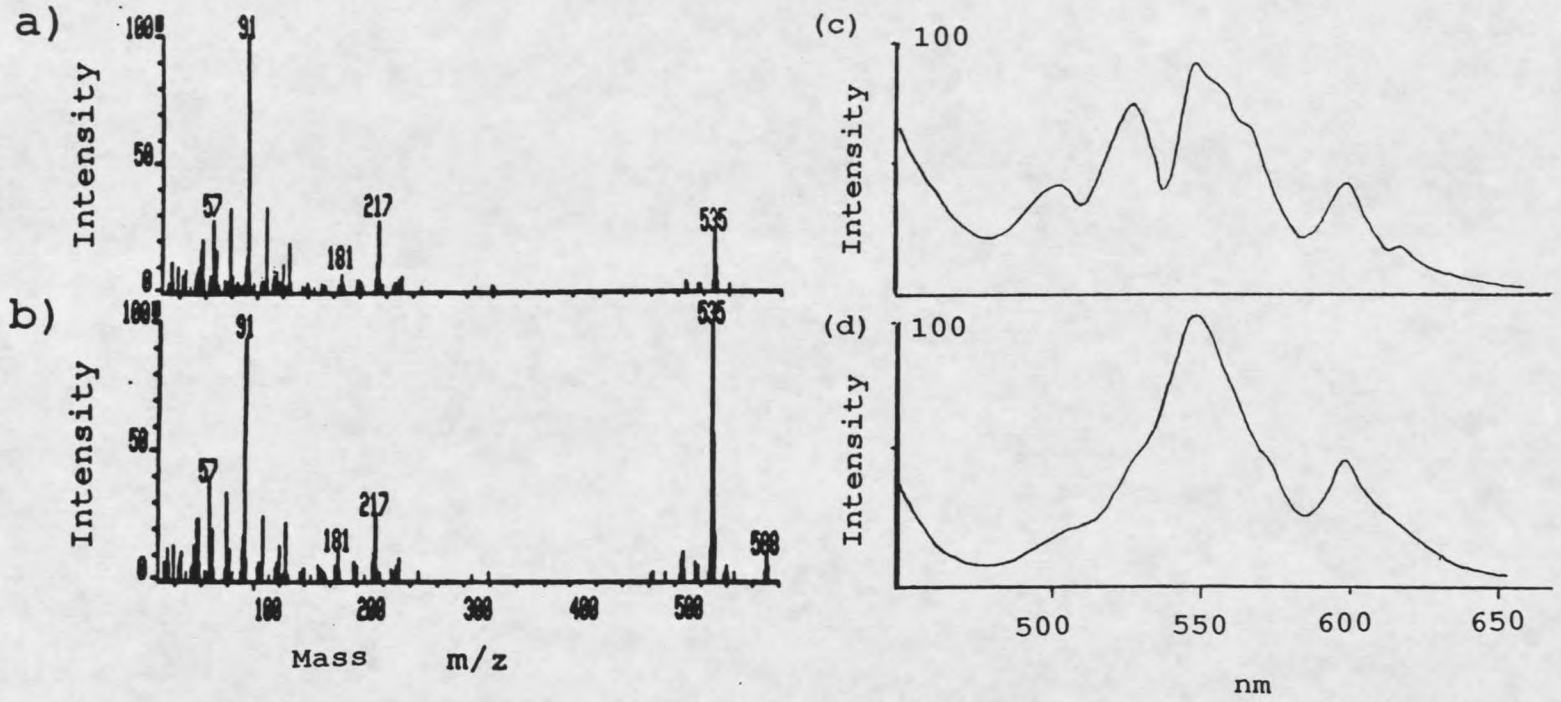

Figure 7. (a) Positive-ion FAB mass spectrum of a 0.005 mol% solution of octaethylporphyrin in thioglycerol prepared by using methylene chloride as a co-solvent. (b) Same as in (a) but solution prepared by gentle heating. (c) Visible absorption spectrum of the samples as in (a) and in (b). (d) Same as in (c) but trifluoroacetic acid was added.

solution indicates that some of the porphyrin molecules are still in a non-solvated form (aggregates). Apparently, they become solvated when acid is added. The aggregation process of a analyte in a supersaturated solution may be expressed by the following reaction sequence.

$$M+M=M_2;\ M_2+M=M_3;\ M_3+M=M_4;.....$$

If the degree of supersaturation is high enough, this aggregation process may occur without an activation energy barrier (Gunton and Droz, 1983). The diffusion-limited rate constant in glycerol is $5x10^6$ $l \cdot mol^{-1}s^{-1}$ with a diffusion constant of 10^{-8} cm^2s^{-1}. Thus, for a 0.1 M solution, the half-life of M would be only ca. 1 μs! Hence, we must be aware of the possibility that extensive formation of analyte aggregates occurs seconds after the co-solvent has evaporated in the vacuum system of the mass spectrometer. Adding acid into the solution blocks the aggregation if the solubility increases sufficiently.

Other interesting results presented here are obtained by using magic bullet (dithioerythreitol/dithiothreitol, 3:1 by weight) and diphenylmethane as matrices. Porphyrin samples (offered by Dr. Czuchajoaski in University of Idaho) dissolved well in both matrices (without the help of heating, acids, or co-solvent). However, in magic bullet a green and in diphenylmethane a reddish solution was obtained. After addition of acid, the diphenylmethane solution turned green.

This means that the porphyrin molecules were protonated in magic bullet but not in diphenylmethane. Even in such different conditions, similar mass spectra were obtained (data not shown) of the porphyrin MH^+ ion from both samples. Again, this suggests that preformed ion formation in FAB may not be so important.

Change in Surface Activity

Ligon and Dorn have investigated acid and base effects on organic amines and carboxylic acids. In their particular studies, they concluded that it is surface activity instead of preformed ion formation that affects the pseudomolecular ion intensity of analytes (Ligon, 1983b; Ligon and Dorn, 1984b; Ligon and Dorn, 1986a). Here, experimental results are reported for a few common biological analytes such as amino acids and peptides.

Figure 8 shows the result of adding concentrated HCl to a solution of the tripeptide Prolyl-Leucyl-Glycine (pro-Leu-Gly) in glycerol. In Figure 8(a), the MH^+ signal is seen to decrease slightly whereas the glycerol signal (GlH^+) increases. This is a clear indication of decreasing analyte concentration at the surface of the matrix. The decrease in analyte signal becomes more pronounced when two other major analyte ions, m/z 70 (major fragment ion) and $[MH+12]^+$ (a product of radiation-induced chemistry), are also considered. The tripeptide possesses highly hydrophobic branched groups

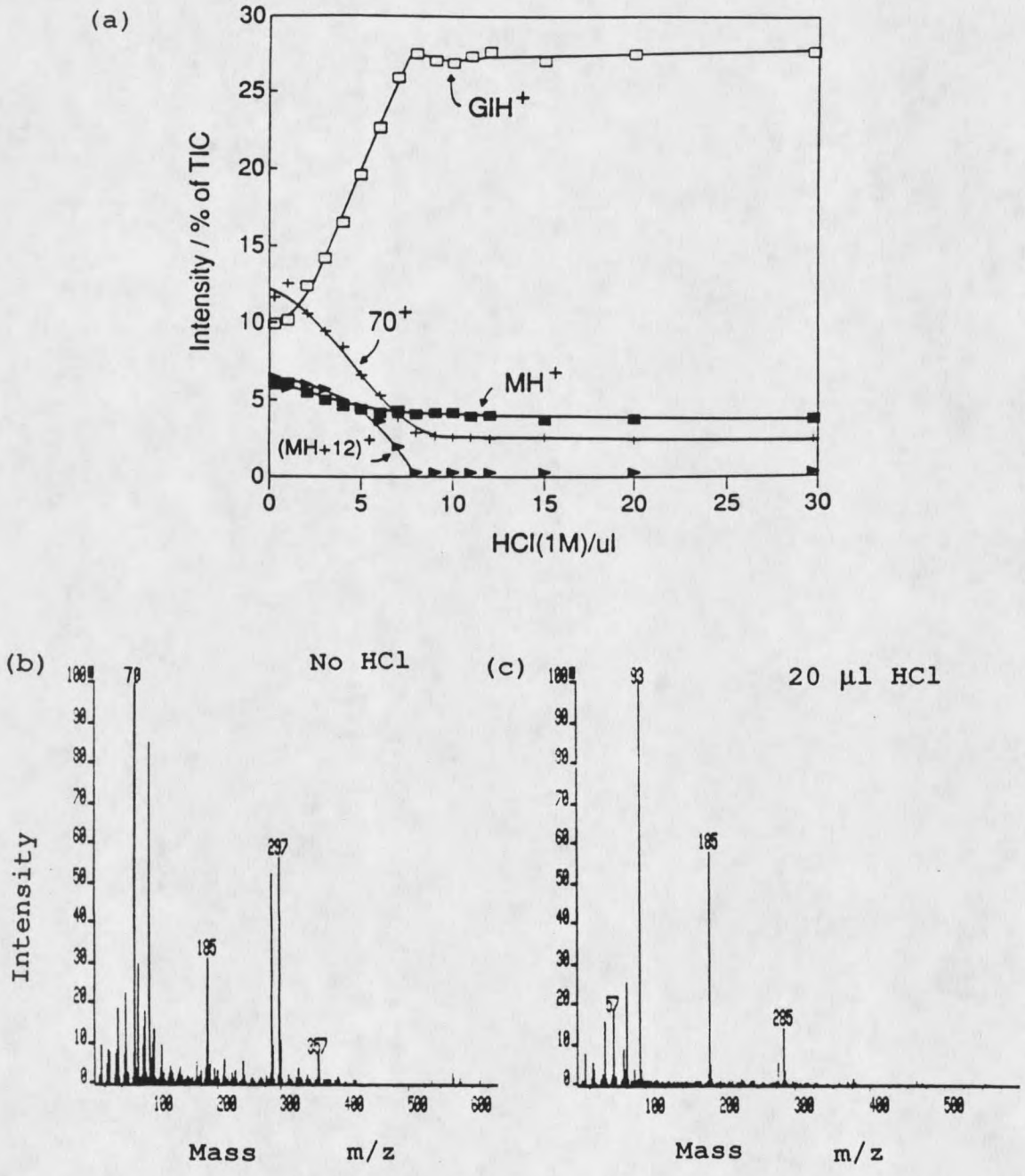

Figure 8. (a) Effect of adding HCl to a 0.1 mol% solution of the tripeptide Pro-Leu-Gly in glycerol. The intensities of three main analyte ions MH^+ (m/z 285), $[MH + 12]^+$ (m/z 297) and m/z 70 in addition to protonated glycerol (GlH^+) (m/z 93) are shown. A 10 µl volume of acid is equimolar with the calculated amount of tripeptide. (b-c) Mass spectra of 0.1 mol% Pro-Leu-Gly in glycerol obtained with and without adding acid.

and should be a good surfactant. After protonation, the peptide should lose some of its surface activity and the concentration of analyte in the surface decrease. This result is analogous to those of Ligon and Dorn (1988) for organic acids and bases.

Figure 9 shows the results of adding p-toluenesulfonic acid (p-TSA) or HCl to solutions of phenylalanine and of glycine (0.1 mol%) in glycerol. It is seen that the pseudomolecular ion signal from the hydrophobic phenylalanine was enhanced by about 9 times when p-TSA was added but was increased only slightly on adding HCl. In contrast, the signal enhancement on adding p-TSA to the hydrophilic glycine was very small (Figure 9(a)).

The relatively small acid effect for the hydrophilic glycine in Figure 9(a) is expected (acid prevents the formation of aggregates) for a non-surface-active compound. However, the strong positive acid effect for phenylalanine is surprising. Phenylalanine is the second most surface-active amino acid (Bull and Breese, 1974), it is significantly enriched at the matrix surface before the bombardment. Addition of acid would be expected to decrease this enrichment, resulting in a decreased signal. In trying to explain this result, several factors must be considered. First, acid addition and the nature of the counter ion will influence the degree of surface enrichment of the analyte (Cooks et al., 1989). Second, it is possible that preformed

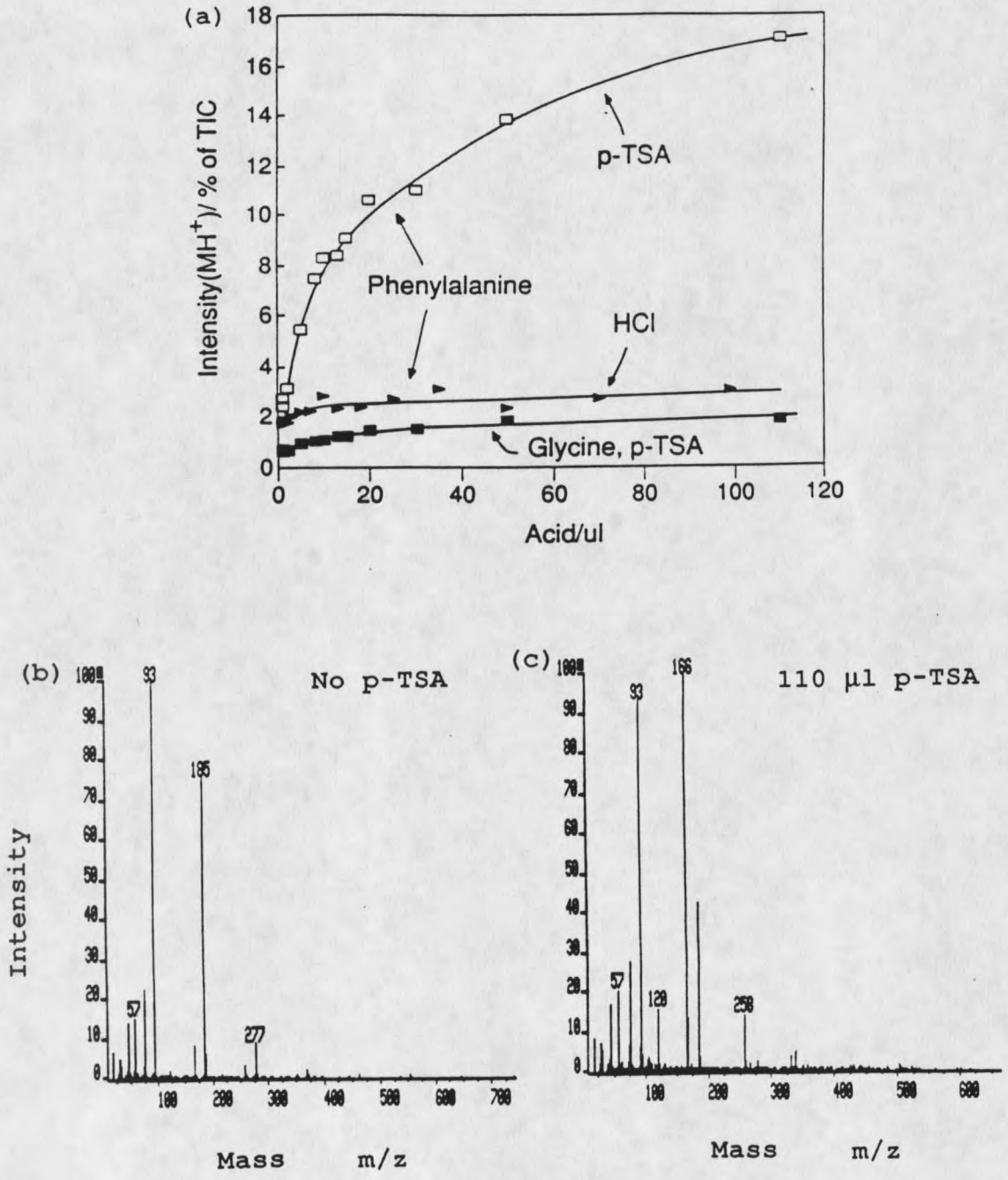

Figure 9. (a) Effect on MH^+ intensity of adding p-TSA or HCl to (separate) 0.1 mol% solutions of the amino acids, glycine and phenylalanine, in glycerol. Acid concentration 1 M in water. A 10 µl volume of acid is equimolar with the amount of amino acid. (b-c) Mass spectra of 0.1 mol% phenylalanine in glycerol obtained with and without adding acid.

ion formation is more important in the uppermost surface layer (< 5 Å) than in the bulk. Third, the chemical environment of the analyte changes which may significantly affect the degree of ionization. In considering all three factors, two different kinds of explanations can be invoked to resolve the problem described in last paragraph. The first explanation focuses on concentrations. Possibly the addition of acids really does increase the surface concentration of phenylalanine. It should be remembered that the amino acids are zwitterionic. The associated strong solvation tends to destablize the amino acid in the surface. Once protonated, only the positive charge remains on the amino acid and an increased surface concentration could possibly result. However, an increase in surface concentration, as the result of protonation, must also depend on the counter ion introduced with the acid. Experimental results suggest that an amphophilic counter ion would be required, such as that provided by p-TSA, to draw the protonated amino acid to the surface. This is supported by the experimental results presented in Figure 9. As the comparison with HCl results shows that the analyte signal is enhanced much stronger in p-TSA (an amphophilic acid).

The second explanation invokes preformed ion formation. Preformed ion formation seems to be unimportant for non-surface-active compounds. However, it is possible that for analytes in the uppermost surface layer (< 5Å), the charge

state is indeed important. In this picture, addition of p-TSA does not significantly increase the surface concentration of phenylalanine, but a larger fraction of the analyte molecules in the surface are in the protonated form.

When the dipeptide Glycyl-Phenylalanine (GP) was used as the analyte, the result was similar to that obtained with phenylalanine (Figure 10). For this sample, a stronger hydrophilic acid (4-hydroxylbenzylsulfonic acid; HBSA) was also used. The MH^+ ion signal is seen to increase only by a factor of 2 in HBSA. It is reasonable to attribute the difference in the enhancement of the MH^+ intensity between the addition of p-TSA and HBSA to surface activity. Deprotonated p-TSA is expected to be amphophilic whereas deprotonated HBSA should be hydrophilic. Thus, with the addition of p-TSA, the protonated GP molecules may be enriched in the surface in order to maintain charge neutrality, as suggested by Ligon and Dorn (1988). This interpretation is supported by the observation that in the negative-ion spectrum, the intensity in percent of TIC of the deprotonated p-TSA behaves similar to that of dipeptide signal in the positive ion spectrum.

As was the case with phenylalanine in Figure 9(a), an alternative explanation seems possible for the dipeptide (GP) in Figure 10. Because of the hydrophobic side chain, the dipeptide is expected to be somewhat surface active and thus enhanced in the surface layer prior to acid addition. One may then speculate that addition of p-TSA has the effect of

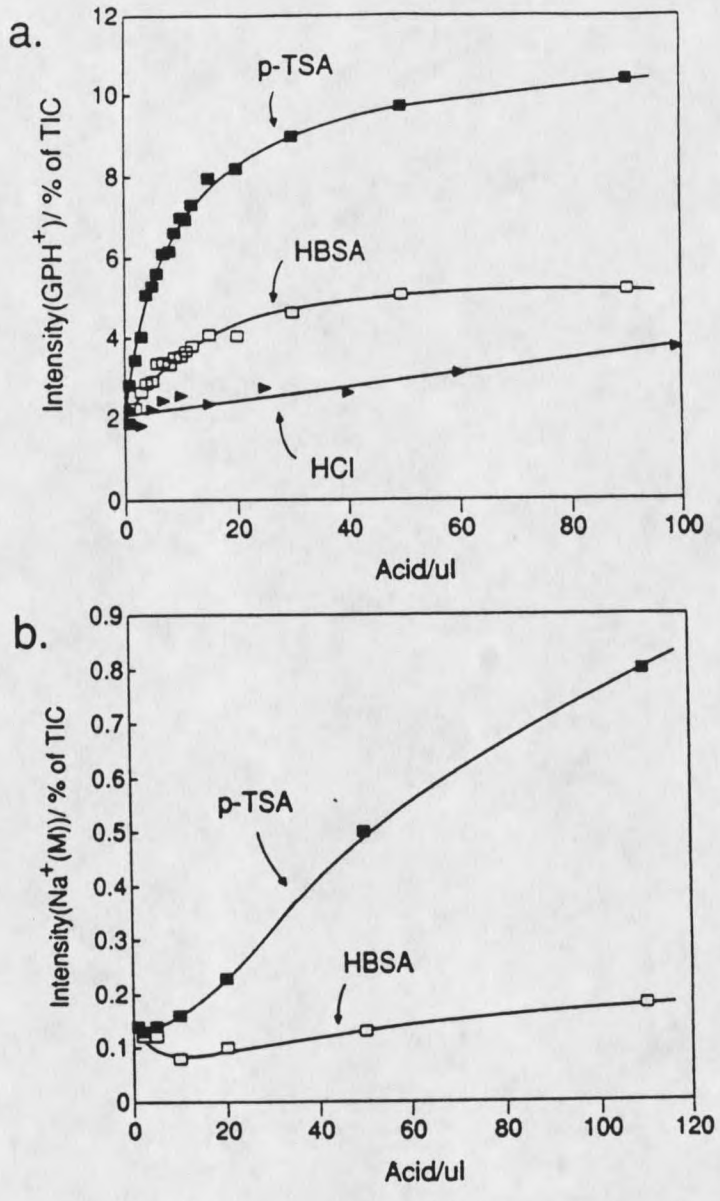

Figure 10. Effect on GPH^+ intensity of adding p-toluene-sulfonic acid (p-TSA), 4-hydroxylbenzylsulfonic acid (HBSA) and HCl to a 0.1 mol% solution of Gly-Phe in glycerol. Acid concentration, 1 M. A 10 µl volume of acid is equimolar with the calculated amount of dipeptide. Additional p-TSA or HBSA results in a decrease and an increase, respectively, in the GPH^+ intensity. (b) The Na^+ probe; effect of adding p-TSA and HBSA to a 0.1 mol% solution of Gly-Phe that has been spiked with 0.15 mol% NaCl. The intensity of $[GP + Na]^+$is shown.

protonating the analyte in the surface. Because of the amphophil nature of deprotonated p-TSA ions, the composition of the surface layers is not much disrupted. In contrast, because of its hydrophilic properties, the deprotonated HBSA molecules cannot protonate the analyte in the surface layers significantly. With HCl, both the protonated analyte and its counter ion are no longer surface active and are able to diffuse freely through the matrix.

A different strategy towards the understanding of the acid effect in Gly-Phe is to use a "sodium probe". Here, a small amount of NaCl (0.15 mole%) is added to the sample solution. The idea is that if the surface concentration of the analyte increases with addition of acid, it should be reflected in an increase in the intensity of the $([Gly\text{-}Phe]+Na)^+$ signal at m/z 245. It is seen in Figure 10 that the signal from this particular ion does increase upon addition of p-TSA but that there is no such effect upon addition of HBSA.

Radiation Chemistry

It has been shown that extensive radiation induced chemical reactions occur during the FAB processes (Field, 1982; Keough et al., 1987; Hand et al.,1987). It seems that many radical species are formed from the impact of a primary atom. These react with matrix or analyte molecules to form new radical species and remain in the matrix. For primary and secondary amines, ions such as $[MH+12]^+$, $[MH+24]^+$... are

frequently observed (Pang et al., 1984; Dass and Desiderio, 1988). Structure of these ions has been suggested as an iminium ion $-NH^{+}=CH_2$ by Pang et al. (1984), but the mode of its formation remains unknown. When neat glycerol was used as the sample in FAB, several large radical compounds were found. Keough et al. suggested that these compounds were formed by the reactions among several carbon-centered radicals and the glycerol molecules (Keough et al., 1987).

The formation of radiation products may interfere in identifying the analyte molecular ions in the mass spectra. An example is given in the mass spectrum in Figure 8(b) and (c). Without knowing the structure of the analytes one might select m/z 297 as MH^{+} ion but that peak is actually the $(MH+12)^{+}$ ion. The MH^{+} ion of this tripeptide (Pro-Leu-Gly) is formed at m/z 285. Fortunately, the intensity of the radiation product is seen to decrease abruptly and reach zero when an equimolar amount of the acid (e.g. HCl) has been added (Figure 8(a)). The most likely explanation is that protonation protects the amine group from attack by the radicals in the matrix. The protective effect of protonation may indeed be very common for peptides. The protective effect shown here is contrary to the observations by Biemann and co-workers (Pang et al., 1984). A possible explanation for the discrepancy is that for their particular analytes the HCl evaporated in the vacuum chamber.

Additional support for the protective effect of

protonation comes from experiments concerning the importance of viscosity on the FAB spectra of diethanolamine (DEA) and diethanolammonium·hydrochloride (DEA·HCl). In these experiments, the viscosity of a 2 mol% DEA solution in glycerol was varied by changing the temperature. As we know, changing viscosity will change the rates of the different transport processes in the liquid/vacuum interface and here serves to highlight the effect of the acid. Figure 11(a) shows the viscosity dependence without adding acid and Figure 11(b) with an equimolar amount of HCl. The radiation products include four of the major even-mass peaks above MH^+, i.e. $(MH+12)^+$, $(MH+24)^+$, $(MH+42)^+$ and $(MH+54)^+$. Without adding acid, it is seen that the radiation product intensity increases substantially up to about 10^4 cP and then again decreases. This maximum for the radiation products is reflected in a corresponding minimum for the $DEAH^+$. With added acid, the initial radiation product intensity is considerably lower and there is only a slow, gradual increase. This is evidence that protonation prevents DEA from radical attack.

The results and interpretations above underscore that collision cascade-induced radiation chemistry may be the major drawback for FAB as an analytical method. In addition to causing most of the chemical background that appear at almost every mass, it also may chemically modify most of the analyte. Protonation and use of matrices that are radical quenchers,

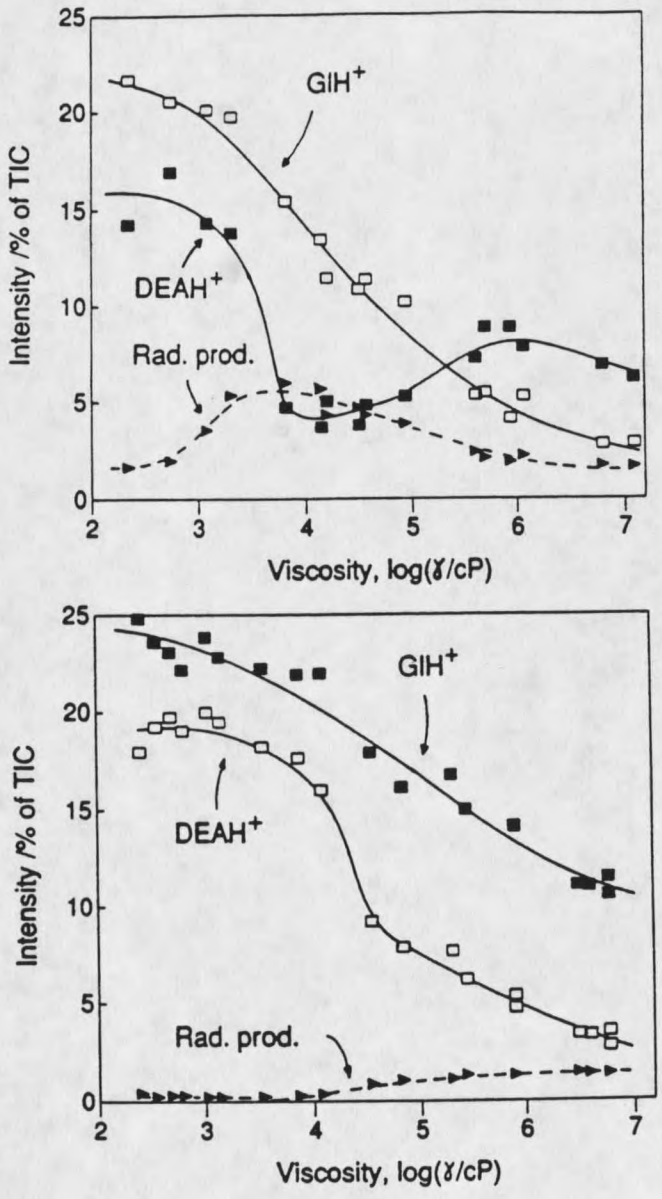

Figure 11. (a) Intensities in FAB mass spectra of 2 mol% diethanolamine (DEA) in glycerol as a function of matrix viscosity. The viscosity was varied by changing the temperature of the FAB probe. Radiation products include ions at m/z 118, 130, 148 and 160. (b) Same as (a) but with an equimolar amount of HCl added to the DEA.

such as thioglycerol, are only stop-gap measures; it is an important goal in analytical mass spectrometry to modify FAB or to replace it with another method that does not suffer from this problem.

Evaporation Effects

Figure 12 shows that with the addition of HCl, the analyte signal from N,N,N',N'-tetramethylethylenediamine (TEMED) in glycerol increases dramatically. Under vacuum, involatile analytes become enriched in the surface layers as the matrix evaporates. The phenomena becomes particularly obvious when a fairly volatile matrix such as thioglycerol is used. However, if the volatility of the analyte is larger than that of the matrix, the surface concentration of analyte will decrease under vacuum and thus the ion signal should decrease. Neutral TEMED is relatively volatile (b.p 120 °C), but protonation significantly increases the interaction between analytes and matrix molecules, thus lowers the volatility and so results in an increased ion signal. Similar results have been found for volatile pyridines and anilines (data not shown).

Desorption Energetics

Figure 13 shows that fragment (m/z 136) to pseudomolecular ion (m/z 268) ratio for adenosine in glycerol initially decreases as concentrated HCl or HBr is added.

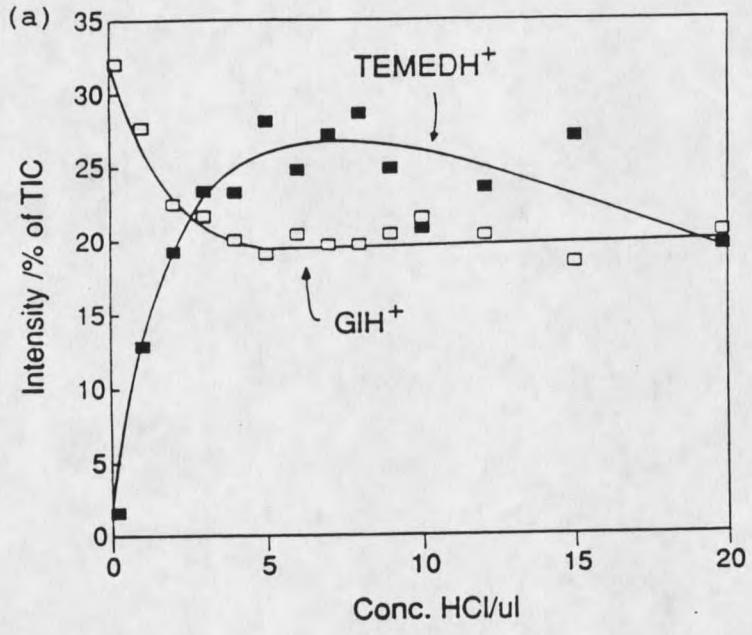

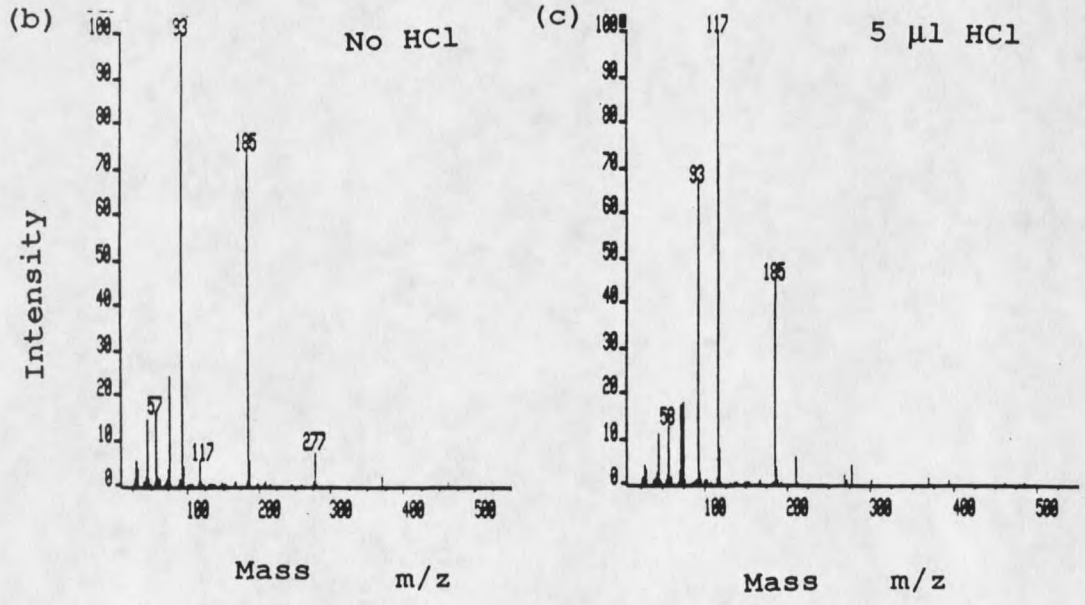

Figure 12. (a) Effect of adding concentrated HCl to a solution of 1 mol% tetramethylethylenediamine (TEMED) in glycerol. The intensities of $TEMEDH^+$ and of GlH^+ are shown. An 8.2 µl volume of acid is equimolar with the amount of TEMED. (b) Mass spectra of 1 mol% TEMED in glycerol obtained with and without adding acid.

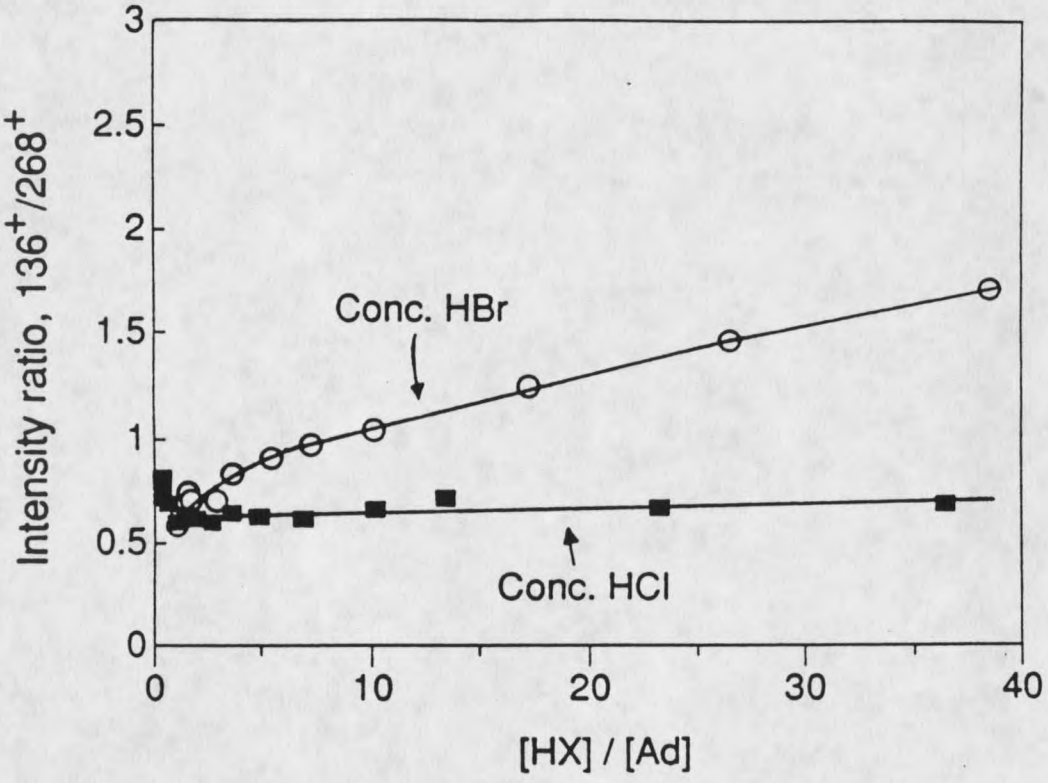

Figure 13. Effect of acid addition on adenosine fragmentation. Ratio of fragment ion at m/z 136, to the pseudomolecular ion, MH^+, at m/z 268 as a function of added acid (μl).

However, this effect is relatively small compared with the subsequent increase in fragmentation as more Hbr is added. The small effect for HCl is probably due to evaporation of HCl in the vacuum chamber. Similar results have been reported by Naylor and Manet (1989). In their experiments, a dramatic increase in the percentage of fragment ions of polypeptides-angiotosin, bradykinin and kemptide was found after addition of H_2SO_4 or $HClO_4$. In general, such a behavior is not

unexpected; a high concentration of acid changes the thermodynamic properties of the matrix and this will influence the energetics of the desorption process (Sunner et al.,1988c).

Preformed Ions

As outlined in the discussion above, a strong acid effect is frequently encountered in FAB. However, in all cases that this study has addressed, and resolved unambiguously, an explanation different than efficient preformed ion formation was found. For non-surface-active compounds there is, at the most, a slight tendency for protonated bases to have a higher sensitivity than the corresponding neutral bases. This can be seen for DEA in Figure 11, for example. This, however, could equally well be due to a slight increase in the surface concentration as a result of protonated DEA being less volatile. For surface-active compounds, the situation is not so clear; it is possible that preformed ion formation is important in the outer-most surface layers as outlined under "change in surface activity". Schronk and Cotter (1986) observed that multiply protonated insulin molecules are obtained from glycerol solutions only when strong acid was added. This constitutes possibly the strongest support to date for preformed ion formation in FAB.

In a strict sense, preformed ion formation must occur in FAB. Alkali and quaternary ammonium ions certainly exist as

preformed ions in the matrix. They are also detected as ions and keep their ionic character in between. The problem is whether preformed ion formation is a more efficient process than ionization of neutral species. We have seen that for protonated bases (at least for a non-surface active species), the acid effect due to preformed ion formation is generally very weak. How can this be explained? There seems to be mainly two types of possible answers. First, the charge states in the sampled surface are different from the bulk or, second, the analytes undergo extensive neutralization and reionization during the desorption event such that any initial differences in ionization states do not matter (Sunner et al., 1986b). The hypothesis that the primary ion bombardment causes extensive ionization in the surface belongs to the first type. This possibility was suggested and has been studied extensively by Todd (1988 and 1989). Todd believed that the primary ion beam causes the establishment of a steady-state concentration of ionic precursors in the matrix surface. These precursors would then protonate analyte molecules between impact events and not during the event as suggested by others (Ligon and Dorn, 1988; Sunner et al., 1988a). In such a case, we do not expect any acid effect, since most of the analytes are already protonated. Indeed, it becomes difficult to explain how acid addition can inhibit radiation-induced chemistry or strongly affect surface activity.

THE SURFACE ACTIVITY EFFECTS IN FAB

It has been shown that ions observed in FAB originate from depths of up to 80 Å beneath the surface (Ens et al., 1981; Ens et al., 1982; Standing, et al., 1982). This observation is particularly important since it has long been recognized that the composition of the first few monolayers of liquid solutions will, in general, differ from the bulk composition (Osipow, 1972; Adamson, 1962). In attempting to elucidate the mechanism of FAB, one must first understand how the surface composition differs from the bulk composition, since it is this surface composition which will be reflected in the mass spectra obtained. In this regard, Ligon and Dorn (1984a) have shown that, for a series of closely related surfactants dissolved in glycerol, differences in sensitivity are due almost exclusively to differences in surface activity. This result has led to the suggestion that it should be possible to use well known principles of surface chemistry to manipulate relative sensitivities in FAB. Based on this idea, several methods have been presented to enhance the sensitivities of surface active or non-surface active compounds. The following is the summary of these methods:

1) Adding a surfactant of positive charge to the solution may bring the small negatively charged analyte to the surface to maintain charge neutrality at the surface, thus, increase the sensitivity of the detection limit

for the negative ions (Ligon and Dorn, 1985).

2) Differences in the relative molar response of closely related analytes in glycerol solution can be minimized if a relatively large quantity of a surfactant of opposite charge is added to the solution before analysis. This added surfactant is chosen to dominate in the surface with the result that differences in surface activity among the species of interest become unimportant (Ligon and Dorn, 1984b).

3) Surface activity of the analytes can be modified by surfactant derivatization. Surfactants such as Girard's reagent, long chain quaternary ammonium hydrazide, dodecanol and 2-dodecen-1-ylsuccinic anhydride have been used as the derivative reagents (Ligon and Dorn, 1986a; Ligon, 1986).

The idea, introduced above, that relative solute composition may be far higher at the surface than in the bulk should immediately suggest a further complication in understanding sputtering from liquid surfaces. As we know, pseudomolecular ions are formed in FAB during continuous erosion of the liquid matrix surface by a high incident atom flux. However, it has been shown by Ligon and Dorn that surface active compounds show higher sensitivities (i.e. more surface active compounds suppress the other compounds in the surface) and the signal intensity decreases in time faster than for non-surface active compounds. Thus, the supply of

molecules from the bulk to the surface of the liquid should be an important factor to the emission current of pseudomolecular ions and, in particular, affects the pseudomolecular ion intensity as function of time. The transportation of molecules from the bulk to the surface of the liquid sample solution can arise from:

1) Diffusion of molecules resulting from a gradient in the chemical potential of the solute between the surface and bulk.
2) Ion migration of charged molecules in the field imposed by secondary emission of ions.
3) Convection of the liquid caused for example by gas evolution and bubble formation in the liquid. Gas evolution can result from electrochemical reactions at the liquid/metal support interface.

Nevertheless, the relative importance of these processes is still unknown. Ligon, however, purposed a surface renewal mechanism for the surface active compounds in polar solvent (e.g. glycerol) in FAB. This mechanism is based on the observation of stirring motions in the solution generated by differences in surface tension. In this experiment, a drop of 0.1 M of solution of cetyltrimethylammonium·bromide in glycerol was placed at the center of the glycerol solution which was covered with a thin film of glass powder beforehand. A fast spreading (807 mm^2 s^{-1}) of this surfactant solution on the glycerol surface was observed (Ligon and Dorn, 1986a). He

then concluded that differences in surface tension are capable of producing very rapid changes in surface composition, even in quite viscous liquids. Sputtering the surface of a glycerol solution is likely to produce just such a situation. Small amounts of hydrophobic solutes can drastically reduce the surface tension of glycerol. However, when the low-energy surface is sputtered away by the primary ion beam, the surface tension of the glycerol in that area became higher. Thus, the surface tension differences generated between adjacent points on the surface of a glycerol target droplet by the sputtering process ensure relatively rapid stirring of both the surface and the bulk. Diffusion may well be important in the relatively short-range process of moving solute molecules from the last few angstroms up to the surface. However, it is macroscopic mixing processes which provide a constantly renewed reservoir immediately below the surface from which short-range diffusion can occur.

The surface renewal process of the surfactant in glycerol solution is well explained by this mechanism. However, it can not explain the suppression effects observed from the simultaneous analysis of a surface active compound and one which is less surface active. To further explore this problem, several studies have been conducted. The effects of viscosity of solution, the irradiation time of sample in FAB, and concentration of surfactants to the analyte signal intensity were examined. The results of these studies will be

discussed below.

Since the intensity of the small inorganic anions can be enhanced by adding a positive charged surfactant (Ligon and Dorn, 1985), it is reasonable to presume that the same strategy can also be applied to positive ion FAB by adding a negatively charged surfactant to enhance the analyte signal. A systematic study of the effect of adding a positive charged surfactant to the solution to enhance the cationic analyte sensitivity has been done here.

Mass Transport Processes

Figure 14 shows the mass spectra of an equimolar mixture of two surface active compounds; n-dodecyltrimethyl-ammonium·chloride (DTMA) and n-hexdecyltrimethyl-ammonium·chloride (HTMA) (a) at high concentration (0.1 M) and (b) at low concentration (0.001 M). The compounds have similar chemical structure except that the chain length of alkyl group is slightly different. Thus, they have nearly the same gas phase basicity (Sunner et al., 1987) and solubility. Presumably, only surface activity differences may affect the signal intensities.

At high concentration (0.1 M) the less surface active DTMA (m/z 228) tends to be excluded from the surface by HTMA (m/z 284). This is shown in the mass spectrum in Figure 14(a) where the intensity of DTMA is approximately one third that of HTMA. It was found that the extent of such suppression

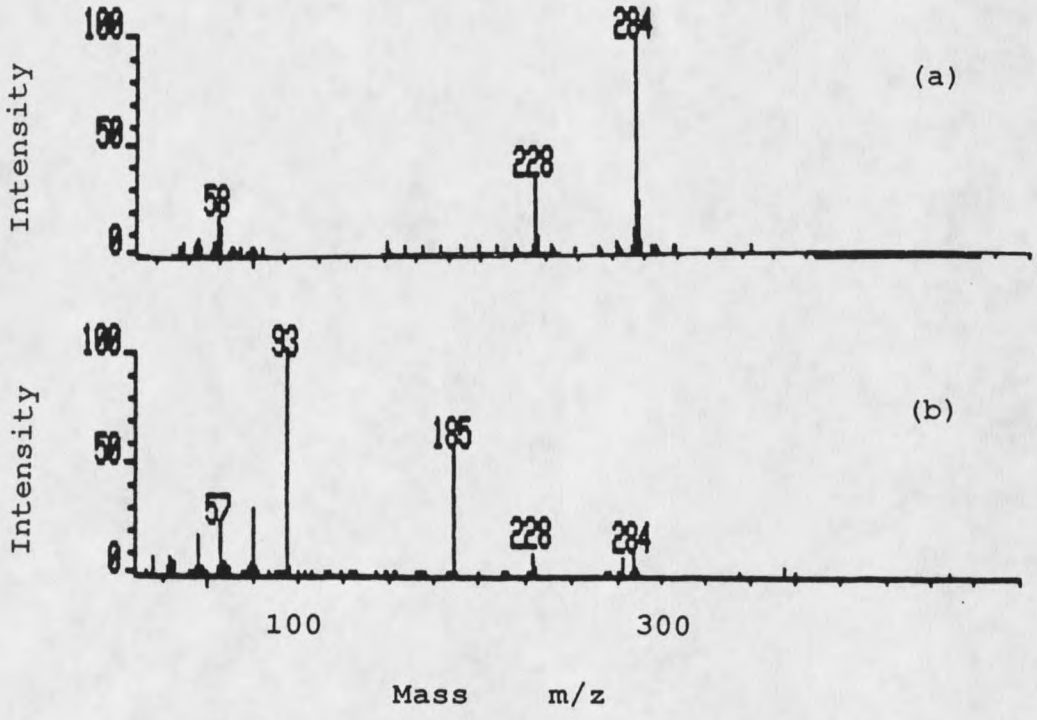

Figure 14. Mass spectra of glycerol solutions which contain equimolar quantities of $C_{12}H_{25}N(CH_3)_3^+$ ($DTMA^+$; M.W. 228) and $C_{16}H_{33}N(CH_3)_3^+$ ($HTMA^+$; M.W. 284) (a) 0.1 M and (b) 0.001 M.

effects will decrease with the surfactant concentration. No suppression effect (i.e. equal signal intensity) is observed when the concentration of both surfactants in the matrix are initially 0.001 M (Figure 14(b)).

The suppression effect observed at high concentration may come from the competition between the two compounds for available surface sites. In that case, the more surface active compound, HTMA, fills the surface sites more efficiently than DTMA. At very low concentration, there are

sufficient surface sites available to enable both compounds to exist in equal concentrations at the surface. Therefore, no competition due to differences in surface activity would be expected. The observation that the sensitivity of both surfactants is the same at low concentration also implies that during the desorption process, the mass transport rate for both molecules from bulk to surface is equally fast even though the surface activity is different.

Figure 15 shows the relative change in ion signal from DTMA and HTMA (0.2 M of each) as a function of time at room temperature. A similar trend has been found for two small peptides with different surface activity in glycerol (Falick et al., 1988). At shorter time, the analyte ion signals show the expected dominance of the more surface-active component. However, at longer times, the signal from less surface active amine becomes increasingly important. This behavior may be due to two competing processes: matrix evaporation and stripping of surface layers by sputtering. The former can account for the increase with time of $(DTMA)^+$ signal due to concentration of the non-volatile analytes as the matrix evaporates. The latter process could account for increased loss of the surface-active analyte with time as the more concentrated surface layers are stripped away.

It is interesting to see that the relative change of ion signal for both amines with time are similar when the viscosity of the solution was increased by decreasing the

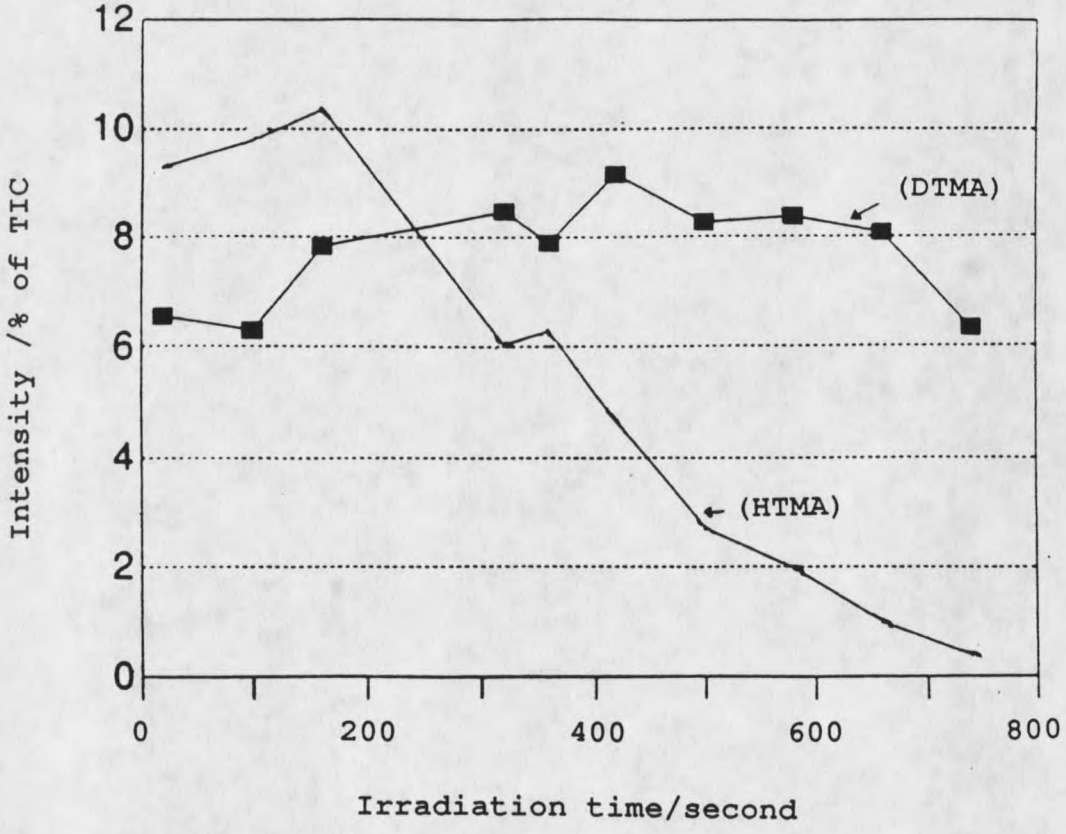

Figure 15. Intensities of M^+ ions of 0.2 M of DTMA and HTMA solution as a function of irradiation time. The more surface active HTMA decrease faster.

temperature (Figure 16(a)). In this experiment, the sample was cooled down to ca. -45°C and then immediately inserted into the ion source.

The ratios of ion intensities of $(DTMA)^+$ to $(HTMA)^+$ in Figure 15 and Figure 16(a) were calculated and shown in Figure 16(b). It was found that in the high viscosity condition the ratio is always nearly equal to 1 even after the sample has stayed in the FAB source for 40 minutes. However, in the low viscosity condition (i.e. at room

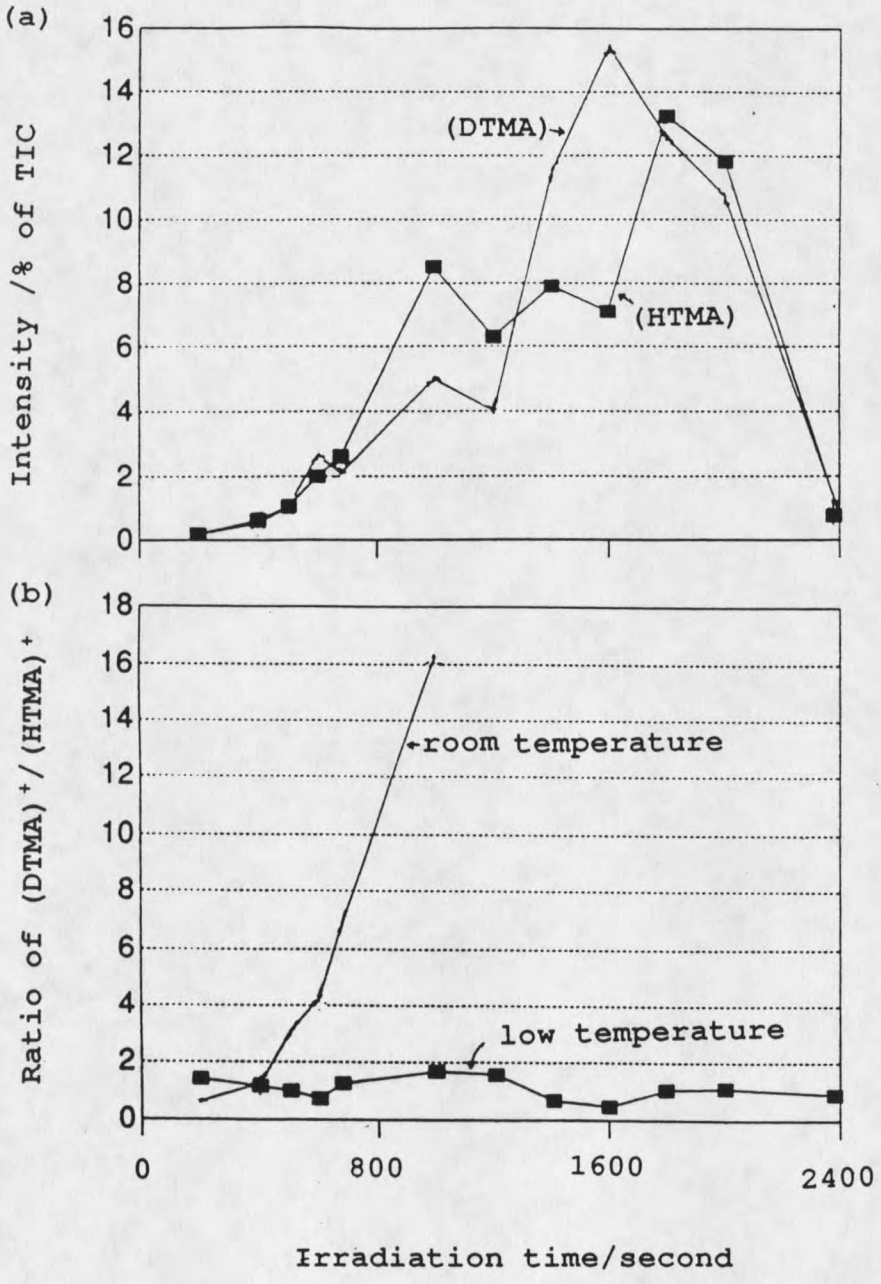

Figure 16. (a) Intensities of $(DTMA)^+$ and $(HTMA)^+$ ions (0.2 M of each) at varying matrix temperature. (b) Ratio of $(DTMA)^+/(HTMA)^+$ vs. irradiation time at room temperature and low temperature condition, the sample composition is the same as in (a).

temperature), the ratio increases abruptly after the sample has been inserted into the source for 6 minutes. The observation clearly shows that when the mass transport process is blocked in high viscosity condition, surface activity effects no longer exist and the intensities of the signal of the analytes in FAB depend only on their bulk concentration. This explains why the changes of ion intensity of both analytes were the same under conditions of low temperature.

It was suggested (Fenselau and Cotter, 1987) that a steady state is achieved between removal of sample and solvent from the surface of the matrix by sputtering and evaporation. This state may contain a sample concentration gradient which would be created by the dynamic forces of convection, diffusion, and ion migration. A sample which contains DTMA and HTMA (0.2 M each) in glycerol was used to explore the effects of concentration differences in the bulk medium and in surface layers during the desorption process in FAB..

In this study, mass spectra were monitored on the computer screen until the ratio of signal intensities of both M^+ ions was nearly equal (Figure 17(a)). The FAB probe was then removed from the source immediately. The solution on the FAB tip was stirred thoroughly. After 10 minutes, the same sample was reinserted into the FAB source. Figure 17(b) shows the first mass spectrum thus obtained. The ratio of relative ion intensities of TIC of $DTMA^+$ to $HTMA^+$ was calculated in both cases. It was found that the ratio increases from 1:1 to 3:1

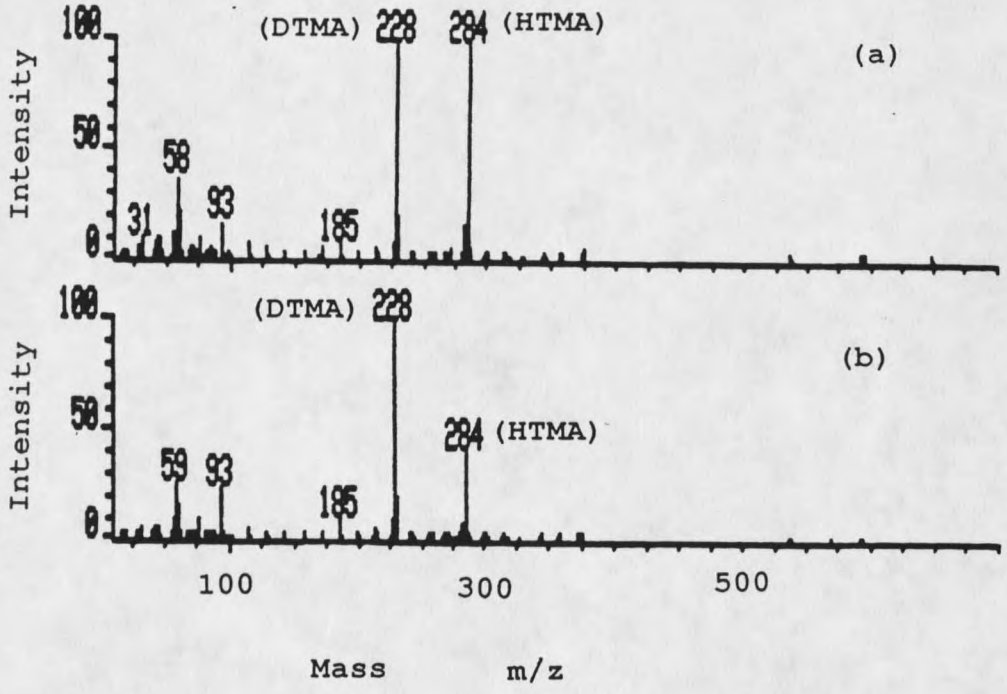

Figure 17. Mass spectra of a sample which initially contains 0.2 M of both DTMA and HTMA. (a) Spectrum obtained after 9 minutes of fast atom bombardment (b) The same sample as in (a), however, after recording spectrum (a) the FAB probe was taken out of the source and stirred, after 10 minutes, the probe was reinserted into the source. The spectrum in (b) was recorded immediately after reinsertion.

after the sample was reinserted.

The sudden increase in the ratio implies that an analyte concentration gradient was generated in the matrix during the previous FAB experiment. Initially, due to the higher surface activity of HTMA over that of DTMA, the surface concentration of HTMA should predominate over the surface concentration of DTMA. In other words, the concentration of DTMA in the bulk

solutions should be higher than that of HTMA. As erosion of the surface layer by the fast atom bombardment process proceeds, more of HTMA should be sputtered away. After 9 minutes, even though the surface concentration for both analytes is the same (because equal signal intensity for both analytes was observed), there will be a relatively small quantity of HTMA left in the bulk solution. Stirring the irradiated bulk solution followed by a 10 minute waiting period will establish a "new" equilibrated distribution of the two analytes based on their bulk concentration and competition for available surface sites. This new distribution is reflected in the initial mass spectrum obtained when the sample is reinserted in the ion source (Figure 17)b)).

Surface Neutrality Effects in FAB

The sensitivity of some small inorganic anions in FAB has been enhanced to nano-gram levels by the addition of long chain cationic surfactants to the solution (Ligon and Dorn, 1985). It was suggested that in order to neutralize the cationic surfactant, the analyte anions must migrate to the surface where they will be more efficiently sampled by the primary particle beam. However, only qualitative results were reported. Here, is reported a systematic and quantitative study of the effect of the addition of a long chain anionic surfactant, sodium dodecylsulfate (SDS), on small inorganic and organic cations.

A 30 mM solution of CsCl in glycerol was prepared to study the influence signal enhancement as the result of surfactant addition. To this solution was added varying quantities of SDS. The mass spectra were obtained and ion signals were compared as a function of SDS concentration. Figure 18(a-d) shows these results. Without adding SDS, the Cs^+ ion signal was only ca. 5% of TIC but after addition of SDS the intensity of Cs^+ ion signal increased. The % of TIC increases by 7 times to ca. 35% TIC when 10 mM of SDS was added. Figure 19 shows the time dependence of the intensities of cesium, glycerol and dodecylsulfate ions from a solution that contains 30 mM of CsCl and 10 mM of SDS. The curves were derived from both positive and negative FAB spectra, because dodecylsulfate does not appear in the positive ion spectrum and cesium is not observed in the negative ion spectrum. It can also be seen in Figure 19 that during the first 20 minutes the signal intensity from Cs^+ dropped simultaneously with the dodecylsulfate signal. This clearly shows that the addition of SDS did affect the intensity of Cs^+ ion signal.

Since the surface activity of dodecylsulfate anion is quite high, through electrostatic binding with this anion the Cs^+ ions will then be brought up to the surface layers and a signal enhancement of Cs^+ ion with the addition of SDS is then observed. When the surface layers of matrix were gradually sputtered away by the bombardment of primary atom beam, the concentration of the surfactant (dodecylsulfate) decreased and

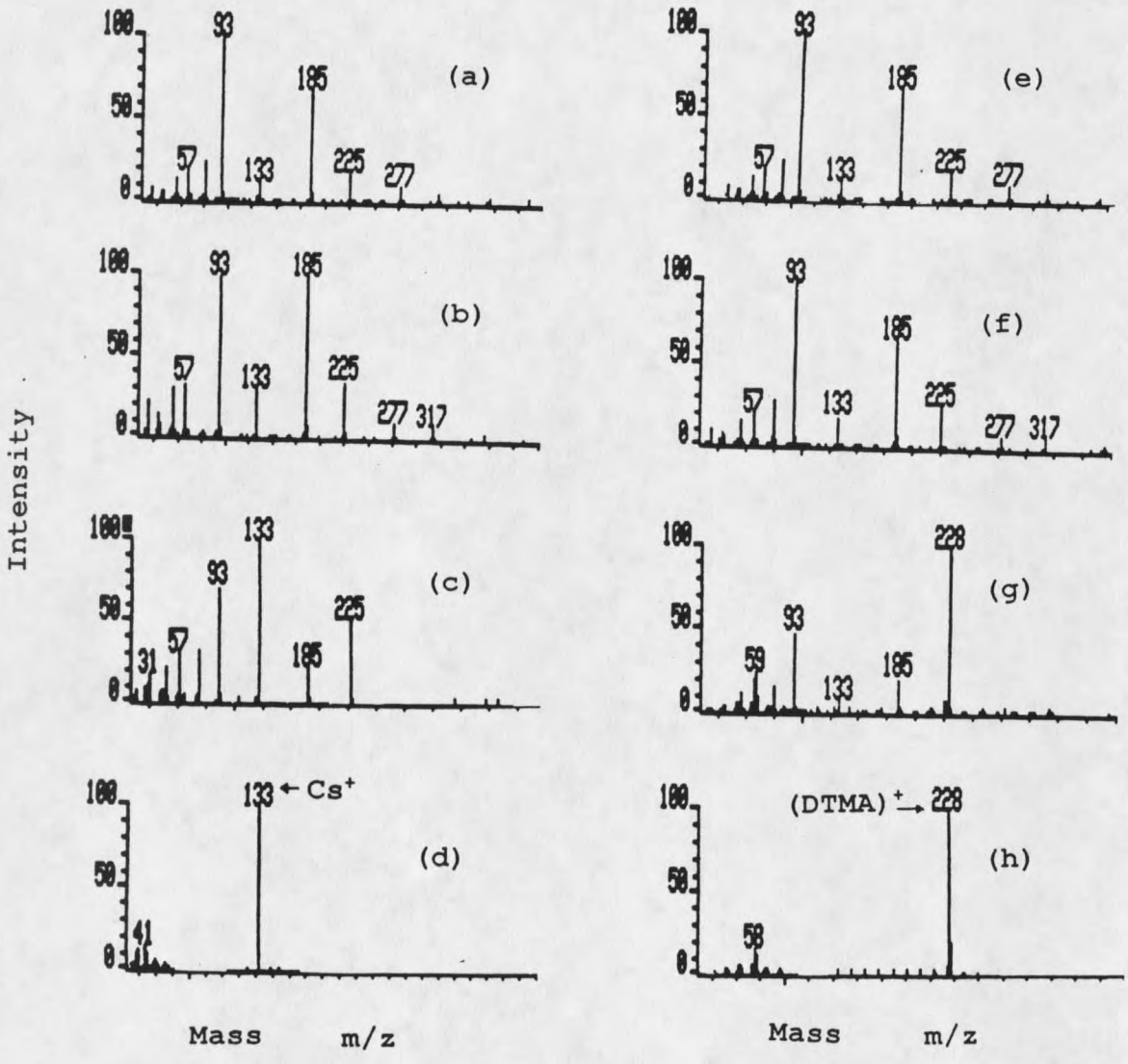

Figure 18. Positive FAB mass spectra of a 30 mM solution of CsCl in glycerol by adding (a) 0 mM, (b) 0.1 mM, (c) 1 mM, (d) 10 mM of sodium dodecylsulfate (SDS) and (e) 0 mM, (f) 0.1 mM, (g) 1 mM, (h) 10 mM of DTMA.

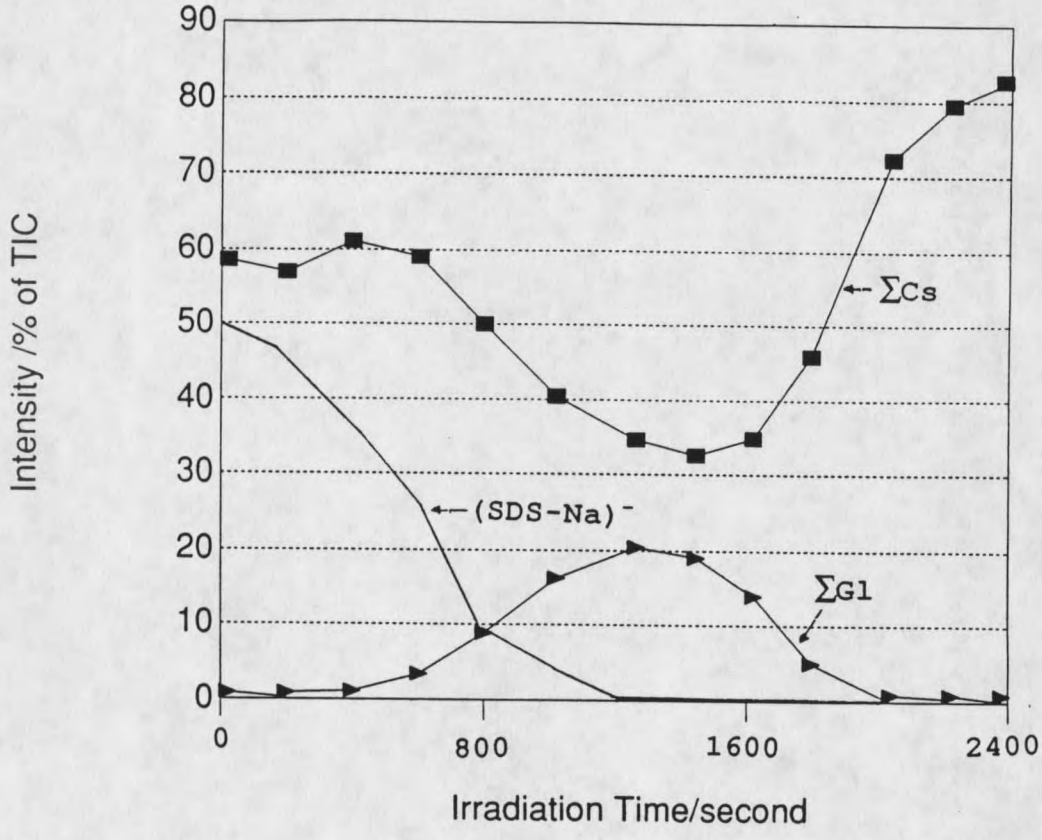

Figure 19. Intensities of Cs^+ of the solution which contains 10 mM of SDS and 30 mM CsCl in glycerol vs. irradiation time. The intensities of summation of glycerol and cesium ions, and dodecylsulfate anion (from negative FAB spectrum) are shown.

so was Cs^+. The decrease of the Cs^+ and surfactant concentration in the surface results in enhancement of the glycerol ion signal (Figure 19). After 20 minutes, the Cs^+ signal increases abruptly as the result of selective evaporation of glycerol from the sample which increases the concentration of cesium salt in the matrix. This is supported by the simultaneous decrease in the signal from the glycerol ions. Figure 20 shows the time dependence of the glycerol

signal for three different concentrations of SDS. It is seen that when more surfactant is added, the signal from glycerol tends to last longer. This is explained simply as a result of the surfactant slowing the evaporation of glycerol.

We have seen that a negatively charged surfactant enhances the signal of Cs^+. It is then interesting to ask what happens if a positively charged surfactant is used

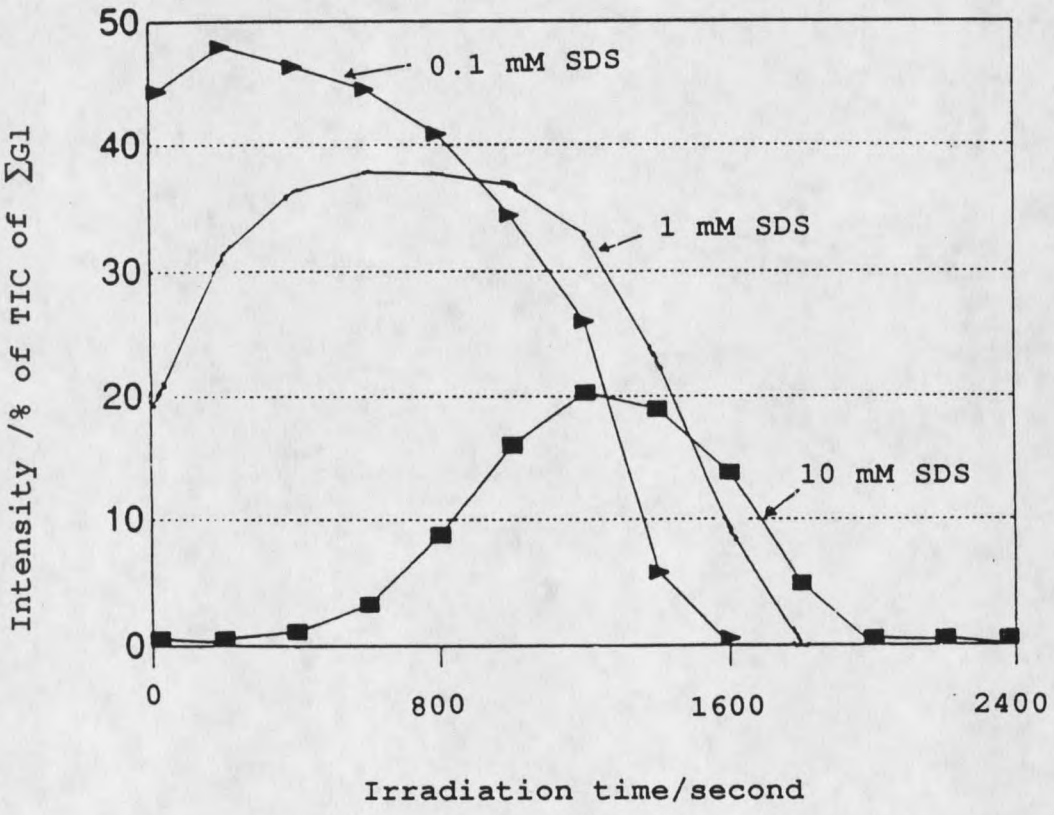

Figure 20. Effect on glycerol ion intensities from the addition of 0.01 mM, 1 mM, and 10 mM SDS to a 30 mM CsCl glycerol solution.

instead. Figure 18(e-f) shows the mass spectra obtained after the addition of DTMA to the glycerol solution which contains 30 mM of CsCl. It was found that the signal intensity from Cs^+ decreased with the addition of DTMA and Cs^+ ion signal disappeared totally after 10 mM of DTMA was added. This can be explained as an effect of the charge repulsion by the positively charged surfactant which removes the hydrophilic cations from the surface layers.

The enhancement of a positive ion analyte signal due to the presence of a negatively charged surfactant can be considerable, not only for inorganic cations, but also for organic species such as diethanolamine (DEA), diethanolammonium·hydrochloride (DEA·HCl), and quaternary ammonium salts. One example is given by using DEA and pre-charged DEA·HCl as analytes. Without SDS, it is observed that ca. 30% of TIC is due to $(DEA)H^+$; whether or not it originates from a 2 mol% solution of DEA or DEA·HCl in glycerol. After the addition of SDS, the intensity of the $(DEA)H^+$ from a DEA·HCl solution was enhanced 10 times but only 3 times for a DEA solution. Since the analyte molecules are pre-charged in the DEA·HCl solution, it is not surprising to see the dramatic enhancement of intensity of the $(DEA)H^+$ signal from this sample. The signal enhancement of DEA by SDS might come from the partial dissociation of DEA molecules in the glycerol.

Another example is the use of 2 mol% of tetraethanol-ammonium·bromide (TEA) (M.W. 194) as the analyte. Before

adding SDS, only about 10% of TIC of signal was from $(TEA)H^+$ ion (Figure 21(a)); after SDS was added, the spectrum was dominated by $(TEA)H^+$ ion (Figure 21(b)). When tetramethylammonium·chloride (TMA) was used as analyte, a very similar result was obtained as those which were observed in the earlier Cs^+ experiments (data not shown).

Because of the large enhancements observed for small organic cations, it seemed interesting to investigate whether

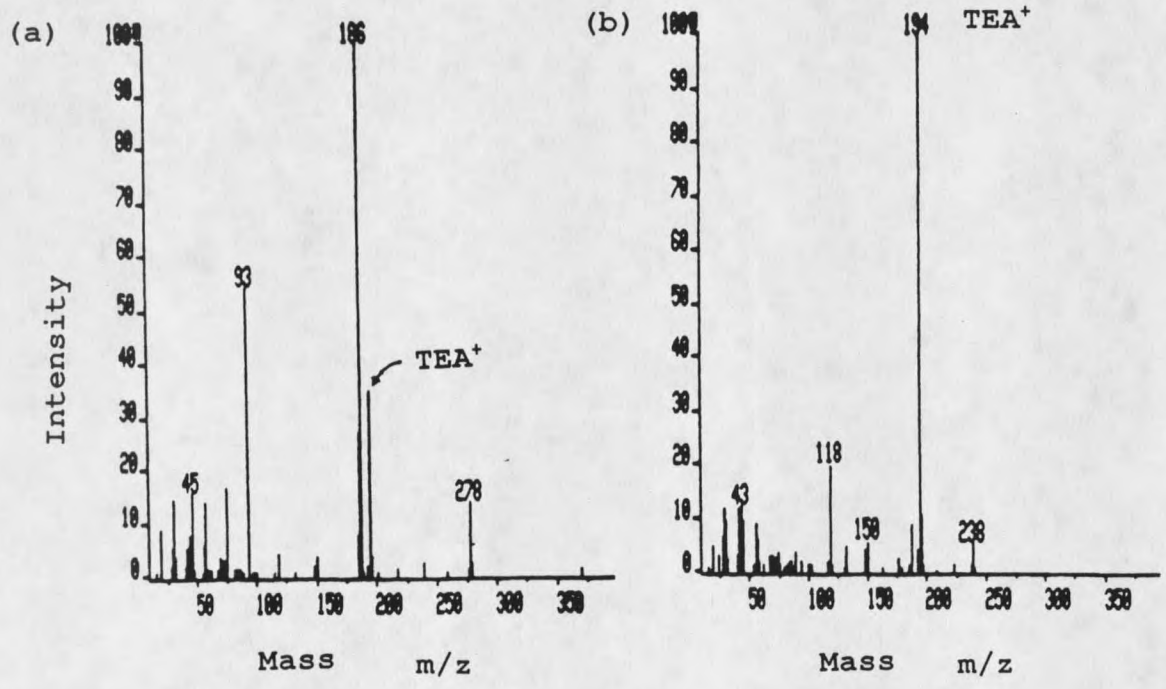

Figure 21. Positive FAB mass spectra of 2 mol% tetraethanolamine (TEA) glycerol solution (a) without adding SDS, (b) with 10 mM SDS addition.

large organic or biochemical compounds might also show the same effect. Unfortunately, when a polypeptide (angiotosin, M.W. 1046) was used as analyte, the addition of SDS didn't increase the MH^+ ion signal. Instead, the signal from this polypeptide was suppressed by adducts of surfactant molecules with sodium ($Na_4(dodecylsulfate)_3^+$ and $Na_3(dodecylsulfate)_2^+$). It is still unclear why the intensity of polypeptide doesn't increase by the addition of SDS.

EFFECTS OF MATRIX VISCOSITY ON FAB SPECTRA

Because of the similarity of timescale in the collision cascade, the desorption mechanism in solid and liquid SIMS (or FAB) is speculated to be quite similar (Magee, 1983; Pachuta and Cooks, 1987). However, the experimental results suggest that there are some differences. The three major different experimental results between the two methods are:

1) the internal energies of desorbed ions are higher in solid SIMS than those in liquid SIMS (Cook and Chan, 1983).
2) the neutral yield is over ten times higher in liquid SIMS than that in solid SIMS (Benninghoven et al., 1987; Gillen, et al., 1988; Jiang et al., 1988; Williams et al., 1981; Wong and Rollgen, 1986). A positive correlation between low yields and high internal excitation energies of desorbed ions is also supported by the observation that internal energies are higher with a lower energy bombarding particle (de Pauw, 1986).
3) the radiation products formed by the primary atom or ion bombardment are largely removed by the desorption process itself (self-cleaning mechanism) in liquid SIMS (Wong and Rollgen, 1986; Wong et al., 1985), whereas this process is much less efficient in solid SIMS (Pachuta and Cooks, 1987).

In spite of the experimental results discussed above, there is no general agreement in the literature that the desorption mechanism in liquid and solid SIMS are significantly different. Some scientists believe that any differences observed are solely due to the transport of analyte and radiation products in the liquid matrix (Pachuta and Cooks, 1987).

Studies of the ionization processes also showed that in liquid SIMS there is considerable evidence for ion-molecule reactions occurring during the desorption processes (Pachuta and Cooks, 1987; Sunner et al., 1986a). As described before, it has been demonstrated that these reactions are governed by gas-phase as opposed to liquid-phase energetics (Sunner et al., 1987; Lacey and Keough, 1989). The lifetime of the intermediate gas phase has been estimated to be in the 10^{-10} to 10^{-9} second range (Sunner et al., 1988a). Combining this with the high neutral yield observation, a simple physical picture of the desorption event-bulk desorption can be given as follows: when the primary atoms or ions hit on the surface of the solution a cavity is formed with its depth longer than width (the order of this cavity is about 100 Å). The molecules in this region are basically the molecules which have been desorbed. Such a picture has also been suggested by several other models of desorption ionization (Pachuta and Cooks, 1987). Other experimental results also support the idea that the process of liquid SIMS desorption has a

character of "bulk" desorption. It has been found that the internal temperature of desorbed glycerol molecules was about 190±40 K when the temperature of the liquid matrix was 267 K (Hoogerbrugge et al., 1988). The same phenomena has also been suggested by Sunner et al. (1988b) from their "phase explosion model" based on thermodynamic considerations of the liquid to gas transition. These are clearly very significant results that strongly suggested a desorption process where collective phenomena are important. Other possible cooling effects are from the processes of declustering or adiabatic expansion in gas phase (Busch et al., 1983; David et al., 1986; Urbassek and Michl, 1987). Both of these proposed processes, in particular adiabatic cooling effect, again implies a bulk desorption process involving many molecules.

Based on the studies described above, the desorption event in liquid SIMS or FAB may be described as a "bulk", thermal or quasi-thermal, collective process, however, a central question becomes to what extent these particular properties are also characterized in solid SIMS. In view of the likely higher internal molecular energies and lower yield in solid SIMS as compared to liquid SIMS one might suspect that the thermal, collective character of the desorption process in solid SIMS should be less pronounced.

In contrast to the uncertainty regarding any mechanistic differences between liquid and solid SIMS, the role of mass transport processes for the desorption is somewhat better

understood. Convection, diffusion, ion migration, sputtering, and evaporation are five major mass transport processes in liquid SIMS. The result of various transport processes is that the surface composition differs from that of the bulk. A steady state concentration profile in the surface is approached (Bartmess and Phillips, 1987; Todd, 1986; Todd, 1988; Wirth et al., 1986; Wong et al., 1985). It is clear that the rate of these processes must be very different in solid SIMS. However, some mixing is still experimentally observed (Pachuta and Cooks, 1987).

It is likely that all the individual mass transport processes, from bulk to the liquid/vacuum interface, involved in liquid SIMS desorption have been identified and been subjected to experimental study. However, the relative magnitudes of the processes under different experimental conditions are still unclear, and thus we can only guess the surface composition in general or the analyte concentration in the surface in particular. This greatly complicates mechanistic interpretation of experimental results.

One approach towards a better understanding of the role of mass transport processes vs. mechanism in SIMS is to study systems which are intermediate between liquids and solids. Of particular interest in this regard is the dependence of FAB spectra on matrix temperature, T_b. Some of these studies to explore the transportation process of surface active compounds have been done and were described in a previous section.

Here, we will be primarily focused on the explanation of the mechanism.

Field and co-workers found that as the matrix temperature decreased the FAB spectra degraded (Katz et al., 1986; Katz et al., 1987a; Katz et al., 1987b). For neat methanol, totally unrecognizable spectra were obtained when the matrix temperature was below 130 K. The authors could not explain their results but only speculate that a small increase in hydrogen bond strengths was responsible for the observation. Sunner and co-workers (Morales et al., 1989) studied the effect of temperature on FAB spectra of solutions of high gas-phase basicity analytes in glycerol. They found that the intensities of cluster ions and of molecular ions decreased and that the intensities of the chemical noise ions increased gradually with decreasing matrix temperature (T_b) in characteristic ways. In fact, the T_b dependence of the different types of ions was successfully reproduced using a kinetic model of ion-molecule reaction processes in FAB that these authors had earlier developed (Sunner et al., 1987). However, one additional assumption had to be made; namely that the time available for these reactions decreased with decreasing T_b. They speculated that at low viscosity (high T_b), the radial expansion of the high-pressure gas in the cavity may become competitive with the expulsion process. Thus, it was concluded it was not the matrix temperature, per se, that is important, but the viscosity of the matrix.

Because of a decrease in pressure, this would slow down the expulsion process. However, changing the viscosity also changes the rate of transport processes from the bulk to liquid/vacuum interface and this introduces uncertainty in the interpretations.

In this study, the problem of the role of transport processes versus the desorption mechanism in liquid and solid SIMS is addressed by varying the viscosity of the matrix. The experimental results will be first presented. The implication of the present findings for the role of transport processes and desorption mechanism in SIMS will then be discussed.

Variation of Viscosity of Glycerol Solution with Temperature and with Chemical Composition

Although water-free liquid glycerol freezes at 18°C (CRC Handbook of Chemistry and Physics, 1984), supercooled liquid glycerol is usually kinetically stable. When cooling liquid glycerol from 40°C to -40°C the viscosity increases exponentially from 10^3 cP (centiPoise) to 10^7 cP. This is shown in Figure 22(a). The viscosity of DEA, another matrix used in this investigation, behaves similarly to that of glycerol except that DEA freezes at 7°C (Figure 22(a)).

To distinguish the effect of temperature, per se, from the effect of viscosity, it is necessary to vary the viscosity at a constant temperature by using an additive. Such an additive must fulfill several requirements. First, it must be able to induce viscosity changes over some range, encompassing

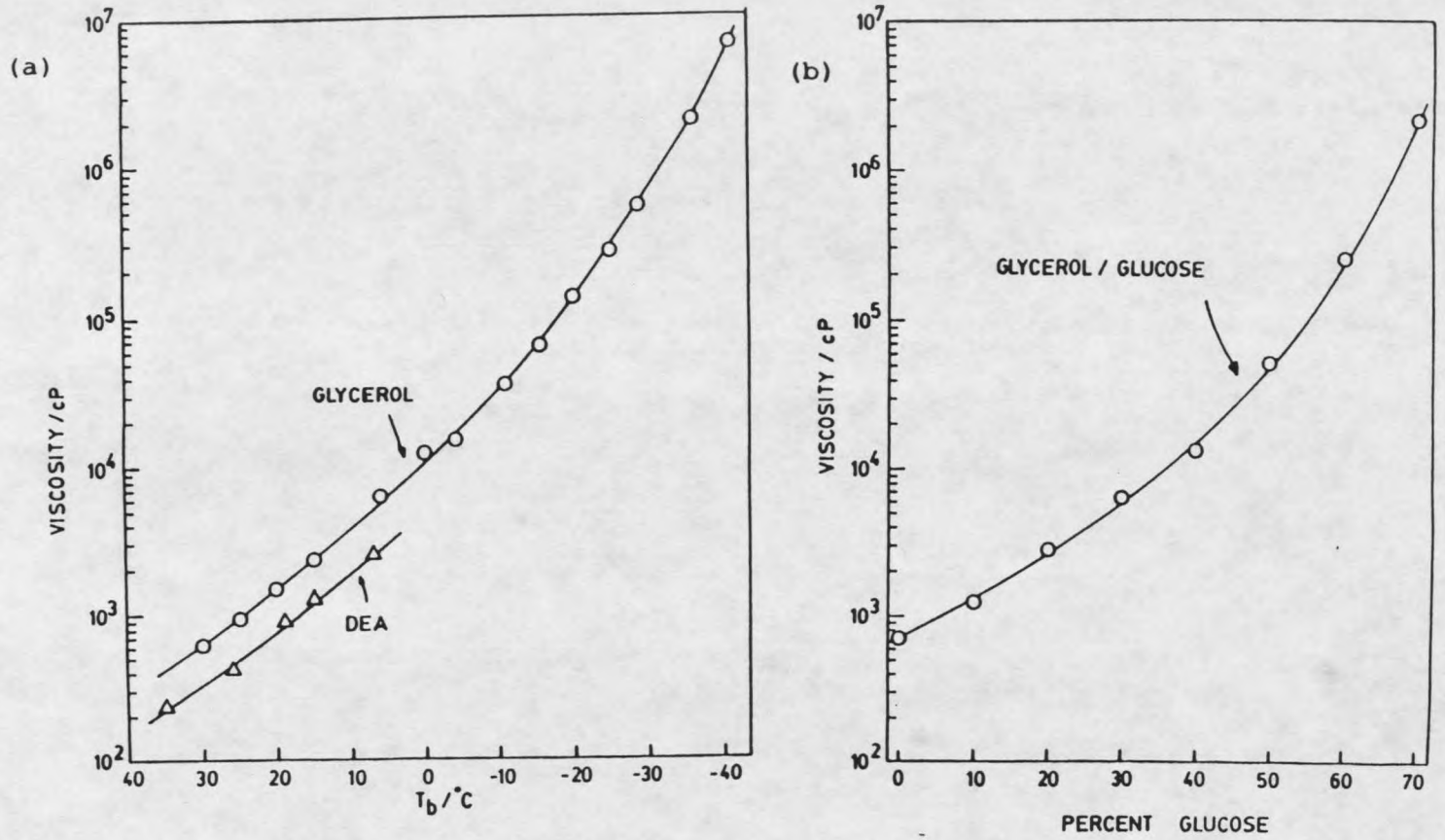

Figure 22. (a) Viscosity in centiPoise of glycerol and of diethanolamine as a function of temperature. (b) viscosity of glycerol/glucose as a function of glucose concentration in wt%.

several orders of magnitude as that covered by varying the temperature. Second, the chemical effects of the additive to the solution must be small. For example, the gas-phase basicity (GB) of the additive must be lower than that of glycerol otherwise the FAB spectrum will be dominated by the additive even at a concentration of 1-2 mol% addition. Several additives were tested and the results are presented here.

Most organic compounds, whether they are liquid or solid, have a relatively small effect on the viscosity when dissolved in glycerol. Water, however, does have a large effect, and the addition of 10 vol% of water decreases the viscosity by a factor of four (Newman, 1968). However, when such a solution is introduced into the vacuum, because of the high volatility of water the surface concentration of water falls almost instantaneously. No effects on the FAB spectra are seen. The same happens when any other volatile, low-molecular weight compound is used as an additive.

Gel-forming compounds, such as polydextran and gelatin, have a dramatic viscosity increasing effect on the glycerol solution. However, because a solidified gel typically consists of a three-dimensional network, the gel is not homogeneous on the length scale of the FAB event, ca. 100 Å. Actually, the FAB spectra of gels were very similar to that of neat glycerol, except that high GB nitrogen-containing groups in the gelatin gel gave intense peaks in that spectrum.

Spectra from acrylamide gels in glycerol, on the other hand, were found to be highly degraded. Presumably, the evaporative loss of glycerol in combination with the induced radiation chemistry in the surface layers resulted in the collapse of the gel structure and the formation of a surface "crust".

It was found that simple carbohydrates such as glucose were suitable as viscosity increasing additives (c_G study). It is noteworthy, here that pure carbohydrates have previously been used as FAB matrices at enhanced temperature (Ackermann et al., 1985). The advantages of using glucose as the additive in this study were:

1) the attained viscosity range largely overlaps that covered by varying the matrix temperature. Figure 22(b) shows the effect on viscosity when glucose is dissolved in glycerol. It is seen that by dissolving up to 70 wt% of glucose, the viscosity is increased from 10^3 to over 10^6 cP. The curve probably extrapolates smoothly to the viscosity of neat glucose, 10^{14} cP.
2) even at high glucose concentrations, only small chemical effects are seen.
3) due to the structural similarity between glucose and glycerol, solutions at any concentration can be made.
4) selective evaporation of the additive is not a problem (However, some selective evaporation of glycerol may be expected.).

Dependence of FAB Spectra on Viscosity

When comparing the glycerol spectrum at +26°C (Figure 23(a)) to the spectrum at -17°C (b) some degradation of the spectra at -17°C is seen to occur. In this degraded spectrum, the glycerol dimer (m/z 185) intensity has decreased and the trimer (m/z 277) has totally disappeared into the chemical noise. There is some increase for the major glycerol fragment ions (m/z 75, 57, 45, 31 and 29) and there is a significant increase for the chemical noise ions. This is similar to previous observations (Katz et al., 1986; Molales et al., 1989). However, compared to the results of Morales et al. (1989), there are some differences in the degree of degradation. A likely major cause is that different mass spectrometers were used. In particular, the angles between the atom gun, the matrix surface and the ion optical axis were different. Also, in the previous study by Morales et al. (1989), the matrix temperature was measured outside the mass spectrometer and might not accurately reflect the true temperature during the bombardment.

Degraded FAB spectra, similar to those observed when decreasing the matrix temperature, are obtained when glucose is added to the matrix (Figure 23(c) and (d)). Thus, when comparing the spectrum of 20 wt% glucose in glycerol (Figure 23(c)) with the neat glycerol spectrum at room temperature (Figure 23(a)), the same trends are observed;

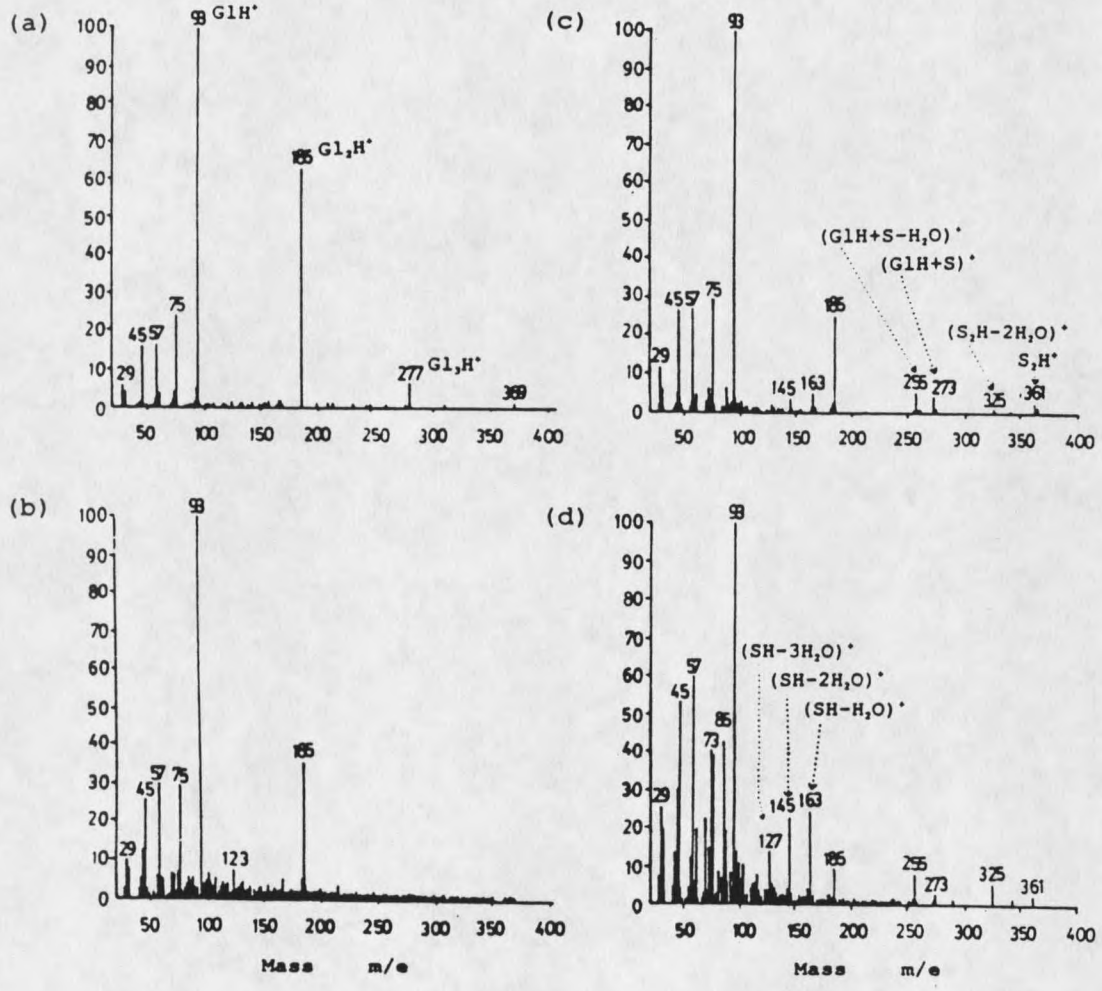

Figure 23. FAB spectra of (a) 100% glycerol at 26°C, 800 cP (b) 100% glycerol at -17°C, 80,000 cP (c) a solution of 20 wt% glucose in glycerol at 23°C, 2,600 cP and (d) a solution of 45 wt% glucose in glycerol at 23°C, 30,000 cP. S=glucose; Gl=glycerol.

namely the ion intensities increase for glycerol clusters, and decrease for fragments and chemical noise. These trends are strongly enhanced in the 45 wt% glucose spectrum (Figure 23(d)). However, the distribution of chemical noise ions is somewhat different for the 20 and 45 wt% glucose solution.

The peaks due to glucose (S) in Figures 23(c) and (d), for example m/z 163 (SH^+-H_2O), 145 (SH^+-2H_2O), 127 (SH^+-3H_2O) and 255 ($GlH^+ + S - H_2O$), are seen to be rather small as expected from the low GB of glucose. When comparing the 45 wt% glucose with the 20% wt% spectrum, some degradation of the glucose part of the spectrum is also found. This is seen both by the increasing water loss and most notably by the large increases for some low mass glucose fragment ions such as m/z 87, 85 and 73. The trends are further strengthened when the glucose concentration is increased beyond 45 wt% (data not shown). Results, such as those shown in Figure 23, are best presented by plotting the intensities of individual ions, or groups of ions, versus the viscosity (γ). Figure 24(a) shows the result of varying the temperature and Figure 24(b) of varying the concentration of glucose. The intensities of glycerol pseudo-molecular, major fragment, and dimer ions as well as the sums of major glycerol ions and of chemical noise ions are plotted in percent of total ion current (TIC). It is seen that the results from the T_b and c_G experiments are quite similar. In both cases, the chemical noise ion intensity increases strongly with viscosity and, at about 40,000 cP makes up for

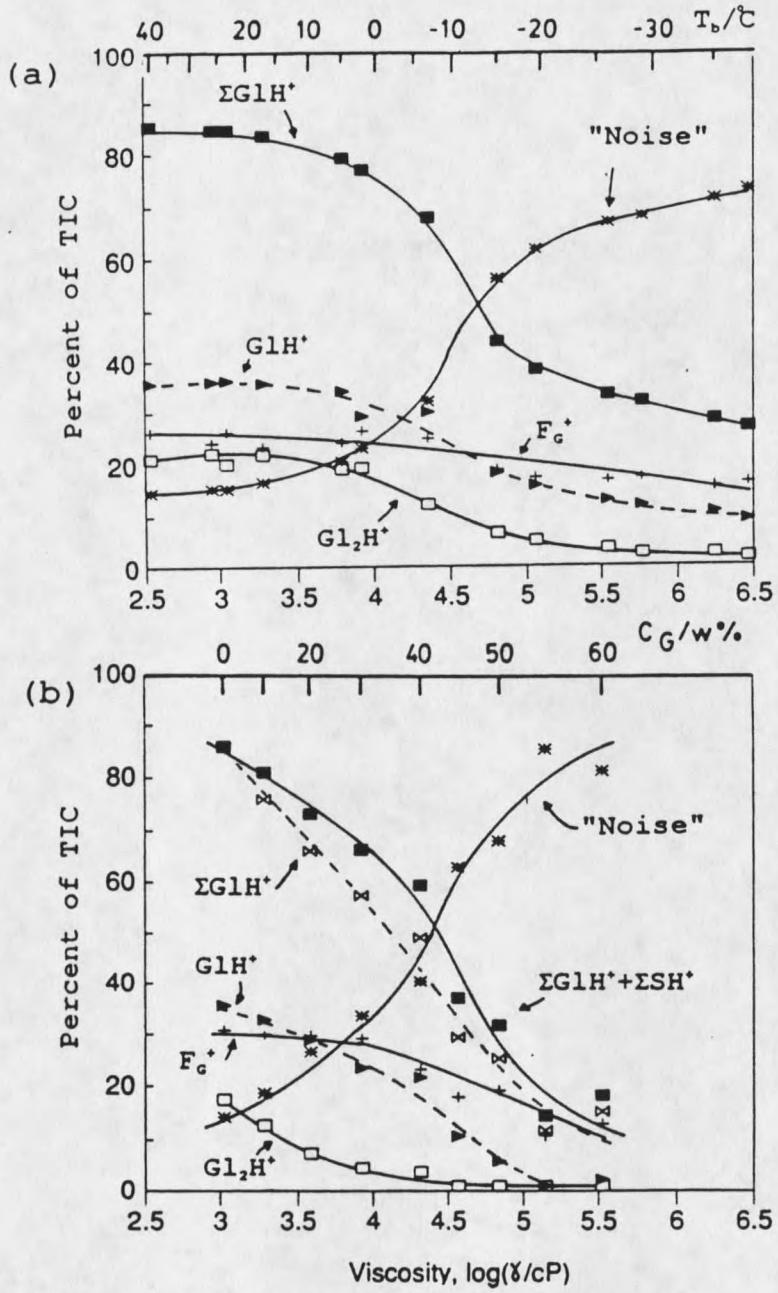

Figure 24. Intensities of major ions vs. viscosity in positive ion FAB spectra. (a) Neat glycerol. The viscosity was varied by changing the matrix temperature T_b. (b) Solution of glucose in glycerol. The viscosity was changed by varying the glucose concentration c_G given in wt%. S=glucose; Gl=glycerol; F^+_G =major glycerol fragments, m/z=75,57,45,31 and 29; $\sum GlH^+$ includes F^+_G as well as Gl_nH^+, n=1, 2,...; $\sum SH^+$ includes m/z=163 (SH^+ - W), 145 (SH^+ - 2W), 127 (SH^+ - 3W), 255 (SH^+ + Gl - W), 273 (SH^+ +Gl), 361 (S_2H^+), 365 (SH^+ + Gl_2), 453 (S_2H^+) and 541 (S_3H^+), W=H_2O; all other peaks were included in the chemical noise ion intensity.

50% of TIC. Also, in both cases, there is a relative decrease in ion intensity follows:

dimer > molecular ion > fragment ions.

Because some ionization of glucose occurs, the sum intensity of glycerol and glucose ions in Figure 24(b) should be compared with the sum of glycerol ions in Figure 24(a). Granting the overall similarity between the results from the T_b and the c_G experiments, there are also some differences. Thus, the different glycerol ions, in particular the glycerol dimer, decrease faster with γ in the c_G than in the T_b experiment.

The viscosity dependence of negative FAB spectra of glycerol was also studied. The results obtained were similar to those from the positive ion spectra and are therefore not presented here.

Because the ionization reactions during the desorption event causes high GB analytes to be preferentially ionized, the behavior of high GB analytes with viscosity is of particular interest. Figure 25 shows the viscosity dependence of the FAB spectra of 10 mol% DEA in glycerol. The overall degradation of the spectra is seen to be quite similar to that found for glycerol. Both in the T_b and in the c_G series in Figure 25, the DEA ions (m/z 106) dominate the spectra at low viscosity, but decrease sharply with increasing viscosity while the chemical noise ions increase. There is a slight decrease for the glycerol ions. The dimer ratios of glycerol

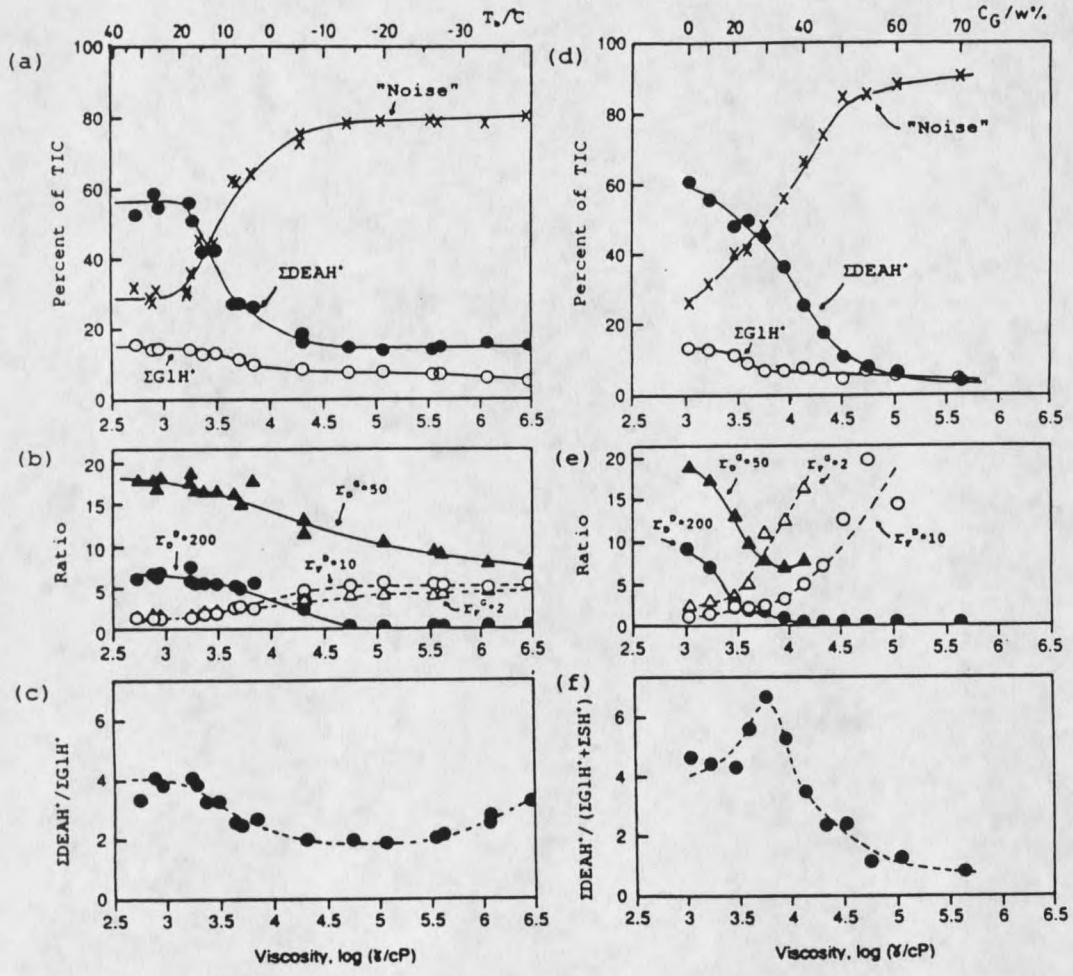

Figure 25. Intensities of major ions vs. viscosity in positive ion FAB spectra of (a-c) 10 mol% DEA in glycerol at varying matrix temperature T_b; (d-f) 10 mol% DEA in glycerol/glucose solutions at varying glucose concentration c_G; DEA=diethanolamine; F^+_D=major $DEAH^+$ fragment ions, m/z=88 and 74; $r_D^D=(DEA_2H^+/DEAH^+)$; $r_D^G=(Gl_2H^+/GlH^+)$; $r_F^D=(F_{DEA}/DEAH^+)$; $r_F^G=(F_{Gl}/GlH^+)$; other notations as in Figure 24. Included in $\sum DEAH^+$ were major $DEAH^+$ ions: $(DEA)_nH^+$, $DEAH^+(Gl)$ and $DEAH^+$+S-mW, m=1, 2,.... as well as the fragment ions F.

(Gl_2H^+/GlH^+) and DEA ($DEA_2H^+/DEAH^+$) decrease and the corresponding fragment ratios (F_{Gl}/GlH^+ and $F_{DEA}/DEAH^+$) (in DEA, m/z 74 and 88 were the major fragment ions (F_{DEA}); in glycerol, m/z 29, 31, 45, 57, and 75 were the major fragment ions (F_{Gl})) increase with increasing viscosity (Figures 25(b) and (e)). However, there are significant differences in these ratios between the T_b and c_G studies. The ratio of $\Sigma DEAH^+:\Sigma GlH^+$ is shown in the bottom curves in Figures 25(c) and (f). In the T_b experiment, there is a decrease of about a factor of two with increasing viscosity. A similar decrease was also found in the previous study by Sunner et al. (1989) where it formed the basis for the kinetic modeling of the FAB ionization process done in that study. In the c_G experiment (Figure 25(f)), the ratio is found to increase first and then to decrease with viscosity.

Comparing Figures 24 and 25, it is striking that severe degradation sets in at a much lower viscosity for the 10 mol% DEA solution than for the neat glycerol. This can be seen by looking at the value of γ_{deg} which was defined as the viscosity where the intensity of chemical noise ions passes 50% of TIC. For 10 mol% DEA this value is about 5,000 cP (Figure 25) where for neat glycerol it is about 40,000 cP (Figure 24). This large effect of the addition of 10 mol% DEA to glycerol was unexpected. Figure 26 shows the variation of γ_{deg} (in T_b experiments only) with the concentration of DEA. It is seen that the addition of few mol% DEA causes γ_{deg} to decrease by a

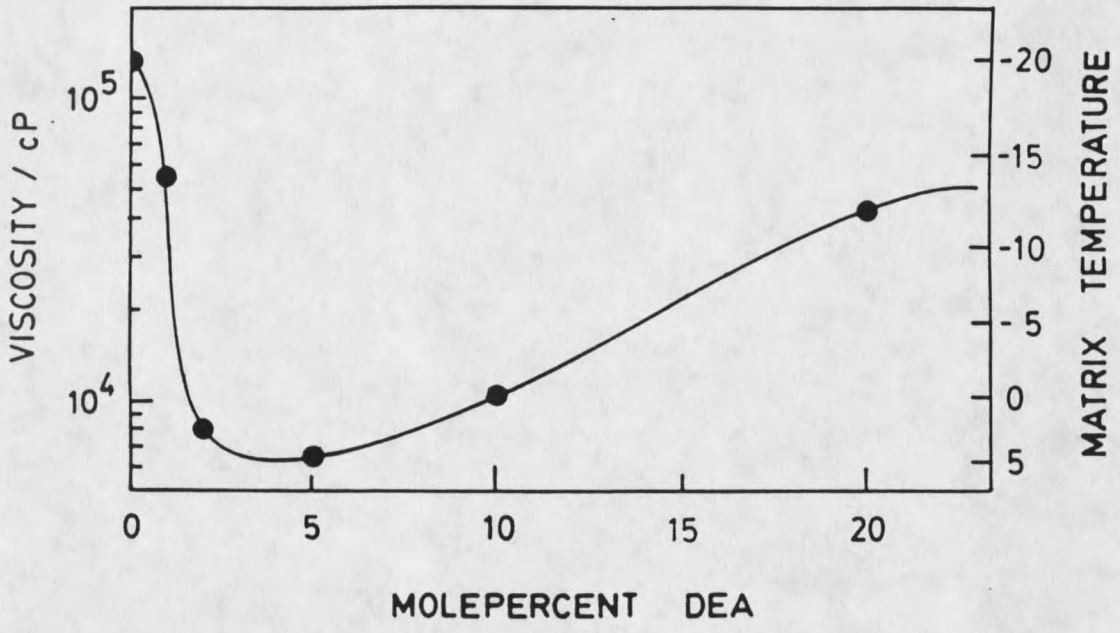

Figure 26. The viscosity at which the noise ion intensity has reached 50%, γ_{deg}, (see text) vs. the concentration of DEA. The scale to the right shows the approximate matrix temperature in degrees centigrade at the corresponding viscosities.

factor of 20. At higher DEA concentrations (over 5 mol%) the trend reverses. Inspection of the spectra shows that the extent of DEA fragmentation decreases monotonically with increasing DEA concentration at constant temperature. Similarly the extent of clustering with glycerol ($DEAH^+(Gl)$) decreases monotonically. This effect by itself should result in a monotonic increase in γ_{deg}. Since the absolute intensities of glycerol fragment ions also decrease with increasing DEA concentration, the reason for the initial

decrease in γ_{deg} in Figure 26 is not an increase in the average excitation energy of desorbed ions, but an increase in the intensities of a number of low intensity background ions. This is illustrated in Figure 27, which shows the sum intensity of four major noise ions (m/z 118,130,148 and 160) as a function of viscosity, at different DEA concentration.

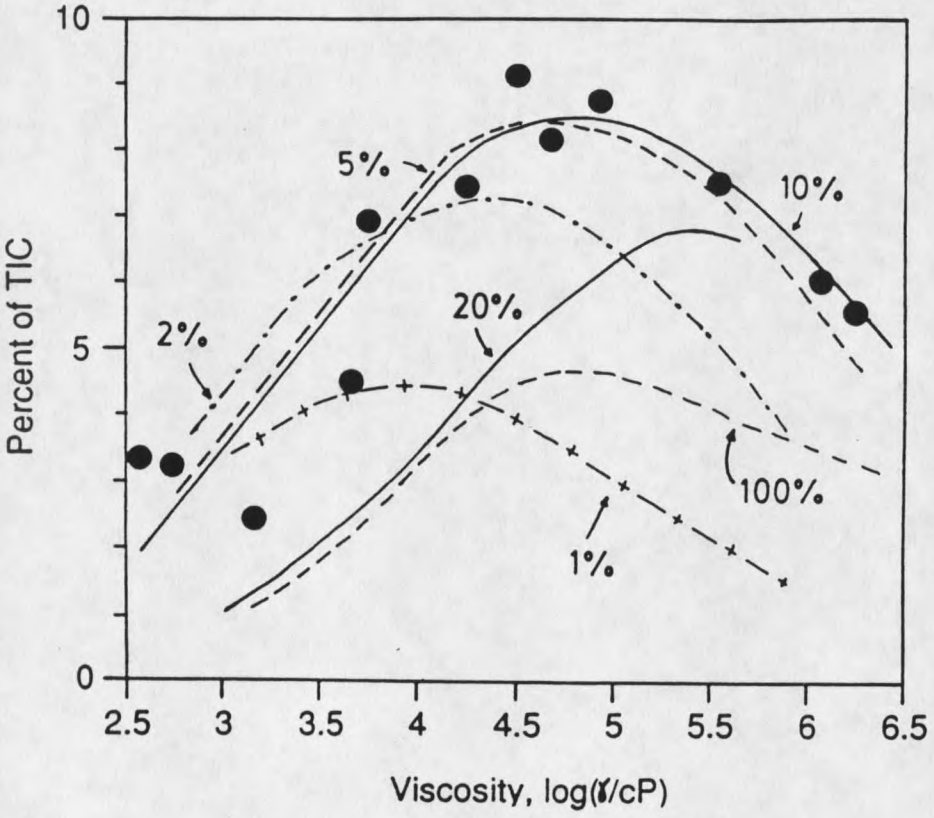

Figure 27. The intensities of four radiation products, noise ions (m/z=118, 130, 148, and 160) in the T_b spectra of 10 mol% DEA in glycerol vs. the viscosity of the matrix for six different DEA concentrations (mol%). Only the experimental points for 10 mol% DEA in glycerol are shown.

It is seen that at a constant DEA concentration, these four ions pass through a maximum. At a constant viscosity value of 4.5, the intensity for different DEA concentrations follows the order:

$1 < 100 < 20 < 2 < 5 < 10$ (mol% DEA)

This agrees well with the trend in Figure 26. Since the intensities of these four ions are observed to increase with fast atom irradiation time and bombardment flux, clearly, they are not fragment or cluster ions but should be produced by radiation induced chemical reactions during the desorption event. It is not surprising to find that some radiation products are retained in the solution and are transported into the bulk of the liquid matrix.

Figure 28 shows the viscosity dependence of intensities of the ions from 1.7 mol% adenosine (Ad) solutions in glycerol There is an observed trend of increasing intensity for chemical noise ions and decreasing intensity in glycerol ions with viscosity. This is noted in both the T_b and c_G studies where the trend is the same as for neat glycerol and the DEA solution. However, relative to neat glycerol (Figure 24) there is a shift in γ_{deg} towards lower viscosity, similar to the shift observed for 10 mol% DEA in Figures 25 and 26. For the T_b study, the expected decrease for the major adenosine ions (m/z 268 and 136) is seen (Figure 28). Figure 28(b) shows that the intensity of the protonated adenosine ion (m/z 268) decreases faster than that of the fragment ion (m/z 136)

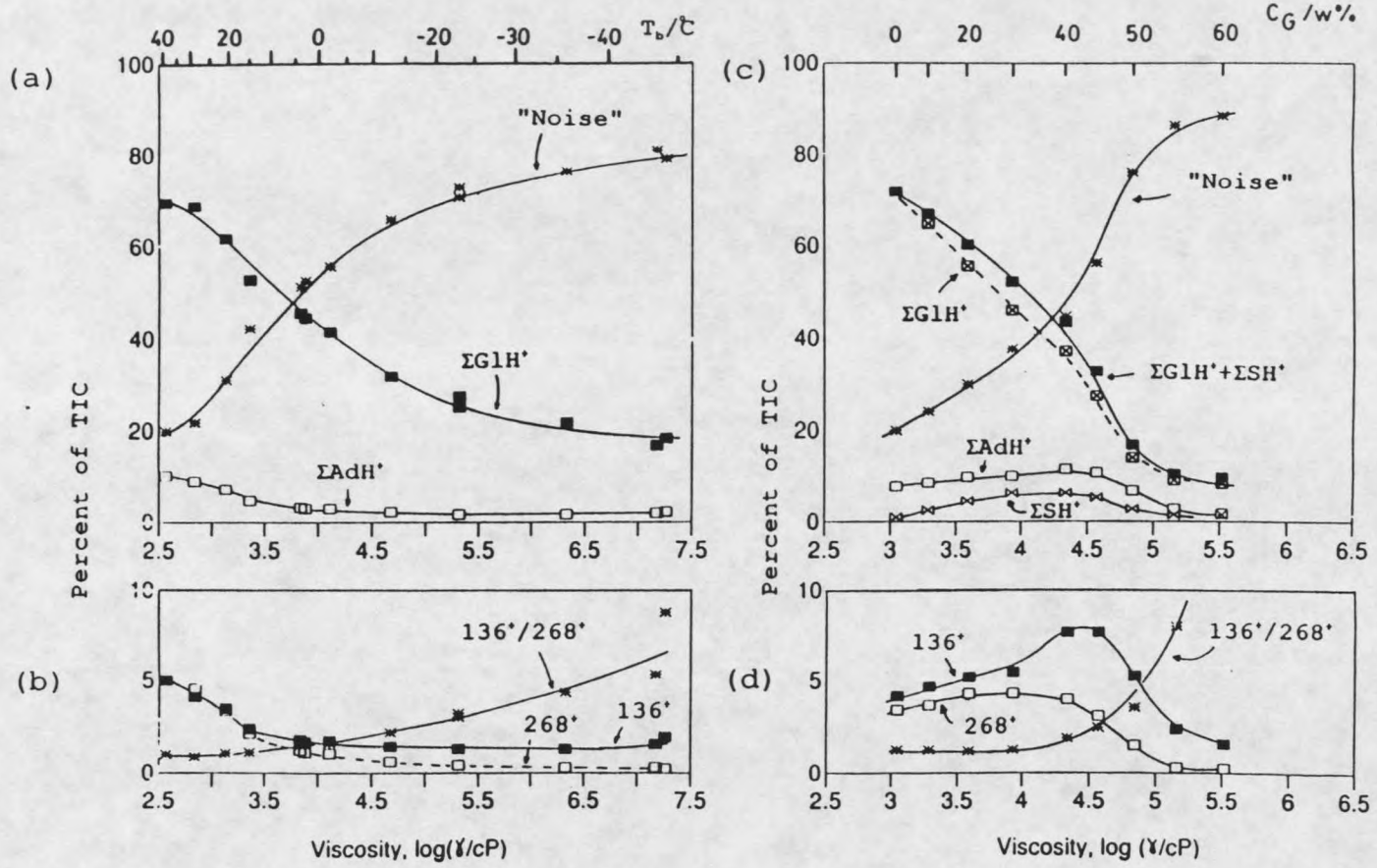

Figure 28. Intensities of major ions vs. matrix viscosity in positive ion FAB spectra of (a-b) 1.7 mol% adenosine (Ad) in glycerol at varying matrix temperature T_b; (c-d) 1.7 mol% adenosine in glycerol/glucose solutions at varying glucose concentration c_G; included in AdH^+ were 268^+ (AdH^+) and the fragment 136^+.

and the 136/268 ratio increases. This is in keeping with the overall pattern of increasing extent of fragmentation with increasing viscosity.

In contrast with the T_b study, the intensity of the adenosine signal in the c_G study was found first to increase to a maximum at about 40 wt% glucose and then to decrease (Figure 28(d)). However, the ratio of fragment to pseudomolecular ions (136/268) still increases with viscosity. The contrasting behavior of the T_b and c_G studies is highlighted in Figure 29.

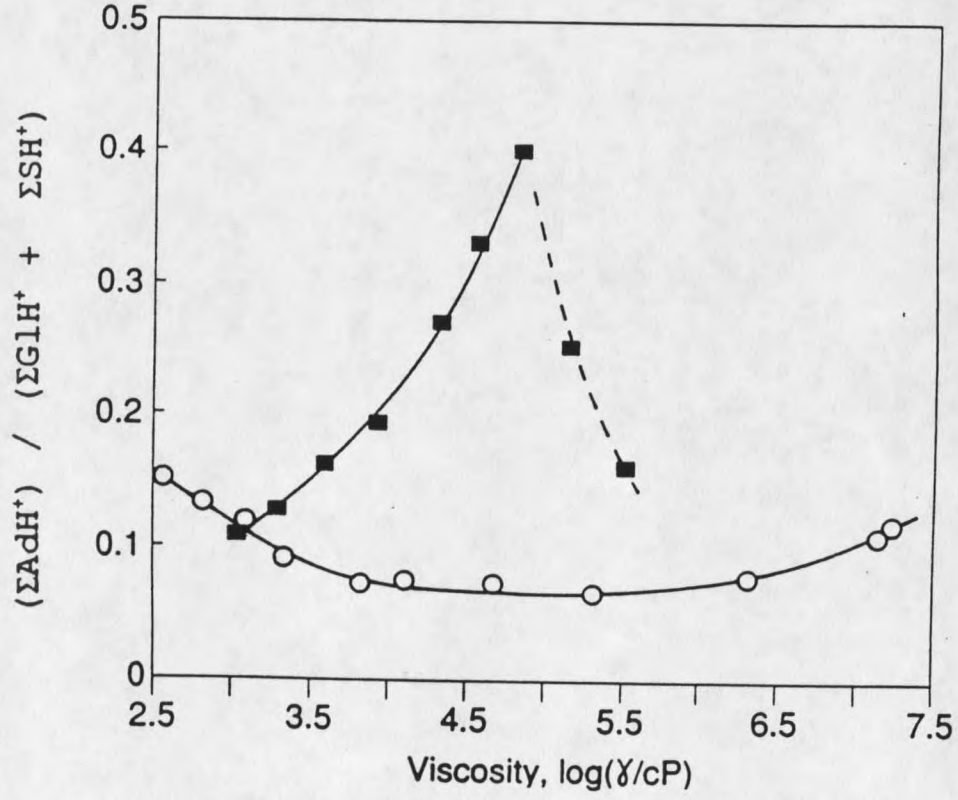

Figure 29. The analyte to matrix ratio AdH^+:(GlH^+ + SH^+) from the T_b(O) and the c_G(■) experiments in Figure 28 vs. the matrix viscosity.

In this figure, the ratio of sum of adenosine ions to sum of glycerol + glucose ions is seen to increase sharply with increasing viscosity in the c_G study, in contrast to the behavior in the T_b study. Similar results were found in the negative ion spectra of the same adenosine solution and also for a solution of adenosine in DEA. A reasonable explanation for this unusual behavior for adenosine will be discussed later.

The viscosity dependence of FAB spectra of solutions of alkali chlorides in glycerol was also investigated. Figure 30 shows the results for 2 mol% KCl in glycerol. The glycerol and chemical noise ions behave as expected. However, in this case the sum of potassium ions (which include the ions: K^+ (m/z 39), K^+(KCl) (m/z 113), K^+(Gl) (m/z 131), and $K^+(K^+(Gl-H)^-)$ (m/z 169)) does not decrease and indeed changes only slightly. At high temperature, the major potassium ions are clusters of the potassium ion with glycerol or KCl. At low temperature, the bare K^+ ion dominates the spectrum. The decrease in the $K^+(Gl)/K^+$ ratio is shown in Figure 30(b). Also shown in Figure 30(b) are the fragment and dimer ratios for glycerol which behave as expected. Thus, both the analyte and the matrix part of the spectrum again degrade with increasing viscosity. It is the analyte-to-matrix ratio that behaves differently than in the previous cases.

It was found by Sunner et al. (1986b) that the alkali ion glycerol cluster ratio ($M^+(Gl):M^+$, M is alkali ion) was closely

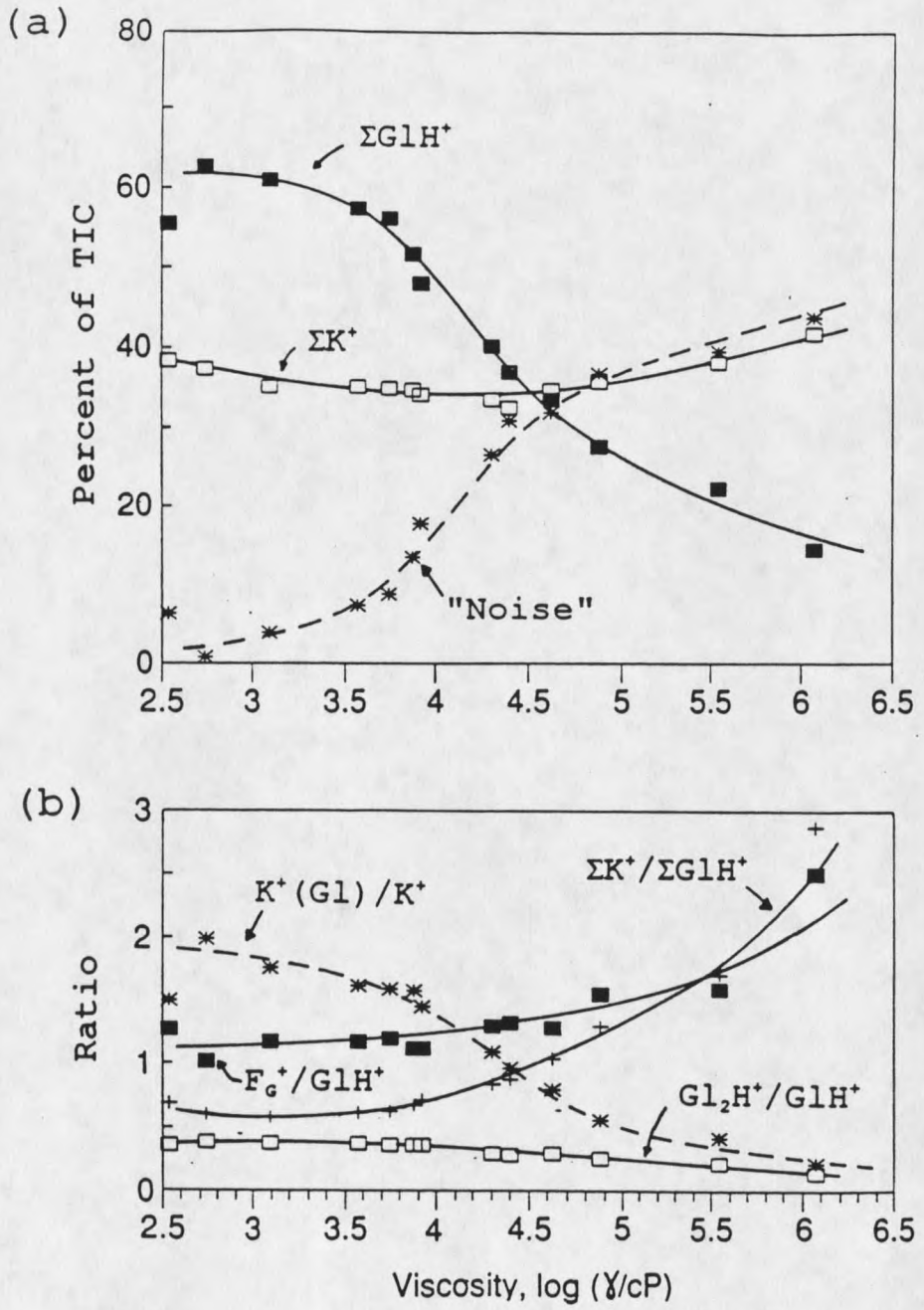

Figure 30. (a) Intensities of major ions in positive ion FAB spectra of 2 mol% KCl in glycerol at varying matrix temperature T_b. ΣK^+ includes ions $K^+(Gl)_n$ and $K^+(KCl)_n$, n=0, 1, 2,...; (b) intensity ratios; for notation see Figure 24.

approximated by an exponential function of the (estimated) ΔH^e for the reaction:

$$M^+(Gl) = M^+ + Gl$$

where as the estimate of ΔH^e, ΔH_0^e for reaction the following was used

$$M^+(H_2O)_2 = M^+ + 2H_2O$$

In Figure 31, $\log(M^+(Gl)/M^+)$ is plotted versus ΔH_0^e for the five alkali ions (Li, Na, K, Rb and Cs) at three different

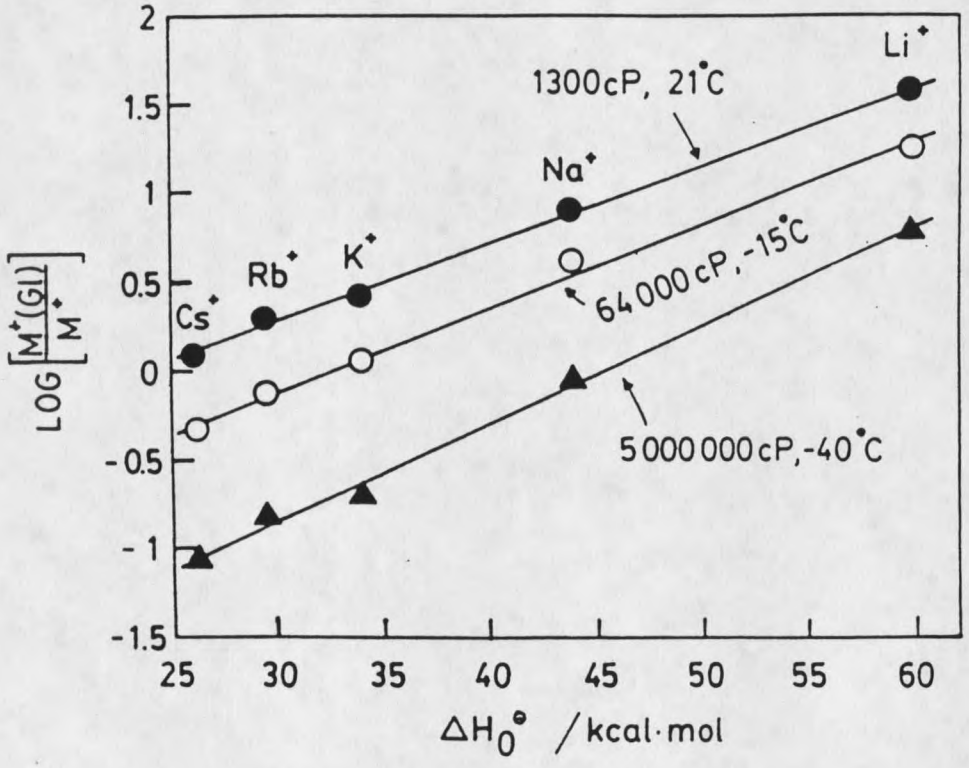

Figure 31. The logarithm of the matrix cluster ratio ($M^+(Gl):M^+$) for M=Li, Na, K, Rb, and Cs, measured in FAB spectra of dilute solutions of the alkali chlorides in glycerol, vs. ΔH_0° for reaction $M^+(H_2O)_2=M^+ + 2H_2O$ at three different values of the viscosity.

temperatures and viscosities. Though the cluster ratio varies substantially, the exponential dependence on $\Delta H_0^{\ominus}$ is seen to hold over a wide viscosity range.

Implications for Mechanisms of Desorption Ionization

The results above can be summarized as follows. Good quality FAB spectra with strong analyte pseudomolecular ion peaks and with a minimum of chemical noise is obtained at a viscosity of ca. 10^3 cP. In contrast, at 10^5 cP and above, the FAB spectra are severely degraded. Typically there is little or no pseudomolecular ion signal, fragmentation is extensive and the spectra are dominated by chemical noise ions. It is obvious that the viscosity of a matrix is a very important factor for obtaining good quality FAB spectra. Further, since the effects on the spectra are quite similar, whether the viscosity is changed by varying the matrix temperature or by varying the concentration of the glucose additive, strongly suggests that the effect of matrix temperature, per se, on FAB spectra is insignificant. One might argue that the temperature affects the internal energy of the solution which in turn may affect the FAB spectra. However, a temperature increase of the matrix from -40°C to +40°C represents an increase in the internal energy of only 0.4 kJ/cm^3. This may be compared with a vaporization enthalpy of ca. 100 kJ/cm^3 for water.

There are two apparent ways in which viscosity can affect

FAB spectra. Viscosity may be important by affecting the physical processes occurring during the impact event. Alternatively, it is the dependence of the rates of different transport properties in the matrix that are important because they affect the chemical composition of the surface. Certainly, the rates of diffusion and convection are strongly viscosity dependent. These two main alternatives for explaining the dramatic viscosity effects are not mutually exclusive. The "viscosity-per-se" effect will be discussed first and then the possible importance of the transport properties.

Viscosity-per-se Effect

To help the discussion of "viscosity-per-se" effect in FAB spectra, a simple physical picture about the desorption ionization process will be given first. This picture is based on the Phase Explosion and Gas Collision Models which were suggested by Sunner et al. (Morales et al. 1989; Sunner et al. 1988c).

When a 10 keV Xe fast atom impacts the liquid matrix, its kinetic energy is deposited in a cylindrical-like cavity that is deeper than it is wide. The energy density (0.01- 0.1 eV $Å^{-3}$) (Whitlow et al., 1987) initially deposited in the central part of this cavity is high enough to allow a high-temperature gas to be formed. In the peripheral region of the cavity the deposited energy density is too low to form a gas. Instead,

the matrix is heated. With the pressure at or very close to zero, the liquid is in a metastable state even before bombardment. As a result of the heating, the liquid penetrates deeper into the metastable region towards the "limit of absolute instability" or the spinodal. Beyond this limit, the matrix is expected to undergo an irreversible expansion and at the same time cool down very significantly. This results in the formation of a low-temperature gas which contains large cool clusters (Sunner et al.; 1988c). The high-temperature gas that is formed at the top of the cavity can expand freely into vacuum. The extent of fragmentation among these molecules depends on the extent to which the energy deposited by the collision cascade has reached internal vibrational degrees of freedom or has resulted in direct bond-cleavages. Excess energy is expected to go into electronic excitation or ionization as well as into kinetic and rotational energy of the ejected molecules and fragments. This general picture explains the desorption ionization process in FAB. The "viscosity-per-se" effect in FAB spectra will then be discussed as follows.

A high-temperature gas that develops at the bottom of the cavity will take a longer time to expand into the vacuum. As the collision cascade energy is becoming equi-partitioned among the different degrees of freedom, the intermolecular collisions become more violent and the pressure builds up. If the walls of the cavity are rigid (at high viscosity), the

pressure will be released upward, imparting a momentum to the gas and a rapid expulsion of all the hot gas is ensured. Severe fragmentation of these excited molecules is expected to occur in the vacuum, resulting in spectra that are dominated by chemical noise and fragment ions. If, on the other hand, the walls of the cavity yield to the pressure (at low viscosity) the gas can expand radially and the pressure drops. The faster the pressure in the bottom of the cavity is released in the radial direction, the smaller is the momentum transfer to the matrix in the upper part of the cavity. The cavity takes a longer time to empty, energy (or heat) transfer to the surrounding liquid will be more extensive, and a larger volume of liquid matrix is expected to undergo a thermal "phase explosion". A good FAB spectrum with pseudomolecular ions and clusters should then be obtained.

The picture described above explains qualitatively the degradation of FAB spectra as the viscosity of the matrix increases. One may ask however if radial expansion of the liquid really can occur during the 10^{-10} to 10^{-9} seconds that the event may take? In order to approach this question, the expansion of a spherical vapor bubble (radius 50 Å) in liquids with different viscosity was calculated. The equation used in this calculation is

$$\rho r\ddot{r} + (3/2)\rho\dot{r} = \Delta P - 4\gamma\dot{r}/r$$

where ρ is the density of the liquid, ΔP is the over-pressure of the vapor beyond what is required to balance any surface

tension, r is the radius of the expanded vapor bubble and γ is the liquid viscosity. The equation here was obtained by integrating the Navier-Stoke equation (Berry et al., 1980).

The results from this calculation are shown in Figure 32. It can be seen that in low viscosity liquids (γ < 10 cP), radial expansion of the deep cavity within a 10^{-9} to 10^{-10} second time frame is quite facile. For example, at very low viscosity (γ = 1 cP), the bubble expands to twice its

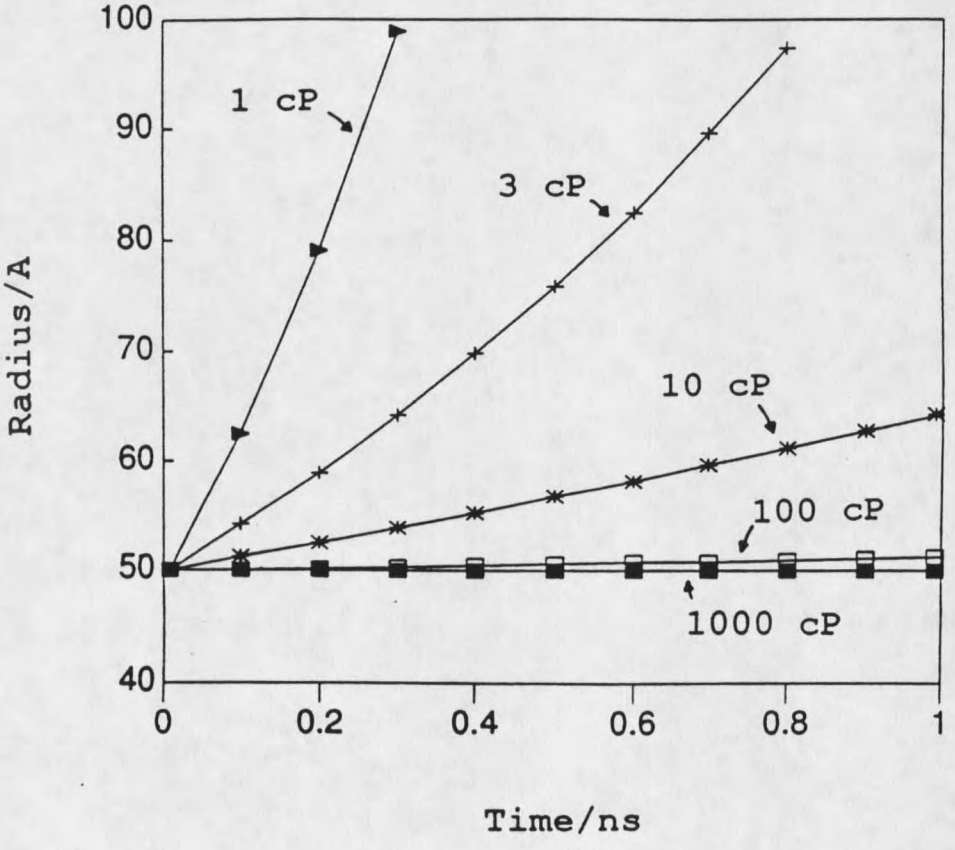

Figure 32. Calculated radial expansion during the first 1 ns of a radius = 50 Å spherical vapor bubble in a liquid with viscosities as shown (see text). The pressure driving the expansion is ΔP = 100 atm.

initial volume in less than 0.2 ns. However, at γ = 1,000 cP, the viscosity of glycerol at room temperature, the calculated volume expansion is only 0.8% after 1 ns. This may seem negligible, but it must be recognized that for a metastable liquid, (dP/dV) is large and a small volume expansion has a large pressure decreasing effect. The calculations also show that most of the viscous resistance to the expansion originates close to the bubble wall, between r and 1.2r. In the FAB event, the liquid in this region is probably at a temperature higher than that of the bulk liquid. The expansion for a given bulk viscosity is then expected to be faster than shown in Figure 32. In addition, there are uncertainties regarding the time scale, the magnitude of ΔP and the applicability of the macroscopic concepts. Thus, the main conclusion that can be made from Figure 32 is only that a radial expansion of the cavity during the FAB event is not unlikely.

The "viscosity-per-se" or radial expansion idea described above has some agreeable features. It explains qualitatively why the spectra become degraded as the viscosity is increased. It also explains the sharp decrease in the intensity of analyte peaks with increasing viscosity in the T_b study (Figures 25 and 29). The reason is that as the gas expulsion becomes faster, less time is available for ion-molecule reactions to occur in the gaseous phase during the desorption event. Thus, with less proton transfer from matrix to

analyte, the analyte to matrix ion ratio is expected to decrease, as observed in Figures 25(c) and 29. This is supported by the result that the T_b dependence of the FAB spectra of DEA in glycerol was well reproduced using a kinetic scheme for ion-molecular reactions (Sunner et al.; 1988a). However, the assumption had to be made that the reaction time for the ions in the gas decreased with increasing viscosity. It is seen that this is in general agreement with the idea of a radial expansion of the FAB cavity.

To explain the high preference observed for alkali ions relative to matrix ions in the FAB mass spectra, it has been suggested that the reactions such as

$$GH^+ + MX = M^+ + XH + Gl$$

occurs in the cavity (M is an alkali ion, X could be Cl^- or $(Gl-H)^-$ and MX is a product of ion-ion recombination reactions). As for high gas phase basicity analytes, one would then expect that the alkali analyte intensity (e.g. K^+ in Figure 30) should decrease with increasing viscosity. However, the initial decrease found for the K^+ in Figure 30 is hardly significant. There are several different possible explanations: 1) the ion-molecule reaction described above may not be important after all; 2) the process responsible for the increase in analyte ion intensity at very high viscosity (see Figures 25(f), 29, 30 and discussion below), may occur at a much lower viscosity for the K^+ ion than for DEA or adenosine; or 3) the decrease observed for high GB compounds may not be

properly understood. An alternative explanation involving transport processes will be discussed later.

It is surprising to find that the analyte signal from K^+ increases at very high viscosity (Figures 25(c)). A tentative explanation for this is that a "preformed ion" mechanism becomes more efficient at high viscosity. This would agree well with a more rapid expulsion process of the desorption volume, since this would result in a larger fraction of the electrolyte ions surviving ion-ion recombination.

Turning now to the results in Figure 31, one may ask why the $M^+(Gl)/M^+$ ratio has an exponential dependence on the bond energy for the $M^+(Gl)$ cluster, ΔH^e, and what the viscosity shifts signify? If it is assumed that the observed effects are entirely due to changes in the internal excitation energies of desorbed ions, a simple analysis is possible. For simplicity, assume that all observed bare M^+ ions were formed from declustering of $M^+(Gl)$ at some stage during the desorption process and also that all $M^+(Gl)$ clusters which had an internal energy larger than ΔH^e dissociated into M^+ and glycerol. The fraction of clusters with energy above ΔH^e can then be calculated and the results are shown in Figure 33(a). The derivatives of the smoothed curves in Figure 33(a) are shown in Figure 33(b). These are approximations of the internal energy distribution of ejected $M^+(Gl)$ clusters. What is particularly noteworthy about these qualitative graphs is the shift towards higher excitation energies with increasing

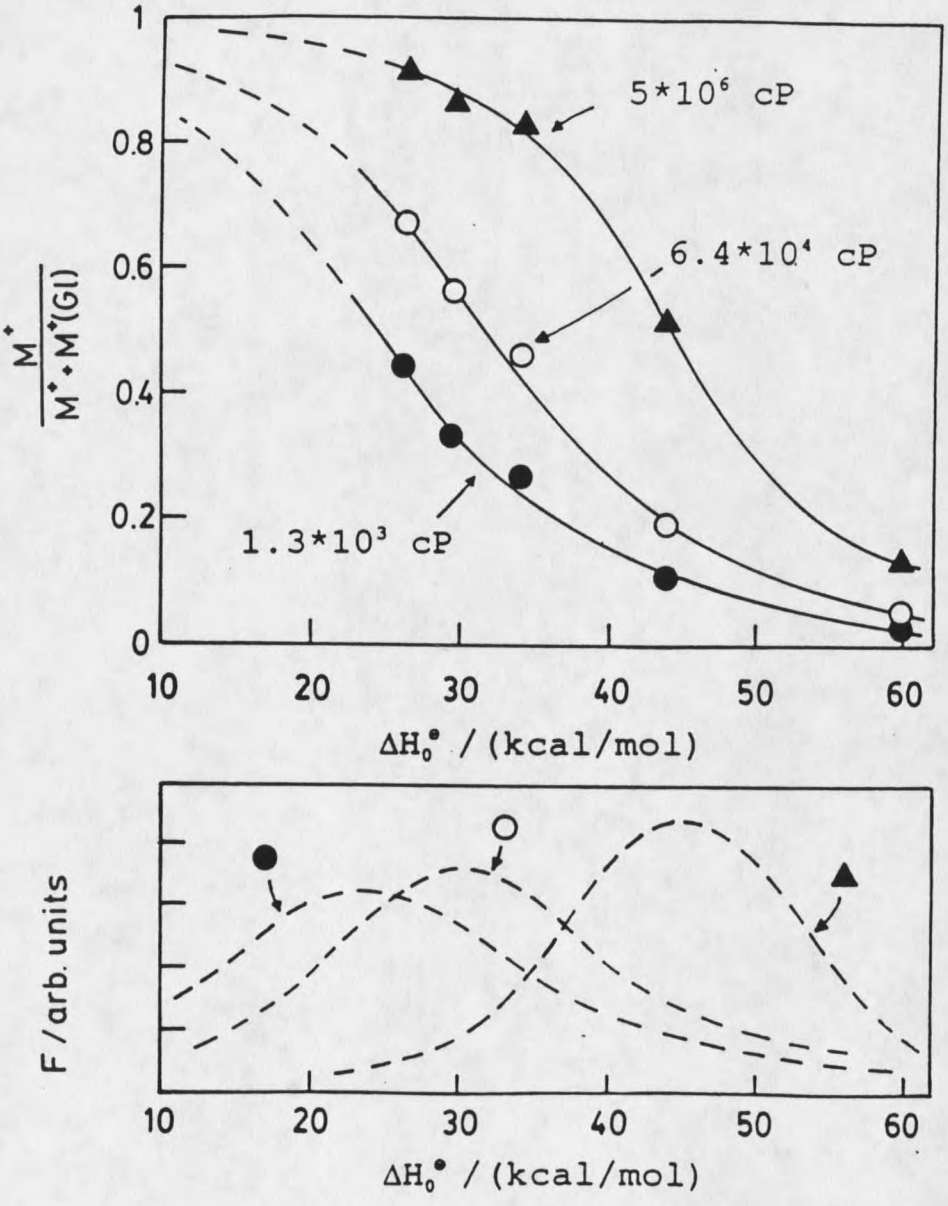

Figure 33. (a) Fraction of ejected $M^+(Gl)$ ions that have an internal energy above ΔH_0°; calculated from Figure 31; (b) the derivatives of the smoothed curves in (a) approximate the distribution of internal excitation energies of ejected $M^+(Gl)$ clusters.

viscosity. gain, this behavior is roughly that expected from the idea of "viscosity-per-se" or radial expansion model.

Viscosity Dependence of Transport Processes

Although the radial expansion concept explains the main experimental observations on the viscosity dependence of FAB spectra, there are still some results that remain unclear. Examples include

1) the initial increase in the intensity of analyte signal in the c_G studies for DEA and adenosine (Figures 25(f), 28(d) and 29)
2) the much faster increase of the fragment ratios for both analyte and matrix in the c_G studies than in the T_b studies (Figure 24)
3) the observed accumulation of radiation-induced products on the surface at high viscosity (Figure 27). These kinds of effects point towards the importance of radiation-induced damage and of transport processes in the liquid/vacuum interface.

As we know, selective evaporation of glycerol molecules from a glucose solution in glycerol will tend to increase the surface concentration of glucose beyond that of the bulk. This tendency is opposed by other processes which include

1) diffusion of glycerol molecules from the bulk matrix toward the surface
2) diffusion of glucose molecules from the surface toward

the bulk matrix

3) sputtering of the glucose-enriched surface by the primary fast atom.

The effect of these processes is a tendency for the surface composition to revert to that of the bulk. If these processes are slow, a solid "sugar crust" could even be formed and this may be the reason why heavily degraded FAB spectra are observed from very viscous solutions which contain more than 50 wt% glucose (Figures 24 and 28). The rate of the transport processes are enhanced by raising the temperature. Since also the viscosity should decrease, one would expect FAB spectra of a 50 wt% glucose solution to improve as the temperature is increased. Instead, the spectra are found to degrade (data not shown). Thus, it seems that the increase in surface viscosity due to selective evaporation of glycerol dominates over the decrease due to the temperature increase. Only at even higher temperatures, where the viscosity of the neat carbohydrate has decreased to 10^5 cP and below, do carbohydrates give good FAB spectra (Ackermann et al., 1985).

The initial increase in the analyte signal in the c_g but not in the T_b studies has a particularly clarifying explanation in terms of the viscosity dependence of the various transport processes that operate at the liquid/vacuum interface. As described before, in the glycerol solution of adenosine, adenosine molecules will be enriched in the surface because of selective evaporation of glycerol molecules in the

vacuum. Again, this tendency is opposed by diffusion and by sputtering. In the T_b study, both evaporation and diffusion are slowed down when the matrix temperature is lowered. In contrast, when glucose is added in the c_g experiment, diffusion is drastically slowed, but evaporation rate still remains relatively fast. The expected result is enhanced enrichment of adenosine in the surface with increasing glucose concentration. This expectation is supported by the observed increase of the adenosine signal in the FAB spectra (Figure 29).

The extent of accumulation of radiation-induced products in the surface layers under high viscosity conditions can be estimated by a simple calculation. The mean-square displacement ($\langle x^2 \rangle$) due to diffusion during a time period(t) is given by (Berry et al., 1980)

$$\langle x^2 \rangle = 6Dt$$

when D is the diffusion coefficient. Its value can be estimated from the Stoke-Einstein law

$$D = \frac{k * T}{6\pi\gamma r}$$

where k is the Bozeman's constant, T is the absolute temperature, r is the radius of the molecule diffusing through a continuous medium and γ is the viscosity of the solution. It is seen that the diffusion coefficient is inversely proportional to the viscosity γ. Substituting the values for glycerol at room temperature ($r \approx 3$ Å and $\gamma \approx 1000$ cP = 1 Pa

s), we find the root-mean-square displacement during 0.1 s to be 6500 Å. If it is assumed that sputtering removes the surface layer of glycerol to a depth of ca. 200 Å in ca. 0.1 s, it is seen that by comparison, diffusion is relatively fast. However, at the higher viscosity of $2 * 10^5$ cP, the root-mean-square displacement is 300 Å, and the rate of diffusion is now comparable to the rate of sputtering. This would be consistent with the dramatic increase in the chemical noise ion intensity at about $2x10^5$ cP as seen above.

The idea of increased accumulation of radiation-induced products in the surface layer under high viscosity conditions offers an alternative explanation to the results shown in Figures 31 and 33. It is possible that as the viscosity increases, these products accumulate in the surface to such an extent that the concentration of intact glycerol molecules significantly decreases. This should decrease the ratio of $M^+(Gl)/M^+$ in Figure 31. However, there is a problem with this interpretation. For example, the parallel increase in the extent of fragmentation of GlH^+ clearly shows that the internal excitation energy of these ions increases with viscosity. There is no reason to exclude the possibility that the same may happen to $M^+(Gl)$ clusters.

From the discussion above, it is concluded that not only the "viscosity-per-se" effect or radial expansion idea but also the viscosity dependence of the transport processes are important in explaining the observation from c_G and T_b studies.

The "viscosity-per-se" effect implies a gradual shift in the desorption mechanism with increasing viscosity. An interpretation of this shift is that the bulk, thermal or quasi-thermal part of the desorption becomes less important at higher viscosity.

ON SENSITIVITY AND COMPETITION EFFECTS IN FAB

The mechanisms involved in FAB and SIMS have been studied by many groups for several years. It is likely that the observed desorbed molecules in the events are from momentum-induced desorption in the collision cascade and also from a thermal spike effect (Pachuta and Cooks, 1987). The former process is similar to that in solid SIMS. The latter may have a character of a bulk, near-thermal transition from liquid to gas (Sunner et al., 1988b). It has been proven that the relative importance of these two extremes vary with the properties of the matrix, analyte and with the projectile used. Ligon and others have pointed out that the surface effect from both matrix and analyte plays an important role in determining the FAB spectra (Ligon and Dorn, 1986a; Naylor et al., 1988). This is also well documented in previous sections of this study.

The idea of "preformed ion formation" has been heavily discussed (Benninghoven et al., 1987; Fenselau and Cotterr, 1987; Todd, 1989). However, as mentioned in the previous section, there are few implications of this effect in FAB. Extensive studies concerning matrix effects in FAB have been conducted by Sunner et al. (1986a). They conclude that the intensity of ion signal is determined mainly by gas phase basicity instead of liquid phase basicity. Based on this idea, a requirement for obtaining an intense protonated

analyte peak in FAB is that the analyte must have a higher GB than that of the matrix molecule. The presence of a second, higher GB analyte will typically result in some suppression of the ion signal from a lower GB analyte (Sunner et al., 1987). It is true that the extent of this analyte/analyte suppression is small, and that suppression effects due to surface activity can be much larger and more significant from a practical point of view (Lacey and Keough, 1989; Naylor et al., 1988). However, the idea of GB effects provides us with greater insight with respect to the DI process.

The mechanistic implication about the DI process from viscosity has been discussed in the last section. Here, the ionization efficiencies of two important categories of preformed ions, namely alkali ions and tertiary alkyl ammonium ions, and the competition effect between them will be discussed. Such results may help to resolve the questions regarding ionization processes in FAB and to build a consistent physical picture of the DI process.

When evaluating different analyte ion signals in FAB under different experimental conditions, it is important to distinguish between sensitivity (ionization efficiency) on one hand and competition effects on the other. The ionization efficiency is judged at low analyte concentrations and refer to the overall efficiency of forming, ejecting and detecting analyte pseudomolecular ions in the spectra. The ionization efficiency of an analyte can be measured by using preference

factors (F_p) which is defined as (Sunner et al., 1986a):

$$F_p = \frac{I_a/X_a}{I_m/X_m} = \frac{I_a}{I_m} * \frac{X_m}{X_a}$$

where I_a and I_m are the intensities of analyte and matrix ions separately, X_a and X_m are the mole fractions of analyte and matrix. It can be seen that F_p measures the sensitivity of the analyte relative to that of the matrix. For a non-surface active analyte, typical F_p values are in the range of 10-20 (Sunner et al., 1986a). This means that for an analyte with F_p value equals to 10, a 10 mol% of the solution will give equal ion intensities to both analyte and matrix ions in the spectra.

Competition effects refer to the suppression of the ion intensity of one analyte by the presence of a second analyte in the matrix. Such suppression effects are frequently observed in FAB at high analyte concentration.

$$R(\text{An 2/An 1}) = \frac{I(An2,An1)/I(An2)}{I(An1,An2)/I(An1)} = \frac{I(An2,An1)}{I(An1,An2)} * \frac{I(An1)}{I(An2)}$$

where I(An1) is the sum intensity of major An1 analyte ions for a solution containing An1 in the matrix only, and I(An1/An 2) is the sum intensity of the An1 ions when the second analyte An2 is also present in the solution. The same definition can be used in I(An2) and I(An2/An1). The sensitivity for an analyte can be seen as a result of competition between matrix and analyte molecules.

Alkali Ions

Figure 34 shows the result of a competition experiment between Na^+ and Cs^+. In each sample, equal amount of NaCl and CsCl were dissolved in glycerol and a concentration study was then conducted. At higher formal concentrations, the analytes were dissolved in glycerol by strongly stirring and gentle heating. However, at certain concentrations, not all the salt was dissolved. This effect will be discussed below. All the major peaks in the spectra were assigned as either major glycerol, sodium or cesium peaks. Mixed clusters, such as $(NaCsCl)^+$ and $(Na_2CsCl_2)^+$ were formally split to sodium and cesium groups. As expected, the TIC of glycerol ions decreases rapidly as the concentration of salt increases, whereas the intensities of sodium and cesium ions increases. At high salt concentration (greater than 7 mol%), the signal of glycerol ions levels out and cesium ions overtake sodium ions (Figure 34(a)). It is also seen that the cluster ratios, $M^+(Gl)/M^+$ for Na^+ and Cs^+ decreases gradually up to about 10 mol% from there both curves level out (Figure 34(b)). Competition experiments between other alkali ion pairs show similar results with the heavier ion winning out at high concentration.

From the results described above and in Figure 34, one may conclude that Cs^+ suppresses Na^+ ions. However, the suppression effect found in Figure 34 is in fact due to NaCl

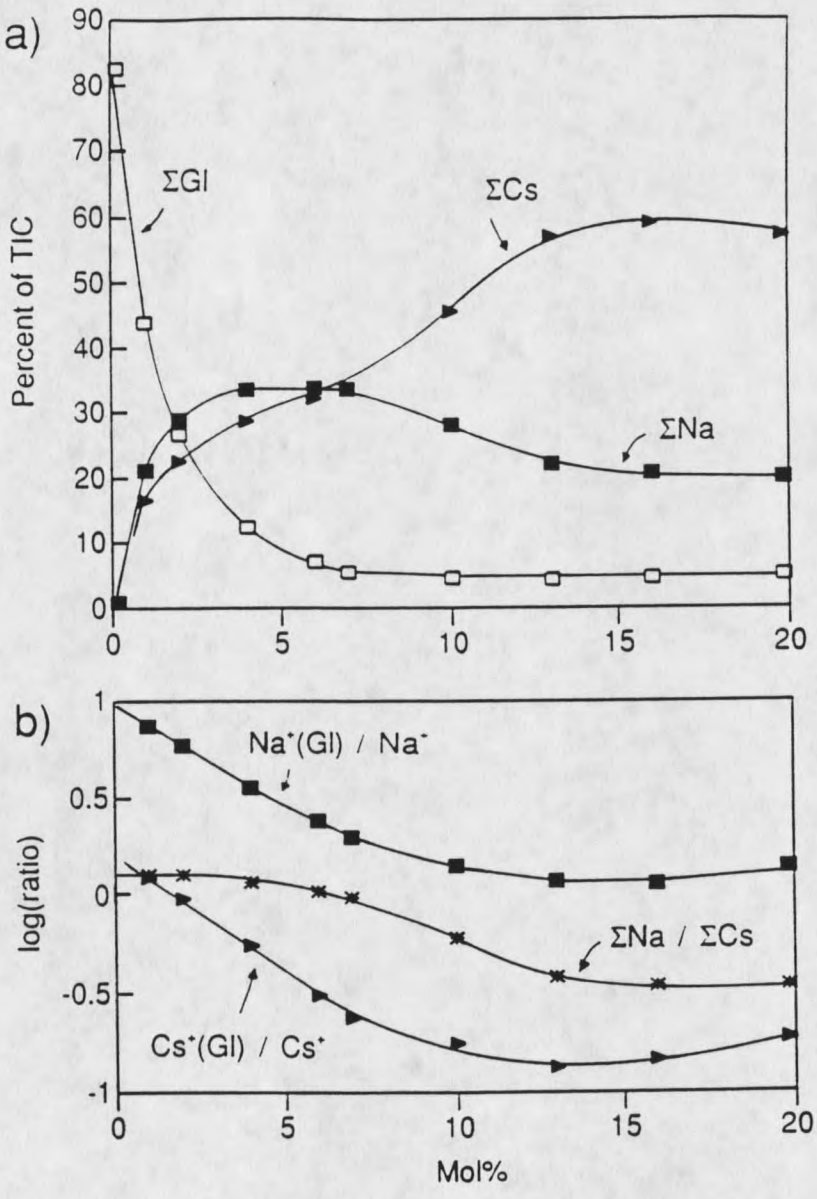

Figure 34. (a) Intensities of major types of ions in FAB spectra of a mixture of equimolar amount of NaCl and CsCl in glycerol as a function of the nominal concentration of each analyte. ΣM^+ includes $Na^+_n\ Cl_{n-1}^+$ and $Na^+(Gl)$ ions where M=Na or Cs; ΣG includes major glycerol fragments ions, glycerol dimer, and protonated glycerol. (b) Alkali ion-glycerol cluster ratios and $\Sigma Na/\Sigma Cs$ ratio as a function of analyte concentration.

not being fully dissolved above 5 mol% and CsCl not above 12 mol%. With the analyte concentration approaching a limiting value, it is expected that the spectra should not change above a certain formal concentration (12 mol% in this study), as observed in the leveling out of the sum of glycerol ion signal as well as of the ratios of $(M)^+(Gl)/M^+$ in Figure 34(b). Further support of this is obtained by analyzing the distribution of the alkali ions in a mixed cluster. Figure 35(a) shows the observed distribution (dark bars) of Na and Cs ions in the cluster $(Cs_nNa_{4-n})^+Cl_3$ from a 4 mol% equimolar solution where both salts are fully dissolved in the bulk glycerol. The gray bars show the binomial distribution, i.e. the relative intensities expected statistically. The expected distribution for each ion in the cluster is calculated by using the following equation:

$$I_n = \binom{4}{n} * p^n * (1 - p)^{(4-n)} ; \quad n = 0,1,2,3,4$$

where p equals to 0.45, the relative concentration of dissolved Cs^+ or Na^+ ions and n is the number of Cs^+ ions in the mixed cluster. It can be seen that the experimental results match well with the statistical expectation. Figure 35(b) shows the same cluster-distribution but at a nominal concentration of 13 mol% for each salt. Because the cesium ion signal is nearly three times stronger than that from sodium ions in this solution (Figure 34), this leads to the tentative conclusion that the concentration of dissolved

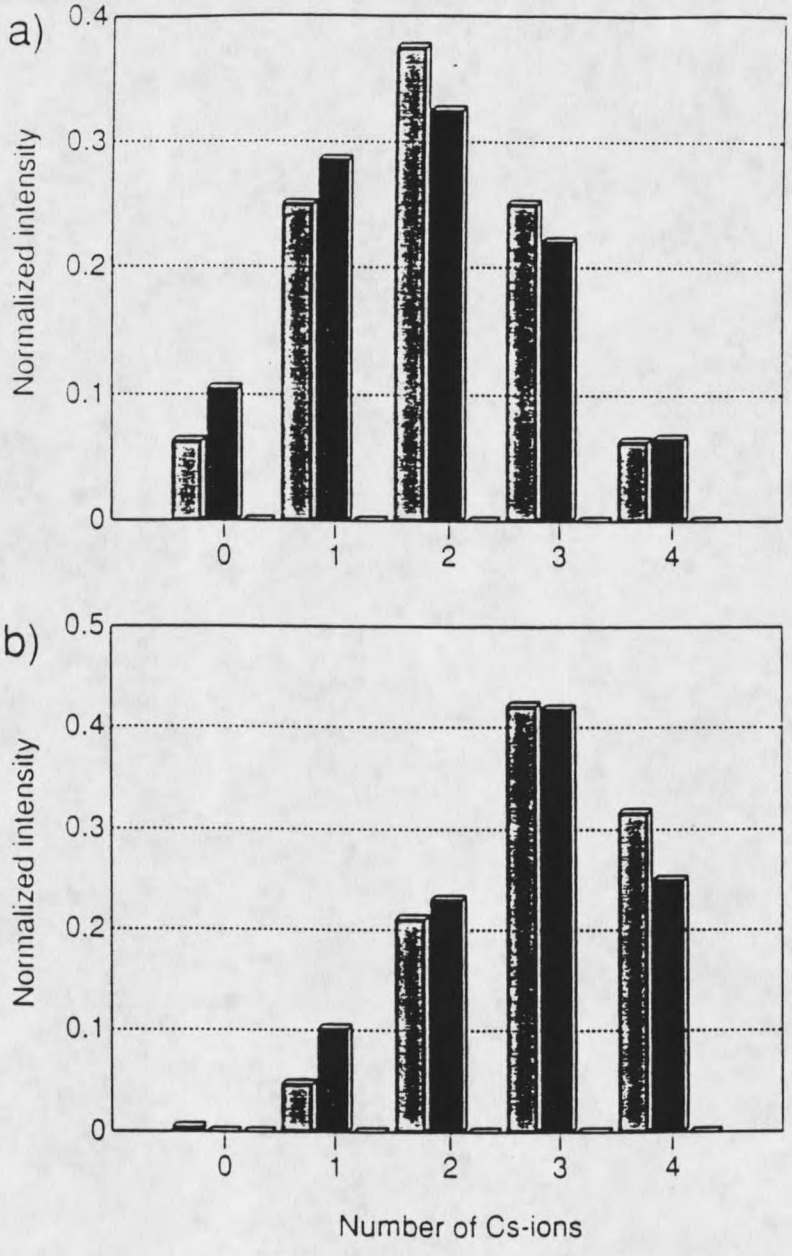

Figure 35. (a) Normalized intensity distribution of $(Na_nCs_{4-n})^+$ clusters in the 4 mol% spectrum used for Figure 34. Black bars: Experimental distribution; Grey bars: Calculated distribution, see text. (b) Same as in (a) but for a nominally 13 mol% solution.

cesium ions is also three times higher than those of sodium ions (i.e. Cs:Na = 0.75:0.25). The statistical cluster distribution for $(Cs_nNa_{4-n})Cl_3^+$ is then recalculated by using a p factor equal to 0.75. The distribution from experimental results is seen to shift toward a higher number of Cs^+ ions, which agrees well with the calculated value. Two important conclusions can be drawn from these results:

1) The cluster formation process is nearly statistical.
2) The energy differences between these clusters are not large enough to significantly affect the intensities.

This is consistent with cluster formation from a homogeneous solution.

As discussed in the last section, it is important to realize that the alkali concentration in the near surface region will be higher than in the bulk because of selective evaporation of glycerol over the non-volatile alkali salts. At low concentrations we expect the salts to be in solvated form whereas at high concentrations unknown fractions of the salts will be in crystalline form. However, from the discussion above, the crystallized CsCl and NaCl in the matrix does not seem to be involved in the formation of significant amounts of either bare alkali ions or clusters ions under these conditions.

Results like those above strongly suggest that there is little or no competition between alkali ions during the FAB process. This means that the reaction

$$Na^+(g) + CsCl(g) = Cs^+(g) + NaCl(g) \qquad H = -21 \text{ Kcal/mol}$$

which contributes to the competition effect may not be important, even though it strongly favors the products.

The F_p for the alkali ions are ca. 20 under this study (calculated from the results in Figure 34). However, it is noteworthy that there are small but reproducible differences between the sodium and cesium ions (i.e. $F_p(Cs^+)/F_p(Na^+)$ = 0.8). The effect of this difference is not only shown in Figure 34 but the distribution of mixed clusters was also somewhat Na^+ shifted, as shown in Figure 35(a). The reason for this difference is unknown.

A viscosity study of 1 mol% NaCl and CsCl in glycerol solution was performed to provide more insight into the competition effect in FAB. Figure 36 shows two FAB spectra of a solution obtained at 8 and -42°C. Spectra like these were used to prepare the graphs in Figure 37(a) which relate the intensity of glycerol, cesium, and sodium ions as a function of matrix viscosity. Most noteworthy in both figures is the large increase in the cesium ion intensity below 0°C, > ca. 10,000 cP. Also a high viscosity glucose solution (40% (w/w) glucose, ca. 10,000 Cp), showed a strong cesium ion enhancement (data not shown). Figure 37(b) shows the ratio of $M^+(Gl)/M^+$ as well as the ratio of cluster and dimer ions of glycerol. The gradual decrease in these ratios with increasing viscosity is in line with previous observations. Furthermore, the lower value for $Cs^+(Gl)/Cs^+$ is in agreement

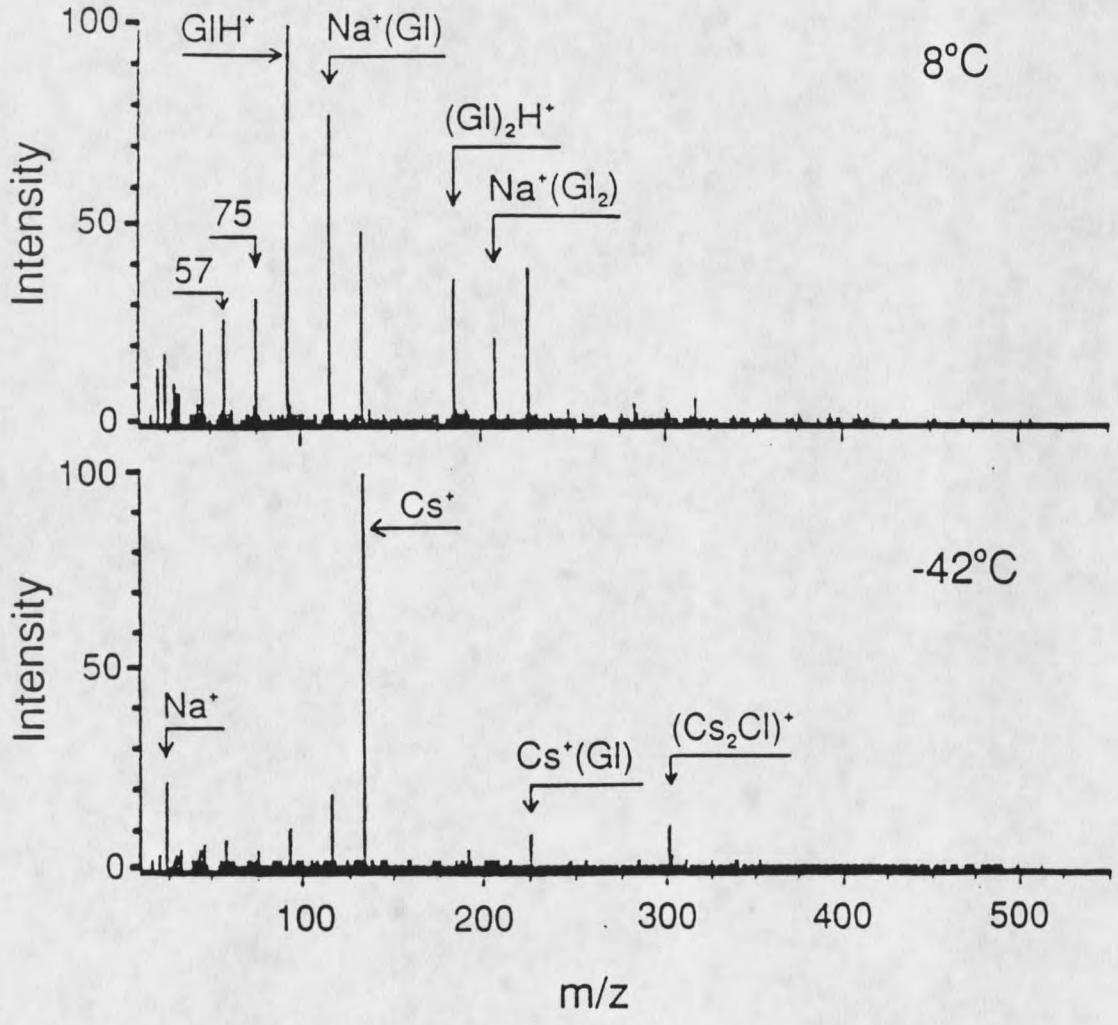

Figure 36. FAB spectra of a solution of 1 mol% NaCl and 1 mol% CsCl in glycerol at 8°C and -42°C.

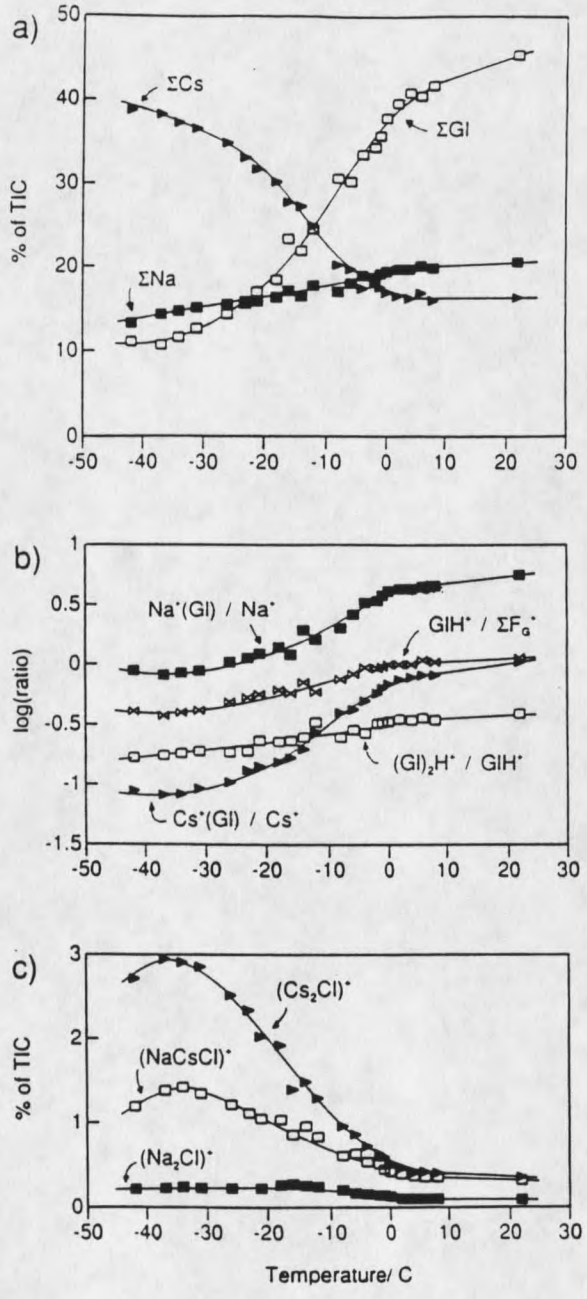

Figure 37. (a) Intensities of major types of ions in the FAB spectra of a mixture of equimolar amounts of NaCl and CsCl in glycerol as a function of the matrix temperature. See also Figure 34. (b) Glycerol cluster ratios for Na^+ and Cs^+ and glycerol fragment and dimer ratios in the spectra in (a). (c) Intensities of $(M_2Cl)^+$ clusters, with M=Na or Cs.

with previous results where $M^+(Gl)/M^+$, at constant matrix viscosity, has an exponential dependence on bond strength between the alkali ion and the glycerol molecule. The intensity trends for the other alkali ions are as might be expected between Na^+ and Cs^+. Furthermore, the observed trend holds over a wide concentration range, from 0.2 to 5 mol%.

The dramatic increase in the signal arising from cesium ions at very high viscosities (>ca. 10,000 cP) is unexpected and difficult to explain. Since an important part of FAB mechanism may be involved in this unusual behavior, different possible explanations will be given here. From the viscosity studies in a previous section, it was concluded that the dramatic changes of FAB spectra at high viscosity were due to changes in the transport properties in the surface layer and to a gradual change in the desorption mechanism. It is true that a change in transport properties such as evaporation rates, diffusion rates, or relative desorption yields will change the relative surface concentration of the analyte. The results presented in Figure 37 could be explained if the Cs^+ concentration increased relative to that of Na^+. However, it is difficult to imagine that the transport processes would strongly favor Cs^+ enrichment or Na^+ depletion in the surface. This is because at room temperature, the effect of selective evaporation of the matrix molecules will result in an enrichment of both salts to the same extent in the surface layers. Also, at low temperatures, enrichment due to

selective evaporation of the matrix should be insignificant.

The most likely explanation for an increased relative Cs^+ concentration would be that the sodium but not the cesium salt precipitates at very high viscosity. This is similar to what was observed in samples of high salt concentration. One major problem with this explanation is that the increase in intensity for cesium ions relative to that of sodium ions is also observed for the solution which contains only very low salt concentrations (0.1 mol%). Under such low concentration, the precipitation of alkali salt in the surface layers due to selective evaporation of matrix molecules is almost impossible. A tentative conclusion can then be made that the precipitation of sodium salt in the surface does not occur and that the increase in the intensities of cesium ions at high viscosity is due to the preference factor (F_p) of cesium ion.

Two possible explanations can be made for an increase in $F_p(Cs^+)$ at very high viscosity. Based on this idea from the phase explosion model, it was suggested that particle-induced desorption from volatile matrices (e.g. glycerol) tend to leave behind a cold matrix after the ejection process. This cooling is caused by the mainly entropy driven, endothermic, spinodal-like disintegration of the matrix. Thermal emission would not occur. However, if the matrix surface is near solid, mainly collision cascade, momentum-induced desorption will occur. In such a case, a "hot spot" must remain and some thermal ion emission may occur. It is well known that thermal

emission of Cs^+ occurs at a considerably lower temperature than does Na^+. For this reason, $F_p(Cs^+)$ becomes larger than $F_p(Na^+)$ at very low temperature and the FAB spectra will be dominated by the cesium ions.

Another explanation for the increase of $F_p(Cs^+)$ at high viscosity is based on a very speculative idea of ion-electron recombination reactions in the desorption event. In FAB, the ion yield is usually very low, 0.1 to 1. This means that the majority of charged alkali ions in the solution must be ejected as neutrals. It is well known that in high pressure and high ion density systems, ion-ion recombination is the major process limiting the ion ejection current. The rate of this process would be high for all the species involved here. In contrast, electron-positive ion recombination is generally fast for all ions except atomic ones (Biondi, 1976). The reason is that the formed neutral atoms are super-excited and have no ready means of dissipating the energy except to re-eject the electron. Thus, an enhanced ion ejection efficiency is observed for those atomic cations that are known to have slow electron-ion recombination rates. However, a full discussion of this subject requires a better understanding of the declustering processes in the early stage of the FAB process. It suffices to conclude here that any real connection between electron-positive ion recombination rates and FAB ion intensities remains an interesting possibility only.

Tertiary Ammonium Chloride vs. Alkali Salts

As we know, tertiary ammonium ions observed in FAB spectra must be "preformed" which are similar to those from alkali ions. Because of their hydrophobic alkyl chains, tetraalkylamines tend to be surface active and consequently have a large F_p value. The F_p value for the least surface active compound in this series-tetramethylamine (TMA) is ca. 35 which is still about two times higher than those of the non-surface active alkali ions. Because surface activity effects would needlessly complicate the interpretation, TMA^+(with Cl^- as its counter ion) was chosen as a model compound for ammonium ions to achieve the goals of this portion of the study.

The concentration dependence of the FAB spectra of TMA in glycerol was studied (data not shown). The FAB spectra showed that with increasing TMA concentration, there is a characteristic decrease in intensity of the glycerol ion signal and an increase in the TMA ion intensity. Generally speaking, the behavior of all the major types of ions in the spectra is very similar to what was reported for diethanolamine (DEA) by Sunner et al. (1988a). In their study, the concentration dependence of DEA in glycerol was explained by a detailed kinetic model. The basic part of this model is a transfer of ionization from protonated matrix molecules to analytes that occurs continuously during the

desorption event (i.e. (Matrix-ions) → (DEA-ions)). A similar explanation is reasonable for TMA because of the relative stability of the TMA ions (i.e. (Matrix-ions) → (TMA-ions)). For DEA, the logical choice is a proton transfer reaction:

$$GlH^+ + DEA = DEAH^+ + Gl$$

but other reactions must be involved for TMA (since it is desorbed "preformed"). Because of the low secondary ion yield, most of the TMA-ions are ejected in neutral form, for example (TMA^+Cl^-) or ($TMA^+(Gl\text{-}H^-)$). Therefore, a reaction such as the following is proposed to explain the formation of the TMA^+ in FAB:

$$GlH^+ + TMA^+Cl^- = TMA^+ + Gl + HCl$$

Since the proton affinity (PA) difference between Cl^- (Hotop and Lineberger, 1985) and Gl (Sunner et al., 1986a) (124 Kcal/mol) is larger than the electrostatic interaction between TMA^+ and Cl^-, the reaction is exothermic. This reaction is analogous to the reaction:

$$GlH^+ + NaCl = Na^+ + Gl + HCl$$

previously proposed to occur in FAB by Keough (1985) and Sunner et al. (1986b). Several other reactions such as:

$$X^+ + TMA^+Cl^- = TMA^+ + (X - H) + HCl$$

X= primary ion or glycerol fragment ion produced in the collision cascade.

are also similar to the above reaction and they would also be expected to contribute to the overall reaction.

With regard to competition effects between TMA and other preformed ions (e.g. NaCl), the expectation is that these should be determined by the difference in bond energy between ion pairs like, Na^+Cl^- and TMA^+Cl^-. With these bonds being purely electrostatic, the larger preformed ions are expected to dominate in the spectra. However, the stability differences are small and heavy ions must be transferred in the reaction; therefore, competition effects may be small. This can be seen as a slight suppression of Na^+ by TMA^+, observable only at high TMA concentration (5 mol%), where TMA^+ dominates the FAB spectrum. It should be remembered that the surface activity of TMA is relatively high to that of Na^+. Thus, the effect from surface activity needs to be considered when one evaluates the competition effect between both analytes.

In contrast to the very small competition effects observed between TMA and alkali ions, there is strong suppression of neutral Bronsted bases (e.g. DEA) by TMA (Figure 38). Thus, ionization transfer from DEA to TMA seems to take place:

$$DEAH^+ + TMA^+Cl^- = TMA^+ + DEA + HCl$$

Such reactions should still be exothermic, although the GB of DEA is ca. 20 Kcal/mol higher than that of glycerol. Protonation of DEA, by addition of acid to the matrix solution had no significant effect on the suppression of DEA by TMA. This is in line with previous conclusions about the ineffectiveness of acid addition.

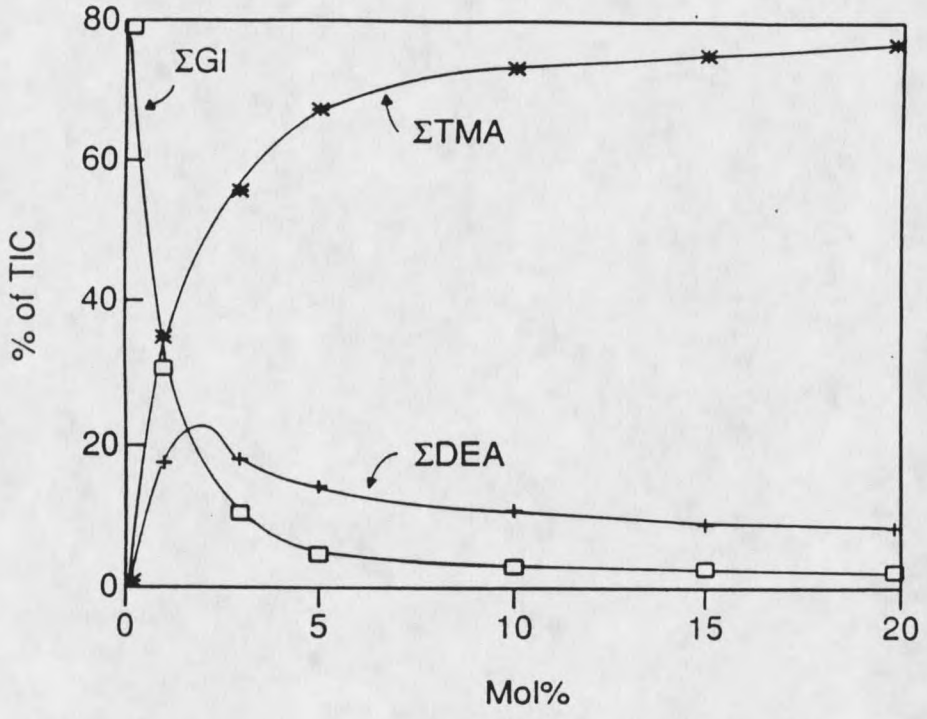

Figure 38. Figure Illustrates suppression of DEA ions by the presence of tetramethylammonium at higher analyte concentrations.

The temperature study of a solution which contained 1 mol% each of CsCl and TMA-Cl in glycerol was performed (Figure 39). As in the previous study, the sum of the cesium ions behaves as before; the sum of the TMA ions behaves similarly to the sum of sodium ions in that the intensity is relatively constant over the whole range. The glycerol ions which contain pseudomolecular ions, fragments and clusters show a normal behavior, reflecting the tendency for the spectra to "heat up" with decreasing temperature. The ratios of

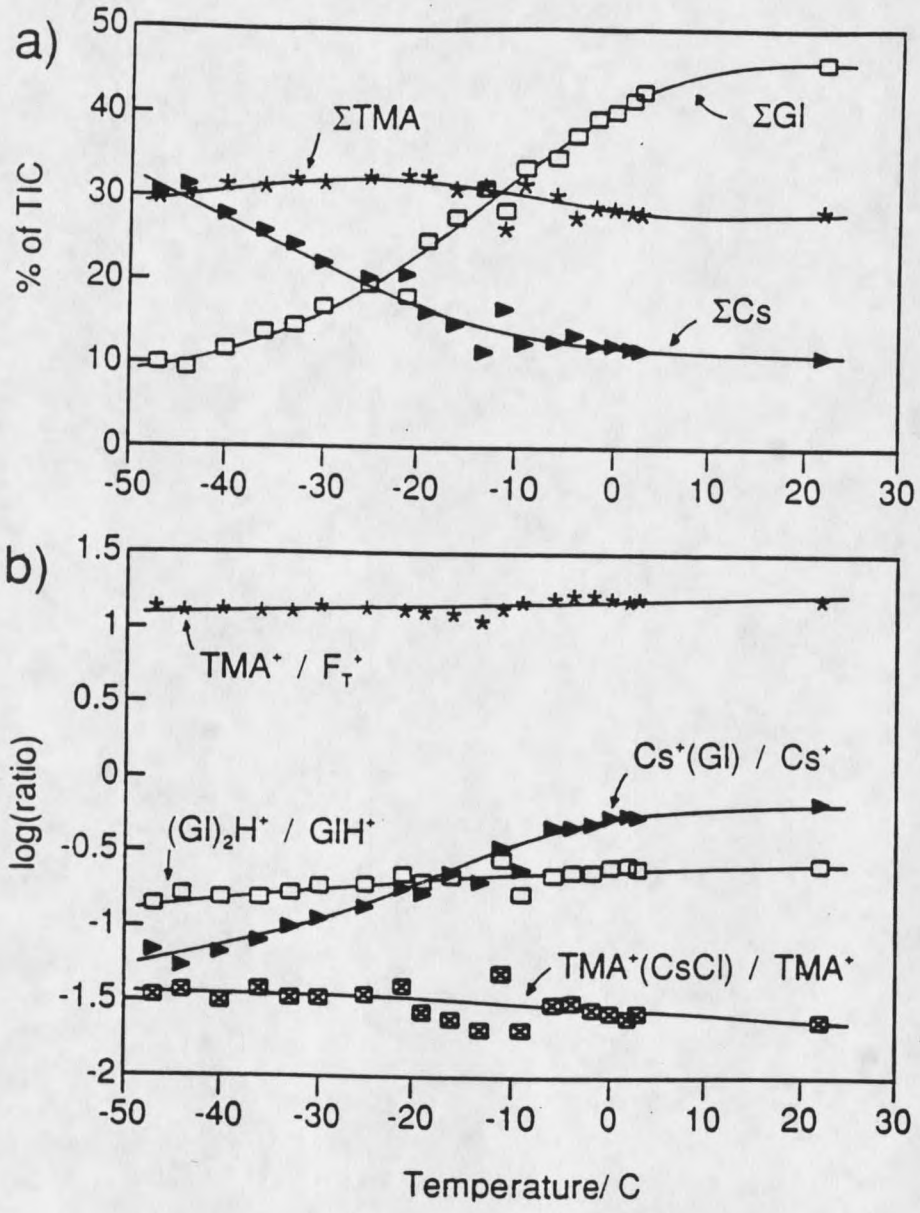

Figure 39. (a) Matrix temperature study of an equimolar solution off CsCl and TMAC. At low temperature, the Cs-signal is enhanced. (b) Fragment and cluster ratios from the spectra in (a).

$(Gl)_2H^+/GlH^+$ and $Cs^+(Gl)/Cs^+$ behave as expected. The decrease in $TMA^+/58^+$ ratio with temperature, where 58^+ is the only major TMA fragment, reflects the internal excitation energies of the desorbed molecules which increase at high viscosity. The explanation for all of the phenomena observed here has been discussed in detail in the last section. It seems that the second analyte in the matrix does not change the desorption process to any great degree. This is true even when the viscosity of the matrix is very high.

MOLECULAR DYNAMICS SIMULATION OF BULK DESORPTION

As discussed before in the previous section, there are major differences between solid and liquid SIMS (or FAB) with respect to the internal energies of desorbed ions and to the neutral yield. The experimental indications are that this may be attributed to a difference in the mechanism of desorption in the two techniques. In solid SIMS, molecular desorption may occur from the uppermost surface layers by momentum transfer in the collision cascade. The process seems to result in a low yield and high internal energies in the desorbed molecules. In liquid SIMS, on the other hand, a "bulk desorption" mechanism is suggested as opposed to momentum-induced desorption. "Bulk desorption" refers to a "phase transition" from liquid to gas presumably in a surface cavity or crater such that the neutral yield is high, ca. 1,000 in the case of glycerol (Jiang et al., 1988; Wong and Rollgen, 1986). Probably, all the molecules in a cavity centered around the original collision cascade are desorbed. The region where these processes occur is often referred to as the "selvedge". Because of their high yield, laser desorption and plasma desorption are also most similar to bulk desorption processes.

As mentioned in the Introduction, a number of studies have explored how the impact energy couples with the matrix and how this energy subsequently causes the ejection of intact

molecules in the different bulk desorption methods. From such studies, numerous models about the desorption event have been presented and have recently been reviewed by Pachuta and Cooks (1987) and de Pauw (1986). These models differ in their predictions on the degrees of freedom of the excitation energy resided during the desorption process. In one extreme view, the excitation energy couples into center-of-mass translation motion of the molecules or clusters without exciting intra-molecular degrees of freedom; the matrix is "mechanically blown apart" into cold fragments or droplets. In the opposite extreme view, the energy is at some point nearly equipartitioned among the different degrees of freedom and statistical methods can be used for the analysis of the desorption process.

Molecular dynamics (MD) calculations have been of great importance in many areas in physics and chemistry by simulating the behavior of molecular and atomic systems (Hedin et al., 1985; Ciccotti, 1986). Because of the complexity, short time and small size scales of the particle-induced desorption process, MD would seem to be ideally suited to resolve the difficult problem of the mechanism of bulk desorption. Indeed, MD simulation has been successfully used by Garrison et al. (Garrison and Winograd, 1982; Garrison and Winograd, 1983; Garrison et al., 1988) to elucidate the momentum-induced desorption process in molecular SIMS. Further, Barber et al. (1982) simulated a two-dimensional FAB

sputtering process from solid KCl. The ejection of large biomolecules in PDMS were simulated by Fenyoe et al. (1989) and also by Hilf et al. (1989). In Fenyoes' calculation, each biomolecule was modelled as a "soft" Lennard-Jones sphere. The spheres along the track of the MeV particle were assumed to undergo an instantaneous expansion. This resulted in an explosive, ejection process involving also the spheres outside of the track.

In their phase explosion model, Sunner et al. (1988b) pointed out that the bulk desorption process may be a result of the matrix becoming mechanically unstable as a consequence of bulk heating. The ensuing spinodal decomposition, a spontaneous phase transition into liquid and gas, is predicted from classical (and statistical) thermodynamics. Although the spinodal decomposition process is well-known for the system such as binary alloys, the spinodal liquid-to-gas transition has not been known to occur; instead homogeneous nucleation is observed (Sunner et al., 1988b). However, the spinodal transition has indeed been observed in MD simulation by Abraham et al. (1982). In their calculation, a two-dimensional Lennard-Jones fluid with 5,000 atoms was used. The system was initialized by running the simulation for a few ps at a temperature slightly above the critical point. As the temperature was suddenly dropped below the critical point, a spinodal state was entered. The system was then followed for 450 ps. In the early stage, $t < 30$ ps, the process is

characterized by "wave creation and growth" during which highly interconnected, high density regions develop and the local density maxima approach that of the condensed liquid. At longer times the simulation is characterized by "wave necking" or breakup and by cluster growth by condensation and coagulation. This simulation gives credibility to the idea that such spinodal-like transitions may occur under proper conditions.

Though the simulation presented by Abraham et al. is thought-provoking it is also clear that the conditions used are different from those of desorption ionization:

1) In Abraham's simulation, the spinodal states are approached through the critical point, whereas in DI they are approached from high density liquid side.
2) The excitation process is more complicated in DI, whereas in Abraham's simulation the system is designed initially equilibrated.
3) In DI, the system is expanding as opposed to the constant volume used by Abraham et al..
4) Abrahams' calculation is isothermal.
5) A real system is three dimensional.
6) Intramolecular degrees of freedom are likely important for BD in molecular matrices.

If the spinodal description of the BD process is correct, we are dealing with a fundamental phase transition that is of extraordinary interest not only for mass spectrometry but for

science in general. Most of what we know about the process is based on theory and conjecture. The goal of this program of MD simulations is then to gradually "develop our intuition" about the bulk desorption process by performing increasingly realistic simulations. It is of particular interest to see, whether spinodal-like transitions occur in the thermal spike regime.

MD Simulation for Neat Matrix

In Figure 40, snapshots of a MD result at -0.2, 0.55, 7.3, and 15.3 ps after impact of a projectile on a neat 2-dimensional matrix, T = 300 K are shown. The target matrix consisted of 1512 atoms (36 by 42) with a mass of 40 Dalton (D). The atomic interactions were Lennard-Jones 6-12 potential

$$V(r) = 4 * \epsilon * \left(\frac{\sigma^{12}}{r^{12}} - \frac{\sigma^{6}}{r^{6}} \right)$$

where ϵ is the depth of the minimum in the potential, σ is the intermolecular distance at which V(r) = 0 and r is the intermolecules distance. For this simulation, ϵ = 5.7 kcal/mole and σ = 3.8 Å were used in calculating V(r). The projectile had a kinetic energy of 200 eV and a mass of 130 D. During the initial thermalization of the matrix, prior to the projectile impact, the matrix was allowed to expand. However, in order to provide some containment of the matrix, the outermost atom layers were given a mass of 500 D.

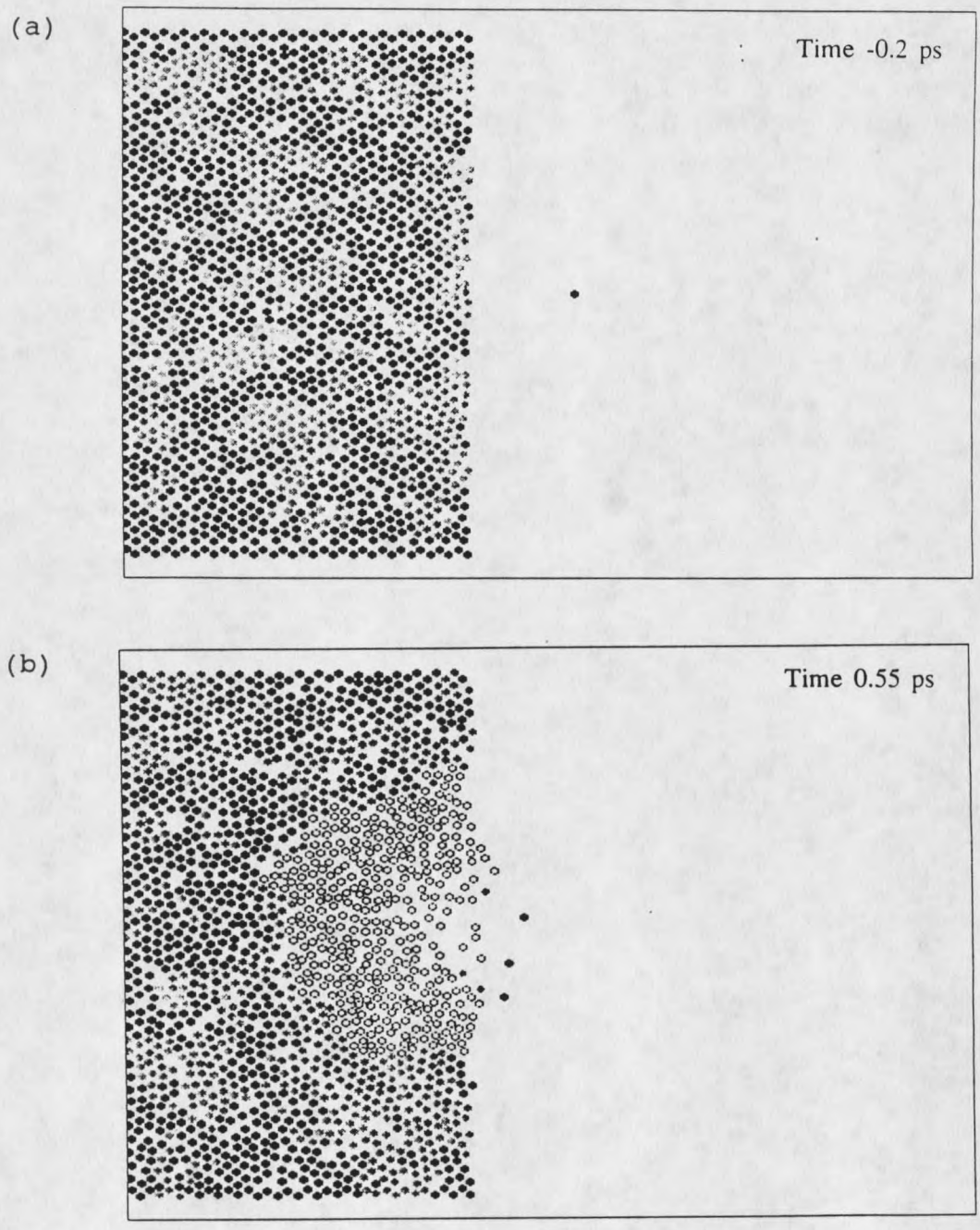

Figure 40. Snapshots from a molecular dynamics simulation of a 200 eV projectile impact on a 2D Lennard-Jones matrix. (a) -0.2 ps (b) 0.55 ps (c) 7.3 ps (d) 15.3 ps.

(c)

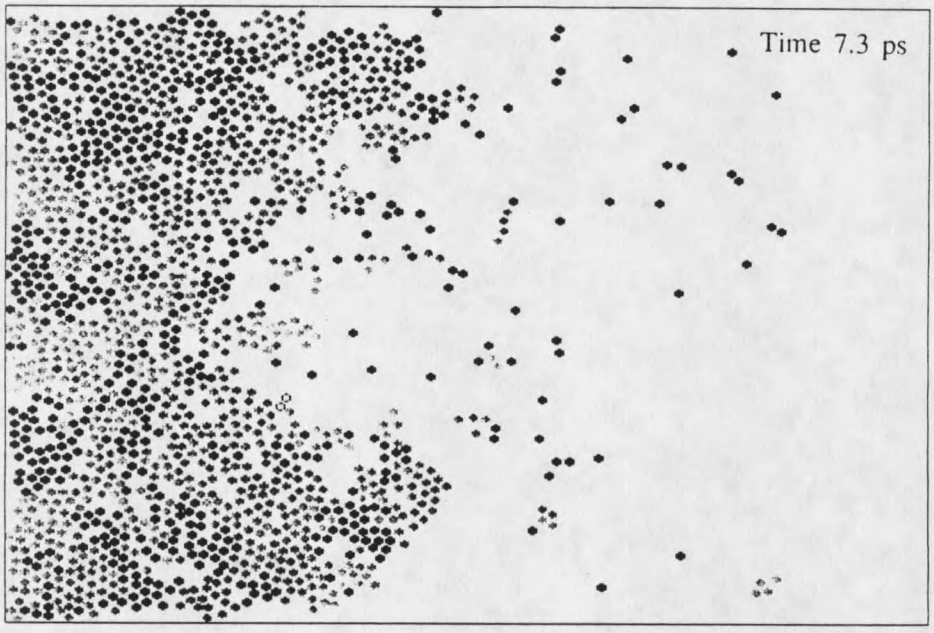

(d)

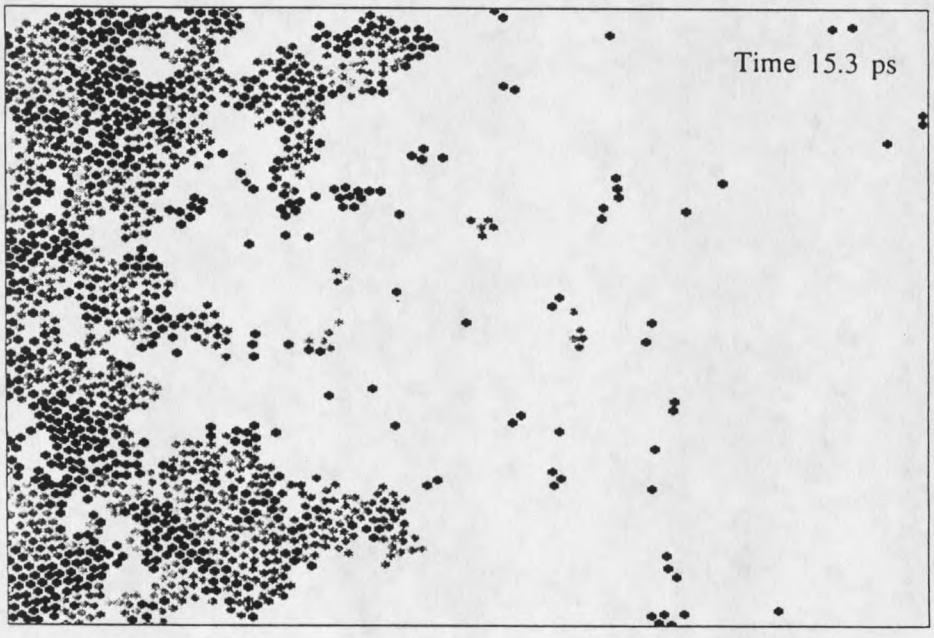

Figure 40. (Continued)

The shading of the atoms in Figure 40 gives information about the local temperature. This was calculated in the following way. The kinetic energy of an atom and its nearest neighbor atoms, within a 9 Å radius, is calculated in the center of mass coordinate for that collection of atoms. The calculated kinetic energy is then translated into temperature and the atoms are color coded according to the temperature. In Figure 40, the following temperature-to-color scale is used: Black: $T < 400$ K; Gray: 400 K $< T <$ 1,000 K and White: $T >$ 1,000 K. It can be seen that at 0.55 ps a semicircular, high temperature region has developed bounded by an outgoing pressure wave. Also, a few atoms with high kinetic energy have been ejected. At 7.3 ps the temperature has decreased substantially as energy goes into disintegration of the matrix. A number of clusters, ranging from dimer to heptamer, are leaving the cavity. At 15.3 ps the desorption process is approaching completion. The neutral yield from this impacting event was 116 atoms. The overall picture for this MD simulation can be described as follows:

1) The impact projectile excites the matrix in the cavity that contains about 350 atoms. One third of these are ejected from the cavity after 15 ps.
2) In the very early stage, a few "first batch" atoms with high kinetic energies are ejected. These atoms originate from the uppermost surface layers in the matrix.

3) A shockwave or "pressure wave", created by the impact atom propagates into the system in all directions. The system is heated by this shockwave and rapid thermalization leaves it in a highly excited, nearly homogeneous, expanding state. All these effects are observed within 2 ps after impact.

4) After ca. 2 ps, some inhomogeneities appear and clear voids in the cavity are seen at around 5 ps. The system now consists of a "highly interconnected network" of cooler, high density regions. Some of these regions "pinch off" and form gas-phase clusters which slowly drift into the vacuum.

The pattern of atoms around the main cavity seen in Figure 40(c) and (d) is quite similar to that observed by Abraham et al. (1982) in their spinodal simulation. The temperature history of a selected region in the matrix in this simulation also gives support to the spinodal interpretation (Figure 41). The region is located along the axis of the incident projectile and 15 - 25 Å below the surface and contains ca. 40 atoms. In Figure 41, the curve shows a initial very sharp increase up to ca. 3,000 K. This is due to the shockwave passing through and represents a highly non-equilibrated system. A subsequent slower heating is followed by a very pronounced decrease such that the final temperature is similar to the initial temperature (ca. 300 K). Such a temperature profile was previously predicted to occur in a spinodal

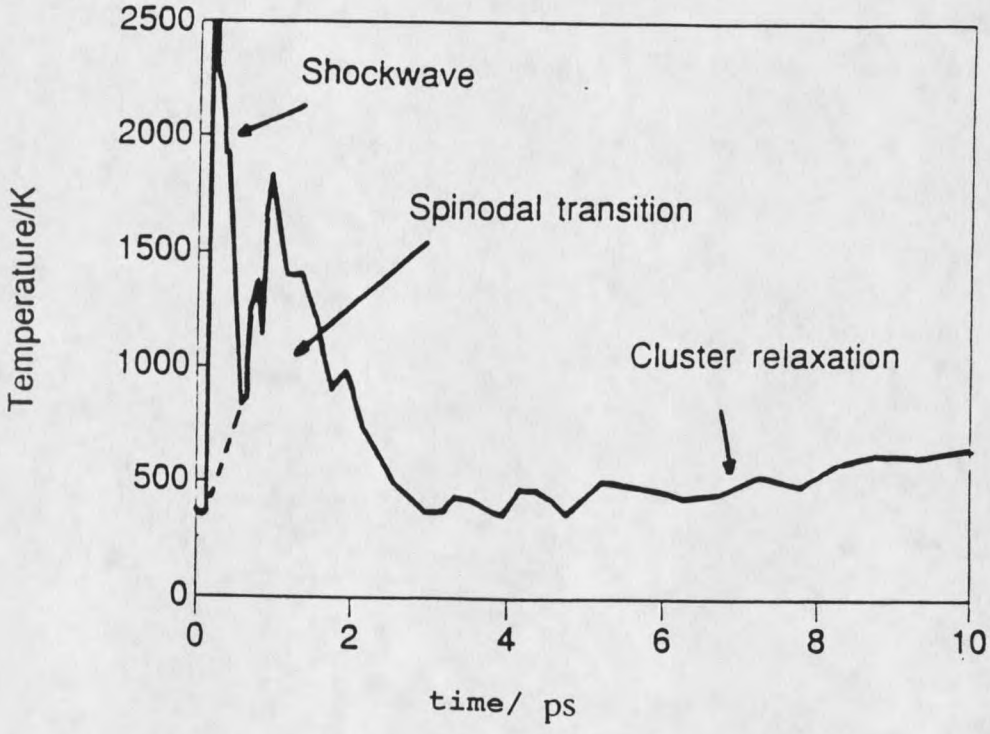

Figure 41. Temperature history of selected region calculated from total kinetic energy in center-of-mass coordinates. Atom impacts at time zero.

liquid-to-gas transition by Sunner et al. (1988b). The final slow temperature increase (after 5 ps) is most likely due to a decrease in potential energy as the clusters and filaments relax.

The kinetic energy distribution for all desorbed atoms whether ejected as monomers or clusters is shown in Figures 42(a) and that for the atoms ejected as monomers only in Figure 42(b). It is clear that the high-energy tail in Figure 42(a) is mostly due to the high kinetic energy

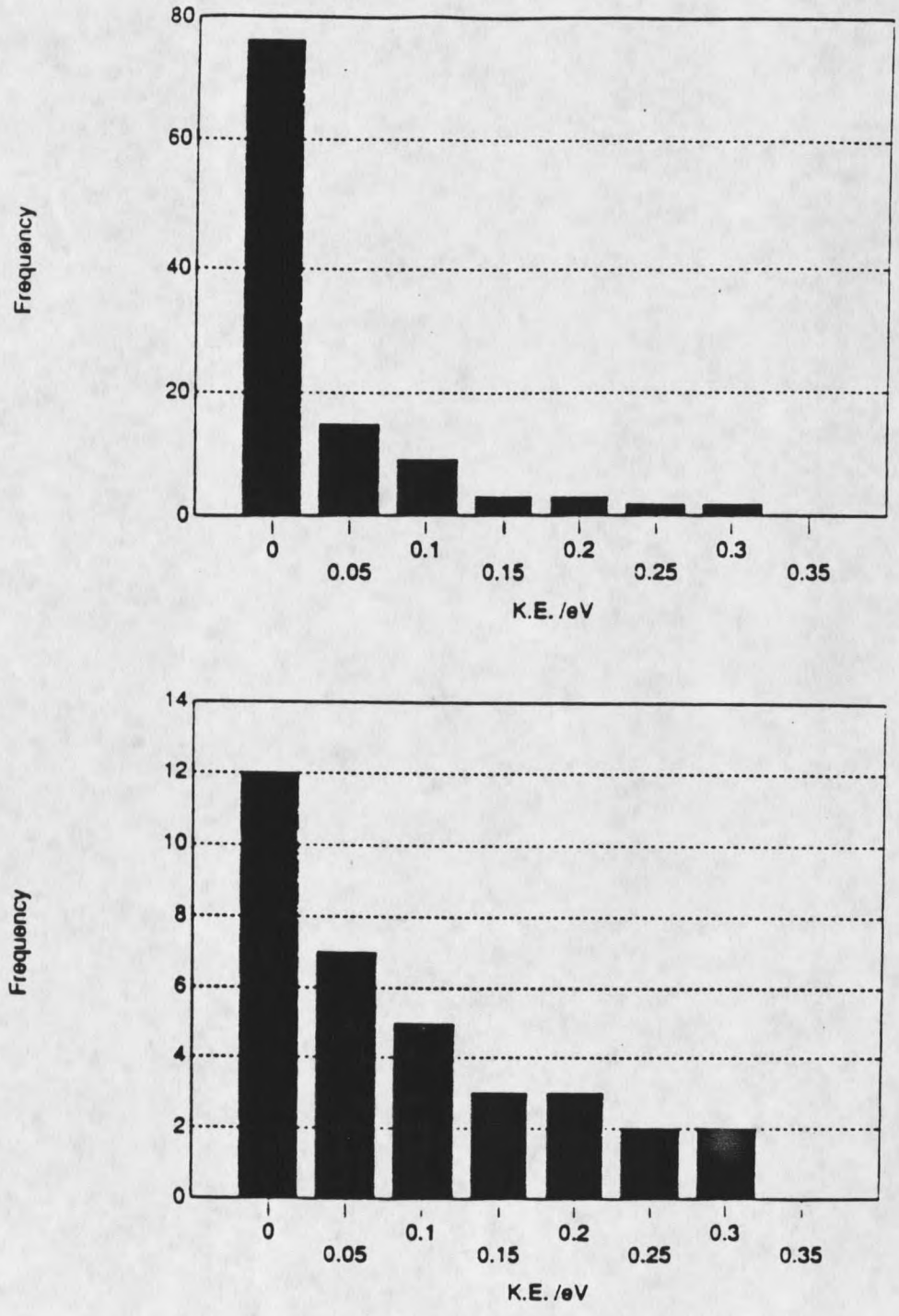

Figure 42. Kinetic energy distributions of (a) all ejected atoms and (b) atoms ejected as monomers only.

monomers desorbed in the very beginning. Also, the kinetic energy of most clusters is clearly low.

As the desorption process evolves there is trend toward ejection of larger clusters. This is illustrated in Figure 43, which shows cluster distributions during the first (0 to 8 ps) and last half (8 to 16 ps) of the simulated time frame. The fraction of atoms ejected as monomers is 45% in the first half and 25% in the latter half. Similarly, the average

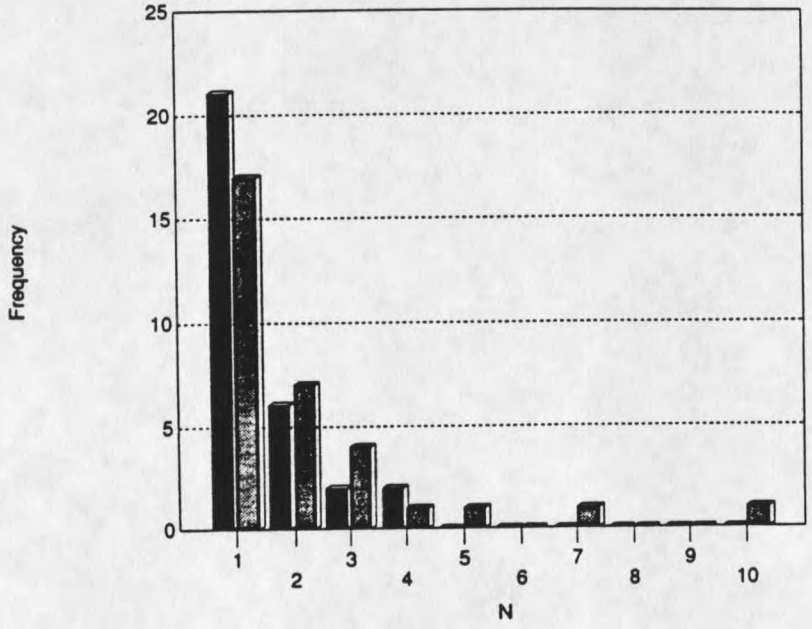

Figure 43. Distribution of ejected clusters ejected in the first (black) and last (gray) half of the desorption process.

cluster size increases from 1.5 to 2.2. The gradual increase in cluster size with desorption time is in agreement with earlier conclusions based on kinetic modelling of FAB spectra by Sunner et al. (1988a).

Molecular Desorption

The question of how thermally labile molecules can survive and be desorbed as intact molecules in FAB is of particular importance. The answer may be provided by Figure 41; the time during which the matrix is hot is too short (ca. 10^{-10} seconds) for any substantial thermal dissociation to occur. This idea was previously forwarded by Sunner et al. (1988b) based on their Phase Explosion Model. Only unimolecular reactions with rates above ca. 10^{10} sec^{-1}, can obviously result in significant fragmentation of the analyte molecules during the temperature spike. The rate constant for a reaction can be written as:

$$k = A * \exp(-E_A / RT)$$

where A is the preexponential factor, E_A is the activation energy, T is the reaction temperature and R is the gas constant. A simple bond fission represents a worst case since such reactions can have A-factors as high as 10^{17} sec^{-1} (Sunner et al., 1988b). If E_A is set equal to the bond energy, then it is found that at 900 K only bonds weaker than 88 kJ/mol have unimolecular dissociation rates above 10^{10} sec^{-1}. Since the chemical bonds are in the range of 250 to 400 kJ/mol the

analyte molecules should easily survive during the FAB event.

A simulation of particle induced matrix assisted molecular desorption is illustrated in Figure 44. In this simulation, the calculational details are essentially the same as for Figure 40, except twenty molecules were set randomly in the matrix. Each molecule is comprised by six neighboring matrix atoms bonded by 25 kcal/mol Morse potentials for this simulation. After 16 ps, the molecular yield from the calculations was found to be 4. These comprised of two intact molecules and the fragments from two other molecules. At 0.6 ps, some shockwave induced radiation damage is found as one of the molecules deep in the matrix has broken into two parts. However, at 4 ps both parts recombine to reform the original molecule.

Generally speaking, the calculations successfully simulate bulk desorption in a 2D system. For example, the shockwave, the spinodal decomposition, the extensive cooling and the molecular desorption are all observed. However, in the present calculations, the region where the spinodal-like transition is observed does not contribute much to the desorption. This means that only few atoms or clusters from this region are actually desorbed. The main reason is the low kinetic energy of the projectile necessitated by the small size of the system. Thus the present simulations reveal an intermediate desorption process that is still far from the spinodal limit. In a larger calculation with a higher

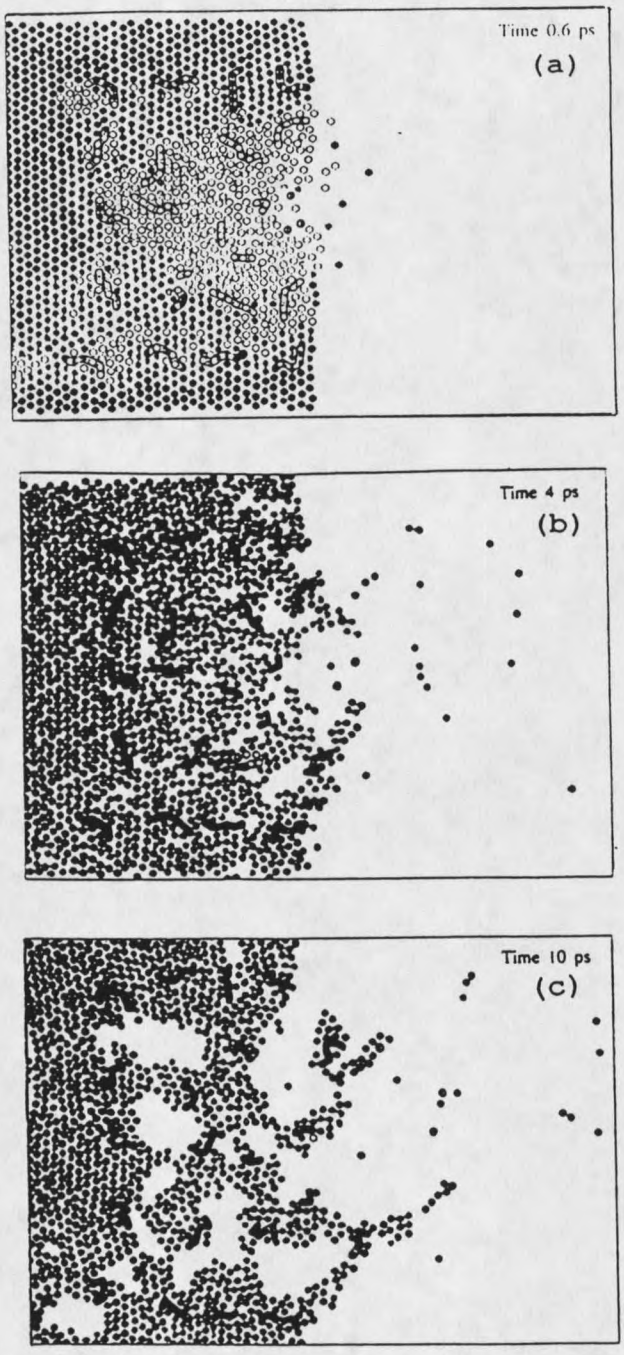

Figure 44. Snapshots from molecular dynamics simulation of a 200 eV projectile impact on a 2D Lennard-Jones matrix with dissolved molecules. (a) 0.6 ps (b) 4 ps (c)10 ps.

kinetic energy projectile, the excited region will be larger, and presumably the spinodal decomposition will be competitive with the quenching due to radial heat loss. Thus, it is expected that the trend towards larger clusters, shown in Figure 43, will continue and an approach to the spinodal limit will be observed.

CONCLUSION

Several mechanistic studies on the desorption process in FAB have been conducted. The objective of these studies is to clarify some controversial ideas previously presented and to obtain further insight into the relationship between the processes in solid and liquid SIMS (or FAB). Although the desorption process in FAB is still not fully explained from these studies, several conclusions which definitely constitute positive contributions to this problem can be summarized as follows:

1) The acid effect in FAB has been critically studied. It was found that the changes in the mass spectra observed on addition of strong acid can be explained as a result of changes in solubility, surface activity, volatility, radiation chemistry and desorption energetics. For non-surface-active compounds, the preformed ion formation effect is, at most, very weak. For surface-active compounds, the situation is not yet clear.

2) It was shown in this study that very low levels of small organic and inorganic cations can be detected in FAB by adding a negatively charged dodecylsulfate surfactant to the matrix. This is the same strategy

previously used by others for the sensitive detection of inorganic anions in FAB by the addition of a positively charged long chain surfactant. The enhancement of analyte ion signal with addition of a surfactant is explained as follows: To maintain charge neutrality in the surface layers, analyte ions are restrained to the vicinity of the surface layer of the oppositely charged surfactant. Therefore, the surface concentration of analyte and also the analyte ion signal in FAB spectra increase.

The transportation of surfactant during FAB irradiation was also explored. At low concentration, there is no competition between the two surfactants with different surface activity. This is in contrast to the strong competition observed at higher concentrations. The result implies that the transport rates for the two surfactants are equally fast. The chain length of the surfactant has no or only very small effect to the mass transport process in FAB. When the mass transport process was slowed at low temperature, there was no competition between the two surfactants, even at high concentration.

3) A very strong dependence of FAB spectra on matrix temperature has previously been reported in the literature. The reasons for this temperature effect

were explored in this study. It was found that the effects on the FAB spectra of decreasing the temperature were closely reproduced merely by increasing the viscosity of the matrix at constant temperature. Thus, it was concluded that the temperature, per se, is not important for obtaining good quality FAB spectra. The very strong dependence on viscosity is explained as a result of changes in the transport processes at the liquid-vacuum interface and of a gradual shift in the desorption mechanism.

The concept that the volume excited by an incident fast atom may undergo a radial expansion is used in interpreting the "viscosity-per-se" effect. At a high matrix viscosity, the pressure of the gas which is formed by energy transfer in the fast atom induced collision cascade will be released upward. In this case, little time is available for ion-molecule reactions to occur in the gaseous phase during the desorption event. Thus, with less proton transfer from matrix to analyte, the analyte to matrix ion ratio is decreased. Further, because of inefficient removal of radicals and radiation-induced products, the FAB spectra are dominated by chemical noise. On the other hand, at low matrix viscosity, the walls of the gaseous cavity may yield to the pressure. The gas expands radially and the pressure drops. The faster

the pressure in the bottom of the cavity is released in the radial direction, the smaller is the momentum transfer to the matrix in the upper part of the cavity. The expulsion is slower and there is more time available for the ionization of analyte. The viscosity dependence of the transport processes that operate at the liquid/vacuum interface is also important in explaining the change of the FAB spectra with viscosity.

The effects from selective evaporation and of accumulation of radiation-induced products in the surface layers were found to be important and were discussed. The increase in analyte signal at very high viscosities may indicate that a "preformed ion formation" mechanism becomes more efficient at high viscosity.

4) The ionization efficiencies and competition between alkali ions and tertiary alkyl ammonium ions have been investigated. The preference factors (F_p) for tetramethylammonium and alkali ions are somewhat higher than for Bronsted bases (e.g. diethanolamine), whether protonated or not. The competition (i.e., the suppression of one analyte ion signal by the presence in the matrix of a second analyte) between these preformed ions is small or non-existent. However,

both types of ions strongly suppress the ion signal from the Bronsted bases, whether protonated or not. This is explained as a result of ionization transfer from the bases to the alkali or ammonium ions. Most likely, these are proton transfer reactions.

Formation of mixed alkali/halide clusters in FAB is nearly statistical; the energy differences between these clusters are not large enough to significantly effect the intensities. This is consistent with cluster formation from a homogeneous solution.

5) The bulk desorption process, observed in FAB and related techniques, was investigated by a 2D molecular dynamics calculation. The shockwave, the spinodal decomposition, the extensive cooling and the molecular desorption are all present. Kinetic energy and cluster distributions are obtained. Early in the process, mainly high kinetic energy monomers are ejected. As the process evolves the kinetic energy decreases and the clusters gradually grow. This is in agreement with ideas from the Gas Collision Model. The temperature history of the molecules in a small region were calculated. The initial very sharp temperature peak reflects the passage of the shockwave. A subsequent slower heating followed by a very pronounced decrease in temperature profile is

interpreted in terms of a spinodal decomposition.

LITERATURE CITED

Abraham, F.F.; Koch, S.W. and Desai, R.C. (1982) Phys. Rev. Lett., 49, 923.

Ackermann, B.L.; Watson, J.T. and Holland, J.F. (1985) Anal. Chem., 57, 2656.

Adamson, A.W. (1962) Physical Chemistry of Surface, Interscience, N.Y.

Allmaier, G. and Schmid, E.R. (1985) Spectrosc. Int., 4, 297.

Anderson, C.A. and Hinthorne, J.R. (1973) Anal. Chem., 45, 1421.

Barber, M.; Bordoli, R.S.; Elliott, G.J.; Sedgwick, R.D. and Tyler, A.N. (1982) Anal. Chem., 54, 645A.

Barber, M.; Bordoli, R.S.; Sedgwick, R.D. and Tyler, A.N. (1981a) J. Chem. Soc. Chem. Commun., 325.

Barber M.; Bordoli, R.S.; Sedggwick, R.D. and Tyler,A.N. (1981b) Nature (London), 293, 270.

Bartmess, J.E. and Philips, L.R. (1987) Anal. Chem., 59, 2012.

Beckey, H.D. (1969) Int. J. Mass Spectrom. Ion Phys., 2, 500.

Beckey, H.D. (1977) Principles of Field Ionization and Field Desorption Mass Spectrometry; Pergamon: New York.

Benninghoven, A. (1983a) Surf. Sci., 53, 596.

Benninghoven, A. (1983b) Int. J. Mass Spectrom. Ion Phys., 53, 85.

Benninghoven, A.; Jaspers, D. and Sichtermann, W. (1976) Appl. Phys., 11, 35.

Benninghoven, A.; Rudenauer, F.G. and Werner, H.W. (1987) Secondary Ion Mass Spectrometry. Basic Concepts, Instrumental Aspects, Applications and Trends, Wiley, New York.

Benninghoven, A. and Sichtermann, W.K. (1978) Anal. Chem., 50, 1181.

Berry, R.S.; Rice, S.A. and Ross, J. (1980) Physical Chemistry, Wiley, New York.

Biondi, M.A. (1976) In Principles of Laser Plasma (Editor: Bekefi, G.), Wiley, New York, p.125.

Brenner, D.W. and Garrison, B.J. (1986) In Secondary Ion Mass Spectrometry, SIMS V., (Editors: Benninghoven et al.) Spring Ser. Chem. Phys., Vol. 44, A. Springer-Verlag, Berlin, p.462.

Bull, H.B. and Breese, K. (1974) Arch. Biochem. Biophys., 161, 665.

Busch, K.L. and Cooks, r.G. (1982) Science, 218, 247.

Busch, K.L.; Hsu, B-H.; Xie, Y.-X. and Cooks, R.G. (1983a) Anal. Chem., 55, 1157.

Busch, K.L.; Hsu, B.H.; Xie, Y.-X. and Cooks, R.G. (1983b) In Ion Formation from Organic solids; (Editor :Benninghoven, A.) Springer Ser. Chem. Phys., 25; Springer-Verlag, Berlin, p.138.

Busch, K.L.; Unger, S.E.; Vincze, A.; Cooks, R.G. and Keough, T. (1982) J. Am. Chem. Soc., 104, 1507.

Ciccotti, G. (1986) Molecular Dynamics Simulation of Statistical-Thermodynamic Systems, North-Holland, Amsterdam.

Cook, K.D. and Chan, K.W.S. (1983) Int. J. Mass Spectro. Ion Processes., 54, 135.

Cooks, R.G. and Busch, K.L. (1983) Int. J. Mass Spectrom. Ion Phys., 53, 111.

Cook, K.D.; Todd, P.J. and Friar, D.H. (1989) Biomed. Environ. Mass Spectrom., Vol 18, 492.

CRC Handbook of Chemistry and Physics, 64th edn., CRC Press Inc., Boca Raton, FL, (1984).

Daniels, F. and Alberty, R.A. (1961) Physical Chemistry, Wiley, Boca Raton, FL, p.350.

Dass, D. and Desiderio, D. M. (1988) Anal. Chem., 60, 2723.

David,D.E.; Magnera, T.F.; Tian, R.; Stulik, D. and Michl, J. (1986) Nucl. Instrum. Meth. Phys. Res., B, 14, 378.

Day, R.J.; Unger, S.E.; Cooks, R.G. (1980) Anal. Chem., 52, 557A.

Detter, L.D.; Hand, O.W.; Cooks, R.G. and Walton, R.A. (1988) Mass Spectrom. Rev., 7, 465.

Ens, W.; Standing, K.G.; Chait, B.T. and Field, F.H. (1981) Anal. Chem., 53, 1241.

Ens, W.; Standing, K.G.; Westomore, J.B.; Ogilvie, K.K. and Nemer, M. (1982) J. Anal. Chem., 54, 960.

Falick, A.M.; Jiang, K.E.,; Gibson, B.W. and Walls, F.C. (1988) Proceeding of the 35th ASMS Conference on Mass Spectrometry and Allied Topics. Denver, p. 318.

Falick, A.M.; Walls, F.C. and Laine, R.A. (1986) Anal. Biochem., 159, 132.

Fenselau, C.J. (1984) Nat. Prod., 47, 215.

Fenselau, C. and Cotter, R.J. (1987) Chem. Rev., 87, 501.

Fenyoe, D.; Sundquist, B.U.R.; Karlsson, B. and Johnson, R.E. (1989) J. Phys., Colloq. (C2, Int. Workshop MeV keV Ions Cluster Interact. Surf. Met. 2nd, 1988), C2-33.

Field, F.H. (1982) J. Phys. Chem., 86, 5115.

Franks, J. (1983) Int. J. Mass Spectrom. Ion Phys., 46, 343.

Garrison, B.J. (1982) J. Am. Chem. Soc., 104, 6211.

Garrison, B.J. (1983) Int. J. Mass Spectrom. Ion Phys., 53, 243.

Garrison, B.J. (1985) In Desorption Mass Spectrometry. Are SIMS and FAB the same? (Editor: Lyon. P.A.) Am. Chem. Soc. Washington, D.C. p. 43.

Garrison, B.J. and Winograd, N. (1982) Science, 216, 805.

Garrison, B.J. and Winograd, N. (1983) Chem. Phys. Lett., 97, 381.

Garrison, B.J.; Winograd, N.; Deaven, D.M.; Reimann, C.T.; Lo, D.Y.; Tombrello, T.A.; Harrison, D.E. and Shapiro, M.H. (1988) Phys. Rev. B, 37, 7197.

Gegarly, A.; Van den Heuvel, H. and Claeys, M. (1989) Spectrosc. Int., 7, 133.

Gillen, G.; Christiansen, J.W.; Tsong, I.T.S.; Kimbal, B. and Williams, P. (1985) Rapid Commun. Mass Spectrom., 2, 67.

Gnaser, H. (1984) Int. J. Mass Spectrom. Ion Processes., 61, 81.

Gower, J.L. (1985) Biomed. Environ. Mass Spectrom., 12, 191.

van Gunsteren, W.F. (1988) In Mathematical Frontiers in Computational Chemical Physics (Editor: Truhlar, D.G.), Springer-Verlag, New York, p. 136.

Gunton, J.D. and Droz, M. (1983) Introduction to the Theory of Metastable and Unstable States, Springer, Berlin.

Hakansson, P.; Kamensky, I.; Sundqvist, B.; Peterson, P.; McNeal, C.J. and MacFarlane, R.D. (1982) J. Am. Chem. Soc., 104, 2948.

Hand, O.W., Scheifers, S.M., and Cooks, G. (1987) Int. J. Mass Spectrom. Ion Processes, 78, 131.

Harrison, D.E., Jr. and Delaplain, C.B. (1976) J. Appl. Phys., 47, 2252.

Harrison, D.E., Jr.; Kelly, P.W. and Garrison, B.J. (1978) Surf. Sci., 76, 311.

Harrison, D.E., Jr.; Levy, N.S. and Johnson, J.P.,II and Effron, H.M. (1968) J. Appl. Phys., 39, 3742.

Harrison, D.E., Jr.; Moore, W.L., Jr. and Holcombe, H.T. (1973) Radiat. Eff., 17, 167.

Hedin, A.; Hakansson, P. and SundqvistB. (1985) Phys. Rev. B 31, 1780.

Hilf, E.R.; Kammer, H.F. and Nitzschmann, B. (1989) In Ion Formation from Organic Solids, IFOS IV. (Editor: Benninghoven, A.), Wiley, p.97.

Hoogerbrugge, R.; Bobeldijk, M.; Kistemaker, P.G. and Los, J. (1988) J. Chem. Phys., 88, 5314.

Hotop, H. and Lineberger, W.C. (1985) J. Phys. Chem. Ref. Data, 14, 731.

Inchaouh, J.; Blais, J.C.; Bolbach, G. and Brunot, A. (1984) Int. J. Mass Spectrom. Ion Processes, 61, 153.

Jiang, L.F.; Barofsky, E. and Barofsky, D.F. (1988) Proceedings of the 36th ASMS Conference on Mass Spectrometry and Allied Topics, San Francisco, American Society for Mass Spectrometry, East Lansing, MI, p.1209.

Junker, E.; Wirth, K.P. and Rollgen, F.W. (1989) J. Phys. (Paris) Colloq. C2, 52.

Katz, R.N.; Chaudhary, T. and Field, F.H. (1986) J. Am. Chem. Soc., 108, 3897.

Katz, R.N.; Chaudhary, T. and Field, F.H. (1987) Int. J. Mass Spectrom. Ion Processes, 78, 85.

Katz, R.N. and Field, F.H. (1987) Proceedings of the 35th Annual Conference on Mass Spectrometry and Allied Topics, Denver, CO, American Society for Mass Spectrometry, East Lansing, MI, 321.

Kelly, R. (1977) Radiat. Eff., 32, 91.

Kelly, R. and Kerkdijk, C.B. (1974) Surf. Sci., 46, 537.

Keough, T. (1985) Anal. Chem., 57, 2027.

Keough, T. and DeStafano, A.J. (1981) Anal. Chem., 53, 25.

Keough, T.; Ezra, F.S.; Russell, A.F. and Pryne, J.D. (1987) Org. Mass SSpectrom., 22, 241.

Krueger, F.R. (1983) Z. Naturforsch., 38a, 385.

Lacey, M.P. and Keough, T. (1989) Rapid Commun. Mass Spectrom., 3, 46.

Lew, H. (1976) Sources of atoms, In Methods of Experimental Physics 4A (Editor: Hues, V.W. and Schultz, H.L.), Academic Press, New York. p.155.

Ligon, W.V. (1983a) Int. J. Mass Spectrom. Ion Phys., 52, 183.

Ligon, W.V. (1983b) Int. J. Mass Spectrom. Ion Phys., 52, 189.

Ligon, W.V. and Dorn, S.B. (1984a) Int. J. Mass Spectrom. Ion Processes, 57, 75.

Ligon, W.V. and Dorn, S.B. (1984b) Int. J. Mass Spectrom. Ion Processes, 61, 113.

Ligon, W.V. and Dorn, S.B. (1985) Int. J. Mass Spectrom. Ion Processes, 63, 315.

Ligon, W.V. (1986) Anal. Chem., 58, 485.

Ligon, W.V. and Dorn, S.B. (1986a) Anal. Chem., 58, 1889.

Ligon, W.V. and Dorn, S.B. (1986b) Int. J. Mass Spectrom. Ion Processes, 78, 99.

Ligon, W.V. and Dorn, S.B. (1988) J. Am. Checm. Soc., 110, 6684.

Macfarlane, R.D. (1982) Nucl. Instrum. Methods., 198, 75.

MacFarlane, R.D. and Torgerson, D.F. (1976) Science, 191, 920.

Magee, C.W. (1983) Int. J. Mass Spectrom. Ion Phys., 49, 211.

Malorni, A.; Marino, G. and Milone, A. (1986) Biomed. Environ. Mass Spectrom., 13, 477.

Mahoney, J.F.; Goebel, D.M.; Perel, J. and Forrester, A.T. (1983) Biomed. Environ. Mass Spectrom., 10, 61.

Martin, S.A.; Costello, C.E. and Biemann, K. (1982) Anal. Chem., 54, 2362.

McNeal, C.J. and Macfarlane, R.D. (1981) J. Am. Chem., 103, 1609.

Michl, J. (1983) Int. J. Mass Spectrom. Ion. Phys., 53, 255.

Morales, A.; Kebarle, P. and Sunner, J. (1989) Int. J. Mass Spectrom. Ion Processes, 87, 287.

Morris, H.R.; Panico, M. and Haskins, N.J. (1983) Int. J. Mass Spectrom. Ion Phys., 46, 363.

Musselman, B.D.; Watson, J.T. and Chang, C.K. (1986) Org. Mass Spectrom., 21, 215.

Murray, P.T. and Rabalais, J.W. (1981) J. Am. Chem. Soc., 103, 1007.

Naylor, S. and Moneti, G. (1989) Biomed. Environ. Mass Spectrom., 18, 405.

Newman, A.A.(1968) Glycerol, C.R.C. Press, Cleveland.

Osipow, L.I. (1972) Surface Chemistry, Theory and Industrial Applications (Editor: Krieger, R.E.), Huntington, New York.

Pachuta, S.J. and Cooks, R.G. (1987) Chem. Rev., 87, 647.

Pachuta, S.J. and Cooks, R.G. (1985) In Desorption mass spectrometry: Are SIMS and FAB the same? (Editor: Lyon, P.A.); American Chemical Society: Washington, p.1.

Pang, H.; Costello, C.E. and Biemann, K. (1984) Proceedings of the 32nd Annual Conference on Mass Spectrometry and Allied Topics, San Antonio, American Society for Mass Spectrometry, East Lansing, S.A., p.751.

DePauw, E. (1986) Mass Spectrom. Rev., 191.

Poole, R.T.; Jenkin, J.G.; Liesegang, J.; Leckey, R.C.G. (1975) Phys. Rev. B: Solid State, 11, 5179.

Posthumus, M. A.; Kistemaker, P.G.; Meuzelaar, H.L.C. and Ten Noever de Brau, M.C. (1987) Anal. Chem., 50, 985.

Rabalais, J.W. and Chen, J.N. (1986) J. Chem. Phys., 85, 3615.

Rudat, M.A. and McEwen, C.N. (1983) Int. J. Mass Spectrom. Ion Phys., 46, 351.

Schronk, L.R. and Cotter, R.J. (1986) Biomed. Environ. Mass Spectrom., 13, 395.

Schultz, J.A.; Kumar, R. and Rabalais, J.W. (1983) Chem. Phys. Lett., 100, 214.

Sigmund, P. (1969) Phys. Rev., 184, 383.

Sigmund, P. (1981) In Sputtering by Particle Bombardment I (Editor: Behrisch, R.), Topics in Applied Physics 47; Springer-Verlag, Berlin, p.9.

Sigmund, P. and Claussen, C. (1981) J. Appl. Phys., 52, 990.

Smith, K.M. (1975) In Porphyrins and Metalloporphyrins (Editor: Smith. K.M.), Elsevier Scientific Co., New York. p.3.

Soldzian, G. (1975) Surf. Sci., 48, 161.

Standing, K.G.; Chait, B.T.; Ens, N.; McIntosh, G. and Beavis, R. (1982) Nucl. Instrum. Methods, 198, 33.

Sunner, J.; Kulatunga, R. and Kebarle, P. (1986a) Anal. Chem., 58, 1312.

Sunner, J.; Kulatunga, R. and Kebarle, P. (1986b) Anal. Chem., 58, 2009.

Sunner, J.; Morales, A. and Kebarle, P. (1987) Anal. Chem., 59, 1378.

Sunner, J.; Morales, A. and Kebarle, P. (1988a) Anal. Chem., 60, 98.

Sunner, J.; Ikonomou, M.G. and Kebarle, P. (1988b) Int. J. Mass Spectrom. Ion Processes, 82, 221.

Sunner, J.; Morales, A. and Kebarle, P. (1988c) Int. J. Mass Spectrom. Ion Processes, 86, 169.

Thomas, G.E. (1977) Radiat. Eff., 31, 185.

Thompson, M.W. (1968) Philos. Mag., 18, 377.

Todd, P.J. (1986) Proceedings of the 34th Annual Conference on Mass Spectrometry and Allied Topics, Cincinnati, OH, American Society for Mass Spectrometry, East Lansing, MI, 651.

Todd, P.J. (1988) Org. Mass Spectrom., 419.

Todd, P. (1989) paper presented at the Conference on Mechanisms in Desorption Ionization Mass Spectrometry, Sanibel Island, Jan. 23-26.

Todd, P.J. and Groenewold, G.S. (1986) Anal. Chem., 58, 895.

Tommasion, L.; Klein, N. and Solomon, P.J. (1975) J. Appl. Phys., 46, 1484.

Torgerson, D.F.; Skowronski, R.P.; (1974) Biochem. Biophys. Res. Commun., 60, 616.

Urbassek, H. M. and Michl, J. Nucl. Instrum. Methods Phys. Res. Sect. B, in press.

Urbassek, H.M. and Michl, J. (1987) Nucl. Instrum. Meth. Phys. Res. sect. B, 22, 480.

Unger, S.E.; DDay, R.J. and Cooks, R.G. (1981) Int. J. Mass Spectrom. Ion Phys., 39, 231.

Ven der Weg, W.F. and Bierman, D.J. (1969) J. Physica, 44, 206.

Vestal, M.L. (1983) Mass Spectrom. Rev., 2, 447.

Watson, J.T. (1985) Introduction to Mass Spectrometry, Raven Press, New York.

Whitlow, H.J.; Hautala, M. and Sundqvist, B.U.R. (1987) Int. J. Mass Spectrom. Ion Processes, 78, 329.

Williams, P. (1979) Surf. Sci., 90, 588.

Williams, P. and Evans, C.A., Jr. (1978) Surf. Sci., 78, 324.

Wirth, K.P.; Wong, S.S. and Rollgen, F.W. (1986) Proceedings of the 34th Annual Conference on Mass Spectrometry and Allied Topics, Cincinnati, OH, American Society for Mass Spectrometry, East Lansing, MI, 645.

Wong, S.S. and Rollgen, F.W. (1986) Nucl. Instrum. Meth. Phys. Res. B14, 436.

Wong, S.S.; Rollgen, F.W.; Manz, I. and Przybylski, M. (1985) Biomed. Environ. Mass Spectrom., 12, 43.

Wong, S.S.; Wirth, K.P.;and Rollgen, F.W. (1986) In Ion Formation from Organic Solids IFOS III (Editor: Benninghoven, A.), Springer-Verlag, Berlin, 91.

Yu, M.L. and Lang, N.D. (1983) Phys. Rev. Lett., 50, 127.

Yu, M.L. and Lang, N.D. (1986) Nucl. Instrum. Methods Phys. Res. Sect. B, 14, 403

Yu, M.L. and Mann, K. (1986) Phys. Rev. Lett., 57, 1476.

Zakett, D.; Schoen, A.E.; Cooks, R.G. and Hemberger, P.H. (1981) J. Am. Chem. Soc., 103, 1295.

Zhang, M.Y.; Liang, X.Y.; Chen, Y.T. and Liang, X.G. (1984) Anal. Chem., 56, 2288.

APPENDIX

Figure 45. Molecular dynamics program I - Initialization.

```
VAR: 'variable list
     'NPART = number of atoms
     DEFINT I-N
     DEFDBL A-H, O-Z
     DIM X(1550), Y(1550), VX(1550), VY(1550), FX(1550),
     FY(1550)
     DIM LST(1550, 20), M(1550), MOL(30, 30)
     DIM MCOV(200, 2), MOLID(1550)
     CLS
     PRINT "MOLECULAR DYNAMICS CALCULATION"
     PRINT "Initialization"
     PRINT
     GOSUB SETSYS
     END

SETSYS: 'subroutine for set-up of system box, # of particles,
        etc
        'energy/temperature, adiabatic run, cell cut-off
        'time step, graph parameters, total run time
        'inter-atomic potentials
        NHC = 0: NHP = 0: SNR = 0

SS2: 'CLS
     INPUT "Action: Parameters, Coordinates, Save, or eXit
     (P,C,S,X): ", AN$
     IF AN$ = "P" THEN
         GOSUB SSP
     ELSEIF AN$ = "C" THEN
         GOSUB SSC
     ELSEIF AN$ = "S" THEN
         GOSUB SSD
     ELSEIF AN$ = "X" THEN
         INPUT "Are you sure (Y/N) ", A$
         IF A$ = "Y" THEN RETURN
     END IF
     GOTO SS2:

SSP: PRINT "Parameter input "

SSP1: 'CLS
      INPUT "Snap, Default, Write, New, Change, Print, eXit
      (S,D,W,N,C,P,X) ", AP$
      IF AP$ = "S" THEN
         IF SNR = 1 THEN CLOSE #3
         INPUT "Name of file ", SNAS$
         FILE$ = SNAS$
         NFR = 3
         GOSUB DIN
         SNR = 1                    'SNAP-FILE IS LEFT OPEN!
```

```
            NHP = 1
            GOSUB MASSINI
        ELSEIF AP$ = "D" THEN
            FILE$ = "MDPARA.DEF"
            NFR = 4
            GOSUB DIN
            CLOSE #NFR
            NHP = 1
            GOSUB MASSINI
        ELSEIF AP$ = "W" THEN
            IF NHP = 0 THEN
             PRINT "No parameter input yet"
             GOTO SSP1
            END IF
            FILE$ = "MDPARA.DEF"
            GOSUB DOUT
            CLOSE #2
        ELSEIF AP$ = "C" THEN
            GOSUB DCH
            GOSUB MASSINI
        ELSEIF AP$ = "P" THEN
           GOSUB PPOUT
        ELSEIF AP$ = "N" THEN
            GOSUB DNEW
            GOSUB MASSINI
            NHP = 1
        ELSEIF AP$ = "X" THEN GOTO SSP4
        ELSE
        PRINT "Illegal answer "

SSP2: END IF
      GOTO SSP1

SSP4: RETURN

SSC:  'coordinates input
      'RECORD COORDINATE TREATMENT HISTORY AND SAVE

SSC1:'CLS
     PRINT "Coordinates input and change"
     INPUT "Snap, Initialize, Expand, Graph, Check mol.,eXit",
           AR$
     IF AR$ = "S" THEN
           AI$ = "Y"
           PRINT "File name ", SNAS$
           PRINT "Reading from a different snap-file is not
                  implemented"
           PRINT "Start time "; TP2; " /ps "
           INPUT "Change (Y/N)? ", A$
           IF A$ = "Y" THEN
               INPUT "Snap-time /ps ", TP2
           END IF
```

```
            FILE$ = SNAS$

SSC2:  GOSUB SNAPREAD
       IF TP < TP2 THEN GOTO SSC2
       CLOSE #3
       T = TP * 1000                    'master clock
       NHC = 1
       ELSEIF AR$ = "G" THEN
            GOSUB GRAPHINI
       ELSEIF AR$ = "I" THEN
            GOSUB INI
            NHC = 1
       ELSEIF AR$ = "C" THEN
            IF NHC = 1 THEN GOSUB MOLCH
       ELSEIF AR$ = "E" THEN
            GOSUB MATEXP
       ELSEIF AR$ = "X" THEN
            PRINT "N"
            RETURN
       ELSE
            PRINT "Illegal answer "
       END IF
       GOTO SSC1
       RETURN

MOLCH:'checks molecular distances
       PRINT "Check for distances between atoms in molecules "
       FOR J = 1 TO NMOL
       PRINT "Molecule # ", J
       PRINT "Bond #          Distance"
       FOR I = 2 TO NAT
       NQ = MOL(J, I)
       DISTA = SQR(X(NQ) ^ 2 + Y(NQ) ^ 2)
       PRINT I - 1, DISTA
       NEXT I
       INPUT A$
       PRINT
       NEXT J
       RETURN

MATEXP: 'Expands matrix in Y-direction
         PRINT "Expansion ratio  ", CEY
         INPUT "Change (Y/N) ", A$
         IF A$ = "Y" THEN INPUT "Expansion ratio: ", CEY
         FOR I = 1 TO NPART
         Y(I) = (Y(I) - BY / 2) * CEY + BY / 2
         NEXT I
         RETURN

SSD:   'done
       CLS
```

```
SSD1: 'CLS
      INPUT "Action: Graphics, Save, or eXit (G,S,X) ", AQ$
      IF AQ$ = "G" THEN
         GOSUB GRAPHINI
      ELSEIF AQ$ = "X" THEN
         RETURN
      ELSEIF AQ$ = "S" THEN
          IF NHP = 0 THEN
               PRINT "No parameters"
          ELSEIF NHC = 0 THEN
               PRINT "No coordinates"
          ELSE
               INPUT "Name of MD-START file  ", MDSTART$
               FILE$ = MDSTART$
               GOSUB DOUT
               CLOSE #2
               GOSUB COUT
               CLOSE #2
          END IF
      END IF
      GOTO SSD1
      RETURN

GRAPHINI:IF NHC = 0 OR NHP = 0 THEN
                PRINT "Not ready for graphing"
                GOTO GRI2
         END IF
         COL2 = 5
         SCREEN 9
         COLOR 6, 7
         WINDOW (0, 0)-(BX, BY)
         GOSUB GRAPH
         INPUT A$
         SCREEN 0

GRI2:    RETURN

COUT: OPEN FILE$ FOR APPEND AS #2
        WRITE #2, NSNAP, TP
        WRITE #2, EK, PE, PTOT, EKP
        FOR I = 1 TO NPART
        WRITE #2, I, X(I), Y(I), VX(I), VY(I)
        NEXT I
        RETURN

DNEW: 'new default parameters
      N$ = "MOLECULAR DYNAMICS"
      CLS
      INPUT "Title ", N2$

DN1: INPUT "Sputtering, Cluster or Gas calculation (S/C/G) ",
     C$
```

```
DN2: INPUT "Matrix identifier ", ATOM$
     GOSUB POTENT
     IF NAT = 0 THEN
         PRINT "Illegal name"
         GOTO DN2
     END IF
     IF C$ = "S" THEN NP = 1 ELSE NP = 0
     IF NP = 0 THEN
         INPUT "Rotation (Y/N) ", R$
     ELSE
         PRINT "Bombardment process, projectile from the
                right"
         INPUT "Projectile KE/eV ", PKE
         INPUT "Projectile mass/amu ", MP
         PVEL = SQR(PKE / MP) * 138.9
         PRINT "Projectile velocity/ A/ps ", PVEL
         INPUT "Projectile initial position, x/A  ", PX
         INPUT "Angle of incidence/alfa   ", PA: PALFA = PA /
                180 * 3.1415
     END IF
     INPUT "Size of system box, x/A ", BX
     BY = BX * .75
     PRINT "                        y/A ", BY
     INPUT "Number of atoms in crystal, X-axis ", NAX
     INPUT "                            Y-axis ", NAY
     NPART = NAX * NAY + NP
     PRINT "Number of atoms          ", NPART
     INPUT "Interaction cut-off/A  ", RCUT: RC2 = RCUT * RCUT
     INPUT "Initial velocity excitation/ (m/s) ", VMAX
     INPUT "Lattice expansion coefficient ", CEY
     INPUT "Containment mass (None/Mass) ", CM$
     IF CM$ = "M" THEN
         PRINT "Outermost atom layer is given a high mass"
         INPUT "Mass of containment particles ", MC
     ELSE MC = MM
     END IF
     INPUT "Containment walls (Y/N) ", CW$
     INPUT "Containment lid   (Y/N) ", CL$
     INPUT "Time step/fs                        ", TD
     INPUT "Time step for list update/ps", TLP: TL = TLP *
            1000
     INPUT "Time interval for snap shots/ps ", TSP: TS = TSP
            * 1000
     INPUT "Total calculation time/ps       ", TFP: TF = TFP
            * 1000
     INPUT "Energy calculation for each snap (Y/N) ", EC$
     IF EC$ = "Y" THEN
         INPUT "Output to printer (Y/N) ", EP$
         INPUT "Output to file    (Y/N) ", EF$
         IF EF$ = "Y" THEN
         INPUT "Energy-file name ", EFN$
         END IF
```

```
      END IF
      INPUT "Do you want a snapshot-file (Y/N) ", SF$
      IF SF$ = "Y" THEN
          INPUT "Name of file ", SFN$
          INPUT "Sequential files (Y/N) ", SSEQ$
      END IF
      INPUT "Initialize from snap file (Y/N) ", AI$
      IF AI$ = "Y" THEN
          INPUT "Name of file ", SNAS$
          INPUT "Start-time /ps ", TP2
      END IF
      GOSUB DNEWM
      GOSUB DNEWMP
      PRINT "END OF PARAMETER INPUT"
      RETURN

DNEWMP: 'Morse potential parameters
      PRINT "Morse potential parameters "
      INPUT "De (J/molecule) ", DE
      INPUT "'beta' (A(-1))  ", BETA
      INPUT "Equilibrium distance /A  ", R0
      BEDE = 2 * BETA * DE * 1E+21
      RETURN

DNEWM: 'molecule input
      INPUT "Molecule(s) (Y/N) ", M$
      IF M$ = "Y" THEN
          INPUT "Number of molecules ", NMOL
          INPUT "Number of atoms in molecule ", NAT
          INPUT "Integral mass of atoms in molecule ", MA
          PRINT "Enter atom-number for the atoms in
                 'string-molecule'"
          PRINT "from one end to the other "
          INPUT "Enter by request or in sequence (R/S) ", AMOL$
          IF AMOL$ = "S" THEN
              FOR J = 1 TO NMOL
              PRINT "Atom# for molecule # ", J
              GOSUB DNEWM2
              NEXT J
         ELSE
             INPUT "Molecule# ", J
             GOSUB DNEWM2
         END IF
      END IF
      GOSUB CONNMAT
      RETURN

DNEWM2: FOR I = 1 TO NAT

DNM2:    PRINT "Atom#  "; I;
         INPUT MOL(J, I)
         IF MOL(J, I) > NPART THEN
```

```
            PRINT "There are not that many particles!! "
            GOTO DNM2
        END IF
        NEXT I
        RETURN

CONNMAT: 'build connection matrix
        FOR I = 1 TO N
        MOLID(I) = 0
        NEXT I
        FOR I = 1 TO 100
        MCOV(I, 1) = 0: MCOV(I, 2) = 0
        NEXT I
        L = 0
        FOR J = 1 TO NMOL
        FOR I = 1 TO NAT
        L = L + 1
        MOLID(MOL(J, I)) = L
        IF I = 1 THEN
            MCOV(L, 1) = MOL(J, I + 1)
        ELSEIF I = NAT THEN
            MCOV(L, 1) = MOL(J, I - 1)
        ELSE
            MCOV(L, 1) = MOL(J, I - 1)
            MCOV(L, 2) = MOL(J, I + 1)
        END IF
        NEXT I
        NEXT J
        RETURN

DIN: 'reads default parameter values
     OPEN FILE$ FOR INPUT AS #NFR
     INPUT #4, N$
     INPUT #4, N2$
     INPUT #4, C$, NP
     INPUT #4, PKE, MP, PVEL, PX, PA
     INPUT #4, BX, BY, NAX, NAY, NPART
     INPUT #4, ATOM$, MM, EPS, BINE, SIG, SIG2
     INPUT #4, NBX, NBY
     INPUT #4, NX, XMIN, XMAX
     INPUT #4, NY, YMIN, YMAX
     INPUT #4, RCUT, RC2
     INPUT #4, VMAX
     INPUT #4, CEY, CM$, MC, CW$, CL$
     INPUT #4, LIDX, YMAX, YMIN
     INPUT #4, TD, TS, TL, TF
     INPUT #4, TSP, TLP, TFP
     INPUT #4, EC$, EP$, EF$, EFN$
     INPUT #4, SF$, SFN$, SSEQ$
     INPUT #4, AI$, SNAS$, TP2
     INPUT #4, EG$
     FOR I = 1 TO NPART
```

```
      INPUT #4, M(I), MOLID(I)
      NEXT I
      INPUT #4, M$, NMOL, NAT, MA
      FOR J = 1 TO NMOL
      FOR I = 0 TO (NAT + 1)
      INPUT #4, MOL(J, I)
      NEXT I
      NEXT J
      FOR I = 1 TO (NMOL * NAT)
      INPUT #4, MCOV(I, 1), MCOV(I, 2)
      NEXT I
      INPUT #4, DE, BETA, R0, BEDE
      INPUT #4, N
      GOSUB CONNMAT
      RETURN

DOUT:'writes default parametes to file
      OPEN FILE$ FOR OUTPUT AS #2
      WRITE #2, N$
      WRITE #2, N2$
      WRITE #2, C$, NP
      WRITE #2, PKE, MP, PVEL, PX, PA
      WRITE #2, BX, BY, NAX, NAY, NPART
      WRITE #2, ATOM$, MM, EPS, BINE, SIG, SIG2
      WRITE #2, NBX, NBY
      WRITE #2, NX, XMIN, XMAX
      WRITE #2, NY, YMIN, YMAX
      WRITE #2, RCUT, RC2
      WRITE #2, VMAX
      WRITE #2, CEY, CM$, MC, CW$, CL$
      WRITE #2, LIDX, YMAX, YMIN
      WRITE #2, TD, TS, TL, TF
      WRITE #2, TSP, TLP, TFP
      WRITE #2, EC$, EP$, EF$, EFN$
      WRITE #2, SF$, SFN$, SSEQ$
      WRITE #2, AI$, SNAS$, TP2
      WRITE #2, EG$
      FOR I = 1 TO NPART
      WRITE #2, M(I), MOLID(I)
      NEXT I
      WRITE #2, M$, NMOL, NAT, MA
      FOR J = 1 TO NMOL
      FOR I = 0 TO (NAT + 1)
      WRITE #2, MOL(J, I)
      NEXT I
      NEXT J
      FOR I = 1 TO (NMOL * NAT)
      WRITE #2, MCOV(I, 1), MCOV(I, 2)
      NEXT I

      'Morse parameters
      WRITE #2, DE, BETA, R0, BEDE
```

```
      WRITE #2, NSNAP
      RETURN

DCCH1:  'VIEW PRINT 1 TO 20
      CLS '2
      PRINT "DEFAULT PARAMETERS"
      PRINT "1.  Title                              ", N2$
      PRINT "2.  Type of calculation (S/C/G)        ", C$
      PRINT "3.  Projectile KE/eV                   ", PKE
      PRINT "4.              mass                   ", MP
      PRINT "5.              position/A             ", PX
      PRINT "6.  Angle of incidence                 ", PA
      PRINT "7.  Box size, x/A                      ", BX
      PRINT "8.  Number of atoms, x                 ", NAX
      PRINT "9.                 , y                 ", NAY
      PRINT "    Total number of atoms              ", NPART
      PRINT "10. Interaction cut-off /A             ", RCUT
      PRINT "11. Velocity excitation /(m/s)         ", VMAX
      PRINT "12. Containment type (M,N)             ", CT$
      PRINT "13.              mass                  ", MC
      PRINT "14. Time step/fs                       ", TD
      PRINT "15.       list update /ps              ", TLP
      PRINT "16.       snap shot /ps                ", TSP
      PRINT "17. Total calculation time /ps         ", TFP
      RETURN

DCCH2:  'VIEW PRINT 1 TO 20
      CLS '2
      PRINT "DEFAULT PARAMETERS 2"
      PRINT "20. Energy calculation (Y/N)           ", EC$
      PRINT "21.              to printer (Y/N)      ", EP$
      PRINT "22.              to file (Y/N)         ", EF$
      PRINT "23. Energy file name                   ", EFN$
      PRINT "24. Output to snap file (Y/N)          ", SF$
      PRINT "25.       File name (out)              ", SFN$
      PRINT "26. Initialize from snap file (Y/N)    ", AI$
      PRINT "27.       file name (in)               ", SNAS$
      PRINT "28.       time to start /ps            ", TP2
      PRINT "29. Molecule input                     "
      PRINT "30. Morse potential input              "
      PRINT "31. Interaction type                   ", ATOM$
      'VIEW PRINT 21 TO 24
      RETURN

DCH: 'change parameter-values
      INPUT "PRESS ENTER", A$
      NSCREEN = 1
      GOSUB DCCH1

PC2: 'CLS 2
      LOCATE 21, 1
      'PRINT  ERASE
```

```
        INPUT ; "Print number to change (0 for exit, 99 for next
                frame) ", NI
        PRINT "     "
        IF NI = 99 THEN
            IF NSCREEN = 1 THEN
             NSCREEN = 2
             GOSUB DCCH2
            ELSEIF NSCREEN = 2 THEN
             NSCREEN = 1
             GOSUB DCCH1
            END IF
            GOTO PC2
        END IF
        SELECT CASE NI
            CASE 0
            GOTO PC4
            CASE 1
            INPUT "Title  ", N2$
            LOCATE 3, 45: PRINT N2$
            CASE 2

PC1:        INPUT "Type of calculation (S, G, C) ", C$
            IF (C$ = "S" OR C$ = "G" OR C$ = "C") THEN  ELSE GOTO
            PC1
            LOCATE 4, 55: PRINT C$
            IF C$ = "S" THEN NP = 1
            CASE 3
            INPUT "Projectile kinetic energy/eV  ", PKE
            LOCATE 5, 55: PRINT PKE
            PVEL = SQR(PKE / MP) * 138.9
            CASE 4
            INPUT "Projectile mass/amu  ", MP
            LOCATE 6, 55: PRINT MP
            PVEL = SQR(PKE / MP) * 138.9
            CASE 5
            INPUT "Projectile position/A  ", PX
            LOCATE 7, 55: PRINT PX
            CASE 6
            INPUT "Angel of incidence  ", PA
            LOCATE 8, 55: PRINT PA
            CASE 7
            INPUT "Box size, x/A ", BX: BY = .75 * BX
            PRINT "           y/A ", BY
            LOCATE 9, 55: PRINT BX
            CASE 8
            INPUT "Number of atoms in crystal, x-axis/A ", NAX
            NPART = NAX * NAY + NP
            PRINT "Number of atoms ", NPART
            LOCATE 10, 55: PRINT NAX
            CASE 9
            INPUT "Number of atoms in crystal, y-axis/A ", NAY
            NPART = NAX * NAY + NP
```

```
PRINT "Number of atoms ", NPART
LOCATE 11, 55: PRINT NAY
CASE 10
INPUT "Interaction cut-off/A ", RCUT
RC2 = RCUT * RCUT
LOCATE 13, 55: PRINT RCUT
CASE 11
INPUT "Velocity of excitation/ (m/s) ", VMAX
LOCATE 14, 55: PRINT VMAX
CASE 12
INPUT "Containment type ", CT$
LOCATE 15, 55: PRINT CT$
CASE 13
INPUT "Mass for containment atoms  ", MC
LOCATE 16, 55: PRINT MC
CASE 14
INPUT "Time step/fs  ", TD
LOCATE 17, 55: PRINT TD
CASE 15
INPUT "Time for list update/ps ", TLP
LOCATE 18, 55: PRINT TLP
TL = TLP * 1000
CASE 16
INPUT "Time for snap shot/ps   ", TSP
TS = TSP * 1000
LOCATE 19, 55: PRINT TSP
CASE 17
INPUT "Total calculation time/ps  ", TFP
TF = TFP * 1000
LOCATE 20, 55: PRINT TFP
CASE 20
INPUT "Energy calculation (Y/N)  ", EC$
LOCATE 3, 55: PRINT EC$
CASE 21
INPUT "Print energies to printer (Y/N) ", EP$
LOCATE 4, 55: PRINT EP$
CASE 22
INPUT "Energies to file (Y/N) ", EF$
LOCATE 5, 55: PRINT EF$
CASE 23
INPUT "Energy file name  ", EFN$
LOCATE 6, 55: PRINT EFN$
CASE 24
INPUT "Output to snap-file (Y/N) ", SF$
LOCATE 7, 55: PRINT SF$
CASE 25
INPUT "Snapshot filename  ", SFN$
LOCATE 8, 55: PRINT SFN$, DUM$
CASE 26
INPUT "Start from snap file (Y/N) ", AI$
LOCATE 9, 55: PRINT AI$
CASE 27
```

```
          INPUT "     file name  ", SNAS$
          LOCATE 10, 55: PRINT SNAS$
          CASE 28
          INPUT "     start time /ps  ", TP2
          LOCATE 11, 55: PRINT TP2
          CASE 29
          GOSUB DNEWM
          CASE 30
          GOSUB DNEWMP
          CASE 31
          INPUT "Interaction type ", ATOM$
          GOTO POTENT
          END SELECT
          GOTO DC3

PC4: 'VIEW PRINT 1 TO 24
     RETURN
POTENT: 'subroutine for defining intermolecular potentials
        PRINT "Alternatives: AR, XE, PSPH, PSPH2....."

POT1:INPUT "Identifier: ", ATOM$
     NAT = 0
     IF ATOM$ = "AR" THEN
          PRINT "Ar - Lennard-Jones potential"
          EPS = 2!
          SIG = 3.8
          MM = 40
          NAT = 1
     ELSEIF ATOM$ = "PSPH" THEN
          PRINT "'Polar' sphere"
          EPS = 20!
          SIG = 3.8
          MM = 40
          NAT = 1
     ELSEIF ATOM$ = "PSPH2" THEN
          PRINT "Superpolar sphere"
          EPS = 40!
          SIG = 3.8
          MM = 40
          NAT = 1
     ELSEIF ATOM$ = "XE" THEN
          PRINT "Kr - Lennard-Jones potential"
          EPS = 0
          SIG = 0
          MM = 0
          'NAT = 1
     ELSE
     END IF
          SIG2 = SIG * SIG
          BINE = EPS * .14393
          PRINT "M-M-system:   Epsilon/(1e-21J) ", EPS
          PRINT "    M-M bond energy (kcal/mol) ", BINE
```

```
        PRINT "                Sigma/A          ", SIG
        PRINT "                Mass of atom     ", MM
    RETURN

GRAPH:  'subroutine for screen output
    FOR I = 1 TO NPART
    IF M(I) = MM THEN
        NC = 6
    ELSE
        IF M(I) = MP THEN NC = 4
        IF M(I) = MA THEN NC = 9
        IF M(I) = MC THEN NC = 8
    END IF
    'NC=I-3*INT(I/3)+4
    CIRCLE (X(I), Y(I)), SIG / 2, NC
    PAINT (X(I), Y(I)), NC
    NEXT I
    IF EC$ = "Y" THEN
        TP = T / 1000
        PRINT "Time/ps ", TP;
        PRINT USING "  #.####^^^^"; EK; PE; PTOT
    ELSE
        TP = T / 1000
        PRINT "Time/ps ", TP
    END IF
    RETURN

MASSINI: 'initializes mass assignment
    FOR I = 1 TO NAY
    M(I) = MC
    NEXT I
    FOR I = 1 TO NAX - 1
    M(I * NAY + 1) = MC
    M(NAY * (I + 1)) = MC
    FOR J = 2 TO NAY - 1
    M(I * NAY + J) = MM
    NEXT J
    NEXT I
    IF NP = 1 THEN M(NPART) = MP
    IF M$ = "Y" THEN
        FOR J = 1 TO NMOL
        FOR I = 1 TO NAT
        M(MOL(J, I)) = MA
        NEXT I
        NEXT J
    END IF
    RETURN

INI: 'subroutine for initialization of positions and
    velocities.
    IF C$ = "G" THEN
        XSTEP = BX / NAX
```

```
        YSTEP = BY / NAY
    ELSE
        XSTEP = .97208 * SIG
        YSTEP = 1.12246 * SIG
    END IF
    FOR I = 1 TO (NPART - NP)       'counts atom #
        K = INT(I / NAY - .001)
        L = I - NAY * K
        YOFF = INT(K / 2) - K / 2 + .25
        X(I) = XSTEP * K - (NP - 1) * (BX / 2 - (NAX - 1) /
               2 * XSTEP)
        Y(I) = BY / 2 + YSTEP * (L - 1 - (NAY - 1) / 2 +
               YOFF)
    NEXT I
    'projectile data
    IF NP = 0 THEN GOTO INI2
    X(NPART) = PX
    Y(NPART) = BY / 2
    VX(NPART) = -PVEL * COS(PALFA)
    VY(NPART) = PVEL * SIN(PALFA)
INI2:'assign initial velocities
    'REWRITE FOR STATISTICAL DISTRIBUTION
    VM = VMAX / 100!'A/ps
    FOR I = 1 TO NPART - 1
        IF M(I) = MM THEN
            FACT = 1
        ELSEIF M(I) = MA THEN
            FACT = SQR(MM / MA)
        ELSEIF M(I) = MC THEN
            FACT = SQR(MM / MC)
        END IF
         VX(I) = FACT * VM * (2 * RND - 1)
         VY(I) = FACT * VM * (2 * RND - 1)
         IF R$ = "Y" THEN
          VX(I) = VX(I) - (Y(I) - BY / 2) * VM
          VY(I) = VY(I) + (X(I) - BX / 2) * VM
         END IF
    NEXT I
    RETURN

ENERGY: 'energy calculation
       'kinetic energy
    EKT = 0
       FOR I = 1 TO (NPART - NP)
       VT2 = VX(I) * VX(I) + VY(I) * VY(I)
       EKT = EKT + M(I) * VT2 / 836.8'kcal/mol
    NEXT I
    IF NP = 1 THEN
       EKP = M(NPART) * (VX(NPART) * VX(NPART) + VY(NPART) *
             VY(NPART)) / 836.8
       EKP2 = EKP / 23.0609    'eV
       EK = EKT + EKP
```

```
        END IF
        'potential energy
        PE = 0
        FOR I = 1 TO NPART - 1
        FOR J = I + 1 TO NPART
        DX = X(J) - X(I)
        DY = Y(J) - Y(I)
        R = SQR(DX * DX + DY * DY)
        Q = SIG / R
        Q = Q * Q * Q * Q * Q * Q
        PE = PE + 4 * EPS * (Q * (Q - 1))
        NEXT J
        NEXT I
        PE = PE * .143929
        PTOT = PE + EK
        IF EP$ = "Y" THEN
            LPRINT "Calculation time/ ps       ", TP
            LPRINT "   , target  ", EKT, "     kcal/mol"
            LPRINT "   , total   ", EK,  "     kcal/mol"
            LPRINT "Potential energy, total ", PE, " kcal/mol"
            LPRINT "Total energy, pot. + kin.", PTOT, " kcal/mol"
            IF NP = 1 THEN
            LPRINT "  projectile ", EKP, " kcal/mol"

            LPRINT "  projectile ", EKP2, " eV"
            LPRINT "  target     ", EKT, " kcal/mol"
            END IF
        LPRINT
        END IF
        RETURN

SNAPREAD: 'subroutine that reads one snap from file
        INPUT #4, NSNAP, TP  'ZZZ
        PRINT "SNAP#, Time/ps ", NSNAP, TP
        INPUT #4, EK, PE, PTOT, EKP
        FOR I = 1 TO NPART
            INPUT #4, I, X(I), Y(I), VX(I), VY(I)
        NEXT I
        RETURN

PPOUT:
        LPRINT "PARAMETER OUTPUT"
        LPRINT N$
        LPRINT N2$
        LPRINT C$, NP
        LPRINT PKE, MP, PVEL, PX, PA
        LPRINT BX, BY, NAX, NAY, NPART
        LPRINT ATOM$, MM, EPS, BINE, SIG, SIG2
        LPRINT NBX, NBY
        LPRINT NX, XMIN, XMAX
        LPRINT NY, YMIN, YMAX
        LPRINT RCUT, RC2
```

```
LPRINT VMAX
LPRINT CEY, CM$, MC, CW$, CL$
LPRINT LIDX, YMAX, YMIN
LPRINT TD, TS, TL, TF
LPRINT TSP, TLP, TFP
LPRINT EC$, EP$, EF$, EFN$
LPRINT SF$, SFN$, SSEQ$
LPRINT AI$, SNAS$, TP2
LPRINT EG$
FOR I = 1 TO NPART
LPRINT "A: "; I; M(I); MOLID(I);
NEXT I
LPRINT
LPRINT M$, NMOL, NAT, MA
FOR J = 1 TO NMOL
LPRINT "Molecule# ", J
FOR I = 0 TO (NAT + 1)
LPRINT MOL(J, I);
NEXT I
NEXT J
LPRINT "Connection matrix"
FOR I = 1 TO (NMOL * NAT)
LPRINT I, MCOV(I, 1), MCOV(I, 2)
NEXT I
LPRINT
'Morse parameters
LPRINT DE, BETA, R0, BEDE
LPRINT NSNAP
RETURN
```

Figure 46. Molecular dynamics program II - Calculation.

```
DEFINT I-N
DEFDBL A-H, O-Z
DECLARE FUNCTION FORCEMORSE (R, R0, BETA, BEDE)
DECLARE FUNCTION FORCEWAALS (R, R2, SIG2, EPS)

VAR: 'variable list
     'N = number of atoms
     DIM X(1550), Y(1550), VX(1550), VY(1550), FX(1550),
     FY(1550)
     DIM LST(1550, 20), MOLID(1550), M(1550), MOL(30, 30)
     DIM MCOV(200, 2)

COMMAND: 'command interpreter subroutine
     CLS
     PRINT "MOLECULAR DYNAMICS CALCULATION": PRINT
     INPUT "Name of MD-START file ", PARA$
     FILE$ = PARA$
     GOSUB INIREAD
     PRINT "Output snap-file ", SFN$
     INPUT "Change (Y/N) ", A$
     IF A$ = "Y" THEN INPUT "New file name ", SFN$
     IF SF$ = "Y" THEN
         FILE$ = SFN$
         NSP = NSNAP
         GOSUB SNAPINI
         IF SSEQ$ = "Y" THEN CLOSE #1
     END IF
     COL2 = 5
     SCREEN 9
     COLOR 6, 7
     WINDOW (0, 0)-(BX, BY)
     T = TP * 1000                    'master clock
     T2 = 0                           'lap time for snap-shot
     T3 = 0                           'lap time for list update
     IF SF$ = "Y" THEN
         IF SSEQ$ = "Y" AND NSNAP < 1000 THEN
          FILE$ = SFN$ + "." + LTRIM$(STR$(NSNAP))
         ELSE
          FILE$ = SFN$
         END IF
         GOSUB SNAP
     END IF
     GOSUB GRAPH
     GOSUB LSTUP
     QA = TD * .06024
     NSPIN = 0

TSTEP:  T = T + TD
     T2 = T2 + TD
```

```
      T3 = T3 + TD
      GOSUB FORCE
      GOSUB FROGP
      IF T3 >= TL THEN
           GOSUB LSTUP
           T3 = T3 - TL
      END IF
      IF T2 >= TS THEN
          TP = T / 1000
          IF SF$ = "Y" THEN
           IF SSEQ$ = "Y" AND NSNAP < 1000 THEN
               FILE$ = SFN$ + "." + LTRIM$(STR$(NSNAP))
           ELSE
               FILE$ = SFN$
           END IF
          GOSUB SNAP
          END IF
          TPICO = T / 1000
          IF E$ = "Y" THEN GOSUB ENERGY
          CLS
          GOSUB GRAPH
          T2 = T2 - TS
      END IF
      IF T >= TF THEN
          IF SF$ = "Y" THEN
           GOSUB FILEFIN
          END IF
           END
      END IF
      GOTO TSTEP

INIREAD: 'subroutine that reads initiation-file and continues
           MD calculation
      OPEN FILE$ FOR INPUT AS #2
      INPUT #2, N$
      INPUT #2, N2$
      INPUT #2, C$, NP
      INPUT #2, PKE, MP, PVEL, PX, PA
      INPUT #2, BX, BY, NAX, NAY, N
      INPUT #2, ATOM$, MM, EPS, BINE, SIG, SIG2
      INPUT #2, NBX, NBY
      INPUT #2, NX, XMIN, XMAX
      INPUT #2, NY, YMIN, YMAX
      INPUT #2, RCUT, RC2
      INPUT #2, VMAX
      INPUT #2, CEY, CM$, MC, CW$, CL$
      INPUT #2, LIDX, YMAX, YMIN
      INPUT #2, TD, TS, TL, TF
      INPUT #2, TSP, TLP, TFP
      INPUT #2, EC$, EP$, EF$, EFN$
      INPUT #2, SF$, SFN$, SSEQ$
      INPUT #2, AI$, SNAS$, TP2
```

```
      INPUT #2, EG$
      FOR I = 1 TO N
      INPUT #2, M(I), MOLID(I)
      NEXT I
      INPUT #2, M$, NMOL, NAT, MA
      FOR J = 1 TO NMOL
      FOR I = 0 TO (NAT + 1)
      INPUT #2, MOL(J, I)
      NEXT I
      NEXT J
      FOR I = 1 TO (NMOL * NAT)
      INPUT #2, MCOV(I, 1), MCOV(I, 2)
      NEXT I
      INPUT #2, DE, BETA, R0, BEDE
      INPUT #2, ND
      INPUT #2, NSNAP, TP
      INPUT #2, EK, PE, PTOT, EKP
      FOR J = 1 TO N
          INPUT #2, I, X(J), Y(J), VX(J), VY(J)
      NEXT J
      RETURN

DOUT: 'writes default parametes to file
      OPEN "MDPARA.DEF" FOR OUTPUT AS #4
      WRITE #4, N$
      WRITE #4, N2$
      WRITE #4, C$, NP
      WRITE #4, PKE, MP, PVEL, PX, PA
      WRITE #4, BX, BY, NAX, NAY, N
      WRITE #4, ATOM$, MM, EPS, BINE, SIG, SIG2
      WRITE #4, NBX, NBY
      WRITE #4, NX, XMIN, XMAX
      WRITE #4, NY, YMIN, YMAX
      WRITE #4, RCUT, RC2
      WRITE #4, VMAX
      WRITE #4, CEY, CM$, MC, CW$, CL$
      WRITE #4, LIDX, YMAX, YMIN
      WRITE #4, TD, TS, TL, TF
      WRITE #4, TSP, TLP, TFP
      WRITE #4, EC$, EP$, EF$, EFN$
      WRITE #4, SF$, SFN$, SSEQ$
      WRITE #4, AI$, SNAS$, TP2
      WRITE #4, EG$
      FOR I = 1 TO N
      WRITE #4, M(I), MOLID(I)
      NEXT I
      WRITE #4, M$, NMOL, NAT, MA
      FOR J = 1 TO NMOL
      FOR I = 0 TO (NAT + 1)
      WRITE #4, MOL(J, I)
      NEXT I
      NEXT J
```

```
      FOR I = 1 TO 100
      WRITE #4, MCOV(I, 1), MCOV(I, 2)
      NEXT I
      WRITE #4, DE, BETA, R0, BEDE
      WRITE #4, NSNAP
      CLOSE #4
      RETURN

GRAPH:  'subroutine for screen output
      FOR I = 1 TO N
      IF M(I) = MM THEN
          NC = 5
      ELSE
          IF M(I) = MP THEN NC = 6
          IF M(I) = MA THEN NC = 9
          IF M(I) = MC THEN NC = 8
      END IF
      CIRCLE (X(I), Y(I)), SIG / 2, NC
      PAINT (X(I), Y(I)), NC
      NEXT I
      TPD = T / 1000
      PRINT NSNAP; "Time/ps ", TPD; "   Total energy ";
      IF EG$ = "Y" THEN PRINT USING "  #.####^^^^"; PTOT
      RETURN

FORCE: 'force calculation, units = 10(-21) J/A
      FOR I = 1 TO N
      FX(I) = 0: FY(I) = 0
      NEXT I
      FOR I = 1 TO N
      K = LST(I, 0)
      IF K = 0 THEN GOTO FOUT
      FOR JC = 1 TO K
      J = LST(I, JC)
      DX = X(J) - X(I)
      DY = Y(J) - Y(I)
      R2 = DX * DX + DY * DY
      R = SQR(R2)
      IF MOLID(I) = 0 THEN
          F = FORCEWAALS(R, R2, SIG2, EPS)
      ELSE
          IF MCOV(MOLID(I), 1) = J OR MCOV(MOLID(I), 2) = J
      THEN
           F = FORCEMORSE(R, R0, BETA, BEDE)
      ELSE
           F = FORCEWAALS(R, R2, SIG2, EPS)
          END IF
      END IF
      FX = DX / R * F
      FY = DY / R * F
      FX(I) = FX(I) + FX
      FX(J) = FX(J) - FX
```

```
      FY(I) = FY(I) + FY
      FY(J) = FY(J) - FY
      NEXT JC

FOUT: NEXT I
      RETURN

ENERGY: 'energy calculation
      EKT = 0
         FOR I = 1 TO (N - NP)
         VT2 = VX(I) * VX(I) + VY(I) * VY(I)
         EKT = EKT + M(I) * VT2 / 836.8'kcal/mol
      NEXT I
      IF NP = 1 THEN
         EKP = M(N) * (VX(N) * VX(N) + VY(N) * VY(N)) / 836.8
         EKP2 = EKP / 23.0609   'eV
         EK = EKT + EKP
      END IF
      PE = 0
      FOR I = 1 TO N - 1
      FOR J = I + 1 TO N
      DX = X(J) - X(I)
      DY = Y(J) - Y(I)
      R = SQR(DX * DX + DY * DY)
      Q = SIG / R
      Q = Q * Q * Q * Q * Q * Q
      PE = PE + 4 * EPS * (Q * (Q - 1))
      NEXT J
      NEXT I
      PE = PE * .143929
      PTOT = PE + EK
      IF EP$ = "Y" THEN
          LPRINT "Calculation time/ ps       ", TP
          LPRINT "      , target     ", EKT, " kcal/mol"
          LPRINT "      , total      ", EK, " kcal/mol"
          LPRINT "Potential energy, total   ", PE, " kcal/mol"
          LPRINT "Total energy, pot. + kin.", PTOT, " kcal/mol"
          IF NP = 1 THEN
           LPRINT "      projectile ", EKP, " kcal/mol"
           LPRINT "      projectile ", EKP2, " eV"
           LPRINT "      target     ", EKT, " kcal/mol"
          END IF
      LPRINT
      END IF
      RETURN

FROGP:'subroutine for calculation of new velocities, units
       = A/ps
       'and positions, calculates v(t+dt/2) and r(t+dt)
      FOR I = 1 TO (N - 1)
            VX(I) = VX(I) + FX(I) * QA / M(I)
            VY(I) = VY(I) + FY(I) * QA / M(I)
```

```
            X(I) = X(I) + VX(I) * TD / 1000
            Y(I) = Y(I) + VY(I) * TD / 1000
            IF X(I) < 0 AND FX(I) < 0 THEN VX(I) = 0
        NEXT I
            VX(N) = VX(N) + FX(N) * QA / M(N)
            VY(N) = VY(N) + FY(N) * QA / M(N)
            X(N) = X(N) + VX(N) * TD / 1000
            Y(N) = Y(N) + VY(N) * TD / 1000

FROGP2:  RETURN

SNAP:'writes intermediate results to file
     OPEN FILE$ FOR APPEND AS #1
     NSNAP = NSNAP + 1
     WRITE #1, NSNAP, TP
     WRITE #1, EK, PE, PTOT, EKP
     FOR I = 1 TO N
         X! = CSNG(X(I)): Y! = CSNG(Y(I)): VX! = CSNG(VX(I)):
VY! = CSNG(VY(I))
         WRITE #1, I, X!, Y!, VX!, VY!
         NEXT I
     CLOSE #1
     RETURN

SNAPINI: 'initializes the output file
     OPEN FILE$ FOR OUTPUT AS #1
     WRITE #1, N$
     WRITE #1, N2$
     WRITE #1, C$, NP
     WRITE #1, PKE, MP, PVEL, PX, PA
     WRITE #1, BX, BY, NAX, NAY, N
     WRITE #1, ATOM$, MM, EPS, BINE, SIG, SIG2
     WRITE #1, NBX, NBY
     WRITE #1, NX, XMIN, XMAX
     WRITE #1, NY, YMIN, YMAX
     WRITE #1, RCUT, RC2
     WRITE #1, VMAX
     WRITE #1, CEY, CM$, MC, CW$, CL$
     WRITE #1, LIDX, YMAX, YMIN
     WRITE #1, TD, TS, TL, TF
     WRITE #1, TSP, TLP, TFP
     WRITE #1, EC$, EP$, EF$, EFN$
     WRITE #1, SF$, SFN$, SSEQ$
     WRITE #1, AI$, SNAS$, TP2
     WRITE #1, EG$
     FOR I = 1 TO N
     WRITE #1, M(I), MOLID(I)
     NEXT I
     WRITE #1, M$, NMOL, NAT, MA
     FOR J = 1 TO NMOL
     FOR I = 0 TO (NAT + 1)
     WRITE #1, MOL(J, I)
```

```
      NEXT I
      NEXT J
      FOR I = 1 TO 100
      WRITE #1, MCOV(I, 1), MCOV(I, 2)
      NEXT I
      WRITE #1, DE, BETA, R0, BEDE
      WRITE #1, NSP
      CLOSE #1
      RETURN

FILEFIN: 'closes file
      I = 0
      OPEN SFN$ FOR APPEND AS #1
      WRITE #1, I, X!, Y!, VX!, VYS!
      CLOSE #1
      RETURN

LSTUP:  'update of interaction lists
      ERASE LST
      FOR I = 1 TO N - 1
      FOR J = I + 1 TO N
      DX = X(J) - X(I)
      IF DX > RCUT THEN GOTO LSU1
      DY = Y(J) - Y(I)
      IF DY > RCUT THEN GOTO LSU1
      R2 = DX * DX + DY * DY
      IF R2 < RC2 THEN
          LST(I, 0) = LST(I, 0) + 1
          L1 = LST(I, 0)
          LST(I, L1) = J
      END IF

LSU1:   NEXT J
      NEXT I
      RETURN
      SCREEN 1
FUNCTION FORCEMORSE (R, R0, BETA, BEDE)
      F1 = EXP(BETA * (R0 - R))
      FORCEMORSE = BEDE * F1 * (1 - F1)
END FUNCTION
FUNCTION FORCEWAALS (R, R2, SIG2, EPS)
      Q = SIG2 / R2
      Q1 = Q * Q * Q
      Q2 = Q1 * Q1
      FORCEWAALS = 4 * EPS * (-12 * Q2 + 6 * Q1) / R
END FUNCTION
```

Figure 47. Molecular dynamics program III - Temperature calculation.

```
      'reads snapshot files and displays them
      PRINT "Reads new file format (July 10, 90) that
            incorporates temp. data"
      DEFINT I-N
      NZATOM = 1550: NZMOL = 20: NZAIM = 7: NZAIAM = 120: NZN
      = 20
      DIM X(1550), Y(1550), VX(1550), VY(1550), M(1550)
      DIM NCOL(1550)
      DIM LST(1550, 20), TEMP(1550), MOL(20, 7)
      DIM MOLID(1550), MCOV(120, 2)
      PRINT "This program colorcodes atoms according to local
            temperature"
      PRINT "Set 'Caps Lock'"

PC1:  INPUT "Calculate or Read temperature? (C/R/No) ", TI$
      IF TI$ = "c" OR TI$ = "r" OR TI$ = "n" THEN
        PRINT "Did I not tell you to set Caps Lock???? "
        GOTO PC1
        END IF
      IF TI$ = "C" THEN
        INPUT "Are you SURE (You may overwrite previous file)
        (Y/N)  ", A$
        INPUT "Neighbor Distance  ", RC
        RC2 = RC * RC
        IF A$ <> "Y" THEN GOTO PC1
      END IF
      INPUT "Input data file name (no extension)  ", S$
      INPUT "Display mode (S/MS/M)  ", DM$
      INPUT "Frame number (Start for Movie)  ", NFRAME
      IF DM$ = "M" THEN
        INPUT "Step frame numbers by (1,2,...)  ", NFSTEP
        END IF
      SCREEN 9
      COLOR 5, 8
      GOSUB INIREAD
      GOSUB DIMTEST
      IF NERR = 1 THEN END
      GOSUB CLIMIT
      GOSUB GCONT

CYC:  IF NFRAME > 999 THEN
           PRINT "NFRAME too large (>999) "
           INPUT "Frame number (Start for Movie) ", NFRAME
           GOTO CYC
       END IF
           FILE$ = S$ + "." + LTRIM$(STR$(NFRAME))
           OPEN FILE$ FOR INPUT AS #1
           GOSUB ONESNAP
```

```
      IF TI$ = "C" THEN
      GOSUB LSTUP
      CLS
      FOR M = 1 TO N
      GOSUB VTEMP
      NEXT M
      GOSUB SNW
      END IF
      GOSUB COLCODE
      GOSUB GRAPH
      IF DM$ = "M" THEN
        NFRAME = NFRAME + NFSTEP
        GOTO CYC:
        END IF
      IF DM$ = "S" THEN
PC2:   INPUT "New frame number/ Graph control/ End (N/G/E) ",
       A$
       IF A$ = "E" THEN
            END
       ELSEIF A$ = "G" THEN GOSUB GCONT
            GOSUB GRAPH
            GOTO PC2
       ELSEIF A$ = "N" THEN
            INPUT "New frame number ", NFRAME
            GOTO CYC:
       ELSE
            GOTO PC2
       END IF
      END IF
      END
GCONT: 'graph control
     WEX = 1.1: REX = .85: REXP = 85: SIGR = SIG * REX: WEXP
     = 110
     WINDOW (0! * BX, (.5 - WEX / 2) * BY)-(WEX * BX, (.5 +
     WEX / 2) * BY)
GC1: INPUT "What do you want to change
     (All/Radius/Expansion/Move/Default) ", A$
     IF A$ = "D" THEN GOTO GC3
     IF A$ = "A" OR A$ = "R" THEN
       INPUT "Circle radius on graphs, percent ", REXP
       SIGR = SIG * REXP / 100: REX = REXP / 100
       PRINT "Circle expansion by factor of   ", REX
     END IF
     IF A$ = "A" OR A$ = "E" THEN
       INPUT "Window expansion, percent ", WEXP
       WEX = WEXP / 100
       PRINT "Window expansion by a factor of ", WEX
       WINDOW (0! * BX, (.5 - WEX / 2) * BY)-(WEX * BX, (.5 +
       WEX / 2) * BY)
     END IF
     IF A$ = "A" OR A$ = "M" THEN
       PRINT "'Move' not implemented"
```

```
      END IF
      INPUT "Change (Y/N) ", A2$
      IF A2$ = "Y" THEN GOTO GC1

GC3: RETURN

SNW: 'subroutine for writing new snap file
      OPEN FILE$ FOR OUTPUT AS #2
      WRITE #2, NSNAP, TP
       WRITE #2, EK, PE, PTOT, EKP
       WRITE #2, TPT, NZT, RCT
      FOR J = 1 TO N
       WRITE #2, J, X(J), Y(J), VX(J), VY(J), TEMP(J)
      NEXT J
      CLOSE #2
      RETURN
      WRITE #2, TP, N, RC
      FOR I = 1 TO N
      WRITE #2, TEMP(I)
      NEXT I
      CLOSE #2
      RETURN

CLIMIT:   'color number calculation
      TL1 = 400
      TL2 = 500
      TL3 = 1000
      TL4 = 2000
      TL5 = 1000000!
      TL6 = 1000000!
      TL7 = 1000000!
      TL8 = 1000000!
      TL9 = 1000000!
      TL10 = 1000000!
      RETURN

COLCODE:
     NR = 0: NY = 0: NG = 0: NB = 0: NGR = 0
     FOR I = 1 TO N
       IF TEMP(I) < TL1 THEN
        NCOL(I) = 16
        NGR = NGR + 1
        END IF
       IF TEMP(I) < TL2 AND TEMP(I) > TL1 THEN
        NCOL(I) = 7
        NB = NB + 1
        END IF
       IF TEMP(I) < TL3 AND TEMP(I) > TL2 THEN
        NCOL(I) = 7
        NG = NG + 1
        END IF
       IF TEMP(I) < TL4 AND TEMP(I) > TL3 THEN
```

```
        NCOL(I) = 12
        NY = NY + 1
        END IF
       IF TEMP(I) < TL5 AND TEMP(I) > TL4 THEN
        NCOL(I) = 12
        NR = NR + 1
        END IF
       IF TEMP(I) < TL6 AND TEMP(I) > TL5 THEN NCOL(I) = 12
       IF TEMP(I) < TL7 AND TEMP(I) > TL6 THEN NCOL(I) = 12
       IF TEMP(I) < TL8 AND TEMP(I) > TL7 THEN NCOL(I) = 12
       IF TEMP(I) < TL9 AND TEMP(I) > TL8 THEN NCOL(I) = 12
       IF TEMP(I) > TL10 THEN NCOL(I) = 12
    NEXT I
     RETURN

LSTUP:  'update of interaction lists
     PRINT "LSTUP"
     ERASE LST
     FOR I = 1 TO N - 1
     PRINT I;
     FOR J = I + 1 TO N
     DX = X(J) - X(I)
     DY = Y(J) - Y(I)
     R2 = DX * DX + DY * DY
     IF R2 < RC2 THEN
      LST(I, 0) = LST(I, 0) + 1
      L1 = LST(I, 0)
      LST(I, L1) = J
      LST(J, 0) = LST(J, 0) + 1
      L1 = LST(J, 0)
      LST(J, L1) = I
     END IF
     NEXT J
     NEXT I
     PRINT
     RETURN

VTEMP: VXSUM2 = 0: VYSUM2 = 0: VXSUM = 0: VYSUM = 0: L =
     LST(M, 0): MSUM = 0
     IF L = 0 THEN GOTO VT1
     FOR I = 1 TO L
     J = LST(M, I)
      VXSUM = VXSUM + VX(J) * M(J)
      VYSUM = VYSUM + VY(J) * M(J)
      MSUM = MSUM + M(J)
     NEXT I

VT1:  VXSUM = VXSUM + VX(M) * M(M)
      VYSUM = VYSUM + VY(M) * M(M)
      MSUM = MSUM + M(M)
      VCMX = VXSUM / MSUM
      VCMY = VYSUM / MSUM
```

```
        IF L = 0 THEN GOTO VT2
        FOR I = 1 TO L
        J = LST(M, I)
        VXC = VX(J) - VCMX
        VYC = VY(J) - VCMY
        VXSUM2 = VXC * VXC * M(J) + VXSUM2
        VYSUM2 = VYC * VYC * M(J) + VYSUM2
        NEXT I

VT2:    VXC = VX(M) - VCMX
        VYC = VY(M) - VCMY
        VXSUM2 = VXC * VXC * M(M) + VXSUM2
        VYSUM2 = VYC * VYC * M(M) + VYSUM2
        L = L + 1
        VSUM2 = VXSUM2 + VYSUM2
        TEMP(M) = VSUM2 * 5 / L / 8.314
        RETURN

INIREAD: 'reads header file (.  )
     OPEN S$ FOR INPUT AS #1
     INPUT #1, N$
     INPUT #1, N2$
     PRINT N$
     PRINT N2$
     INPUT #1, C$, NP
     INPUT #1, PKE, PMASS, PVEL, PX, PA
     INPUT #1, BX, BY, NAX, NAY, N
     INPUT #1, ATOM$, MM, EPS, BINE, SIG, SIG2
     INPUT #1, NBX, NBY
     INPUT #1, NX, XMIN, XMAX
     INPUT #1, NY, YMIN, YMAX
     INPUT #1, RCUT, RC2
     INPUT #1, VMAX
     INPUT #1, CEY, CM$, MC, CW$, CL$
     INPUT #1, LIDX, YMAX, YMIN
     INPUT #1, TD, TS, TL, TF
     INPUT #1, TSP, TLP, TFP
     INPUT #1, EC$, EP$, EF$, EFN$
     INPUT #1, SF$, SFN$, SSEQ$
     INPUT #1, AI$, SNAS$, TP2
     INPUT #1, EG$
     FOR I = 1 TO N
     INPUT #1, M(I), MOLID(I)
     NEXT I
     INPUT #1, M$, NMOL, NAT, MA
     FOR J = 1 TO NMOL
     FOR I = 0 TO (NAT + 1)
     INPUT #1, MOL(J, I)
     NEXT I
     NEXT J
     CLOSE #1
     RETURN
```

```
DIMTEST: 'Checks sizes of declared matrices
      NERR = 0
      IF N > NZATOM THEN
        PRINT "Number of atoms too large (NZATOM) "
        NERR = 1
        END IF
      IF NMOL > NZMOL THEN
        PRINT "Number of molecules too large (NZMOL)"
        NERR = 1
        END IF
      IF NAT > NZAIM THEN
        PRINT "Number of atoms in each molecule too large
              (NZAIM)"
        PRINT "NZAIM must be 1 larger than number of
              atoms"
        NERR = 1
        END IF
      IF (NAT * NMOL) > NZAIAM THEN
        PRINT "Number of atoms in ALL molecules too large
             (NZAIAM) "
        NERR = 1
        END IF
      PRINT "Maximum number of neighbors is ", NZN
      RETURN

ONESNAP: 'reads one snap-shot
      INPUT #1, NSNAP, TP
      INPUT #1, EK, PE, PTOT, EKP
      FOR J = 1 TO N
       INPUT #1, NM, X(J), Y(J), VX(J), VY(J) ', TEMP(J)
      NEXT J
      CLOSE #1
      RETURN

GRAPH: 'screen output
      CLS
      FOR J = 1 TO N
      IF M(J) = MA THEN
       CIRCLE (X(J), Y(J)), SIGR / 2, NCOL(J)
      ELSE
       CIRCLE (X(J), Y(J)), SIGR / 2, NCOL(J)
       PAINT (X(J), Y(J)), NCOL(J)
      END IF
      NEXT J
      PRINT "TIME "; TP; " ps", "  Frame# "; NFRAME
      RETURN
```